Alma Mater Studiorum

Universitá di Bologna

SCHOOL OF ENGINEERING AND ARCHITECTURE
Forlì Campus

Second Cycle Degree in
INGEGNERIA AEROSPAZIALE/ AEROSPACE NGINEERING
Class LM-20

THESIS
In Fluid Dynamics, ING-IND/ 06

Design, calculation and simulation of a wind tunnel for calibration of hot wire probes

Student: FORNERO, Agustin

Supervisor: Ing. BELANI, Gabriele.

Year: 2018

Content

List of Figures

List of Tables

Introduction:

Anemometry is the process of ascertaining the speed, and direction of wind in an airflow. To do this it requires the use of a device, called anemometer. The anemometer is an instrument used to measure the speed of any gas. There are many different types of anemometers but the most common for aeronautics and aerodynamics use is hot wire anemometry.

Hot wire anemometry measures both speed and pressure of the airflow under the principle that a heated body, in this case a fine wire, placed in a flow will experience a cooling effect. This effect is mainly associated to forced convection heat losses which are strongly velocity dependent. If it's possible to measure this heat loss, then it's possible to retrieve the flow velocity based on the wire's cooling rate. In the hot-wire case this cooling effect can be measured either by measuring the change in the temperature of the sensor (constant current anemometer) or either by measuring the action necessary to keep it at a constant temperature (constant temperature anemometer). The hot wire is made of platinum or tungsten and they range in length between 0.5 and 2 mm and in diameter from 0.6 to 5 microns.

It comes in a single-wire configuration or with two or more wires configuration depending on the application is being used and the purpose of it.

In the constant current anemometer, the hot wire is supplied with a constant current and inserted in a Wheatstone bridge where is kept on balance, later by the equation of Wheatstone bridge the resistance of the wire is retrieved and knowing the current, which is constant, we can calculate the speed of the airflow. In the other method, constant temperature anemometer, the wire is kept in a constant temperature (and therefore resistance), so it measures in a faster way and with a faster response.

The Center for International Collaboration on Long Pipe experiments of the Bologna University, CICLoPE, located in predappio, for the long Pipe wind tunnel. The purpose of CICLoPE is focused on the research of turbulence for High Reynolds number. The CICLoPE wind tunnel ensures a size of the smallest scale of the turbulent boundary layer that is sufficiently large to be resolved with the actual measurement techniques for High Reynolds number. To perform these measurements the hot-wire probes, specially X-probes with two wires to measure two components of the velocity, are used.

Like every other measure instrument, the hot wire needs to be calibrated to have an accurate reading of the speed of the airflow, especially this type of anemometer since it can be affected by contamination and their response is highly dependent on ambient quantities. The calibration is achieved by establishing the relationship between the anemometer output voltage and the magnitude and direction of the incident velocity vector, each hot wire must be calibrated before measurements by exposing it to a set of known velocities and then a calibration curve must be fitted to the calibration points.

The exposition to the set of known velocities is achieved in a calibrating wind tunnel, which is a "blower tunnel" who is designed to have a most laminar possible flow in the open test section to get the most accurate reading of the velocity and it has the possibility to achieve different speeds to make possible the calibration of the probes.

The design of this kind of tunnel is performed to meet the investigation purposes, where the parameters of velocity, dimensions and the uniformity of the flow are set. Then comes the calculation of the power lading factor to maintain these parameters and flow characteristics in the test section. Once this is obtained, the elements that will get the flow to these characteristics needs also to be designed and calculate their pressure losses to know how much power we will need to run the tunnel. The pressure loss for each component depends in the geometry and functionality of it.

Once all components are designed and selected, a model representing the wind tunnel can be made to show how it will work and how the components will be placed and kept there. It can also be done the selection of the power plant that will power the wind tunnel.

The present thesis will be focused on the design and selection of the components for a wind tunnel that will be used to calibrate the probes used in CICLoPE. Inside these components, a comparison between different convergent will be made to select the one who will fit the best this application. It will also select the power plant for this and present a model for a future construction of it.

The specifications prior to the design for the wind tunnel are:

1. The flow in the test-section should be as uniform as possible. A difference of less than 0.5% in the velocity distribution in the test-section is required to achieve a calibration the most accurate possible.

2. The test section will have 10mm height by 500mm wide.

3. The settling chamber where the components to achieve the flow characteristics will have 50mm height by 500mm wide. The length of the settling chamber is not yet defined, it will be defined by the number of components since it will be a separation of 15cm between them for stabilization of the flow.

4. The contraction to the test-section is only in height not in wide making it a two-dimensional contraction. Several options will be tested to find the best solution.

This tunnel is an important one since it says before will calibrate the probes for CICLoPE that allows the research performed there, that's the main reason the flow characteristics of the test-section have high requirements, to ensure a proper functioning that will ensure realistic and accurate results in the research performed at this center.

In the next pages, added to the stated before, an explanation of the functioning of the probes and the calibration method will be written along with an introduction to wind tunnels and the different components of one.

Hot-wire

Introduction

Hot-wire anemometry is the leading technique for velocity measurements in the field of turbulent flows, because with a careful design of the sensor and anemometer system, it can achieve and spatial and temporal resolution far much better than the other measurements techniques, making it an invaluable tool for turbulence investigation. It relies on the fact that the electrical resistance of a metal conductor is a function of its temperature. The essential part of the hot-wire anemometer is, therefore, a miniature metal element, heated by an electrical current and inserted into the flow under investigation. When inserted into the flow it experiences a cooling effect; this effect is mainly associated to forced convection heat losses which are strongly velocity dependent. The transfer of the heat from the element increases with increasing flow velocity in the neighborhood of the element, if we can measure this heat loss, it would be possible to retrieve the flow velocity based on the wire's cooling ratio. To get results that can be trust we need to calibrate the wires with the sensors. There are two methods to measure the cooling effect, either by measuring the chance in temperature of the sensor (constant current anemometer) or by measuring the action necessary to keep it at a constant temperature (constant temperature anemometer).

The popularity of the hot-wire anemometry is mainly because of the advantages of the process:

- The sensitive is small enough not to introduce any disturbance in the flow; although the other parts of the probe may not so it can disturb the flow in the vicinity of the wire.
- The hot-wire anemometer responds almost instantaneously to rapid fluctuations so that high-frequency effects can be recorded without distortion.
- Thanks to its very small physical dimensions, it has a small measuring volume and therefore an extremely good spatial resolution.
- The electrical signal produced by the hot-wire anemometer can be readily statically processed, both by analog and digital systems.

Even though all these advantages, there also a few drawbacks of this type of anemometer; few of those being:

- Hot-wires are limited to low and medium intensity turbulence flows, because they can't recognize a reverse flow in a high turbulence flow due to the velocity vector may be falling outside the acceptance cone.
- They have consistent drift over time, may be affected by contamination and their response is highly dependent on ambient quantities. For this, frequent calibrations are necessary.
- Hot-wires are intrinsically fragile due to their small size, so extreme precaution while handling the probes is needed.

The wires range between 0.5 to 2 mm in length and in diameter from 0.6 to 5 microns. Tungsten, platinum or platinum-iridium wires are the most frequently used materials. They can be found hot-wires probes in different configurations, with one, two or more sensor wires.

This section will provide a general description of the methods; the equations ruling the cooling effect and a brief explanation of different types of probes and the way to calibrate them.

Equations

The sensor heated by the electrical current gives up its heat to the flow into which it's inserted by conduction, by free and forced convection, and by radiation. The last component is, however, relatively small and can be neglected.

In case of a cylinder shaped-body, like a wire, the forced convection coefficient h can be expressed as:

$$h = \frac{N_u k_f}{d_w}$$

where k_f is the thermal conductivity of the fluid, and d_w is the cylinder's diameter, in this case, the wire. N_u is the Nusselt's number, which it's a function of many parameters.

$$N_u = N_u \left(M, Re, Gr, Pr, \gamma, \frac{T_w - T_a}{T_a} \right)$$

Which are the Mach, Reynolds Grashof and Prandtl numbers, the ratio between specific heat at constant pressure and volume, and the wire temperature difference.

If we confine our attention to incompressible flows and ignore frequency spectra and space-time correlations of temperature and velocity fluctuations in the immediate neighborhood of the sensor, we can exclude the Mach number from the dimensionless ratios. In subsonic flows, γ and P_r can be considered constant and, if the heat exchange is dominated by forced convection, which is the case for hot-wires, even the dependency on the Grashof number can be neglected. It's good to point that the Reynolds number significant for the Nusselt number is the one of the wire. Taking all this in consideration the equation for the Nusselt number becomes:

$$N_u = N_u \left(Re_w, \frac{T_w - T_a}{T_a} \right)$$

The heat transfer depends on only these two dimensionless parameters. Different workers have obtained different empirical functions for the Nusselt number, and they usually share the form, for wires;

$$Nu = A_1 + B_1 {Re_w}^n$$

Where A, B and n (which for most of these functions is 0.5) are characteristic constants of the particular correlation function. Considering a specific wire diameter, Re_w can be considered only a function of the velocity U, and the equation can be rewritten as,

$$Nu = A_2 + B_2 U^n$$

The heating in the wire is achieved by means of Joule effect: a current I_w is passed through the wire, and the heat liberated is equal to $I_w^2 R_w$, where R_w is the wire's electrical resistance. The amount of heat transferred to the flow at temperature T_a from a hot wire, heated uniformly to a temperature T_w is,

$$Q = (T_w - T_a)\, Ah(U)$$

Where A is the surface area over which forced convection takes place, and h is the forced convection heat transfer coefficient which is dependent, among other things, on the fluid velocity normal to the wire. Assuming equilibrium heat transfer we obtain:

$$I_w^2 R_w = (T_w - T_a)\, Ah(U)$$

The change in the resistance of the wire is approximately proportional to the corresponding change in temperature, we can replace the temperature difference by a quantity proportional to the resistance difference and then combine this equation with the equilibrium equation and introduce them in the Nusselt equation to obtain the working formula relating the electrical quantities to the flow velocity,

$$\frac{I_w^2 R_w}{R_w - R_a} = A + BU^n$$

Considering the voltage across the hot-wire, $E_w = I_w R_w$ and using the proportional relation between the temperature and resistance the equation becomes,

$$\frac{E_w^2}{R_w} = (A + BU^n)(T_w - T_a)$$

Types of Probes

There are different types of probes with the distinction of how many wires they have and because of that, how many components of the velocity they can measure.

The main configuration is a single wire probe, but in the Ciclope lab the most used ones are two-wire probes to use in the research of velocity fluctuations near the wall of the tunnel.

Single wire probes consist in a single wire mounted in two prongs that keep it in place. It's placed perpendicular to the flow direction and the prongs parallel to it. It is used for uni-directional flows because it can't determine the orientation of the velocity vector.

To carry out two velocity measurements it can be with a single wire inclined relative to the mean-flow direction, but this can only provide a statistical information of the velocity field, because of this, two-wire probes, with the wires placed in a X configuration is used. This probe enables simultaneous measurements of two velocity components. Depending on the application the configuration of the X-probe can vary, depending on the probe-stem orientation. It can have the sensor plane (plane where both wires are lying) parallel to the probe-stem or the sensor plane perpendicular to the probe-stem. Both wires are separated from each other in the direction normal to the sensor plane to reduce aerodynamic and thermal interferences.

Another type of two-wire probe is the v-probe, this one is used for measurements close to the wall and the special resolution in the transversal direction to the wall is of extreme importance. Both wires are placed next to each other instead of one over the other.

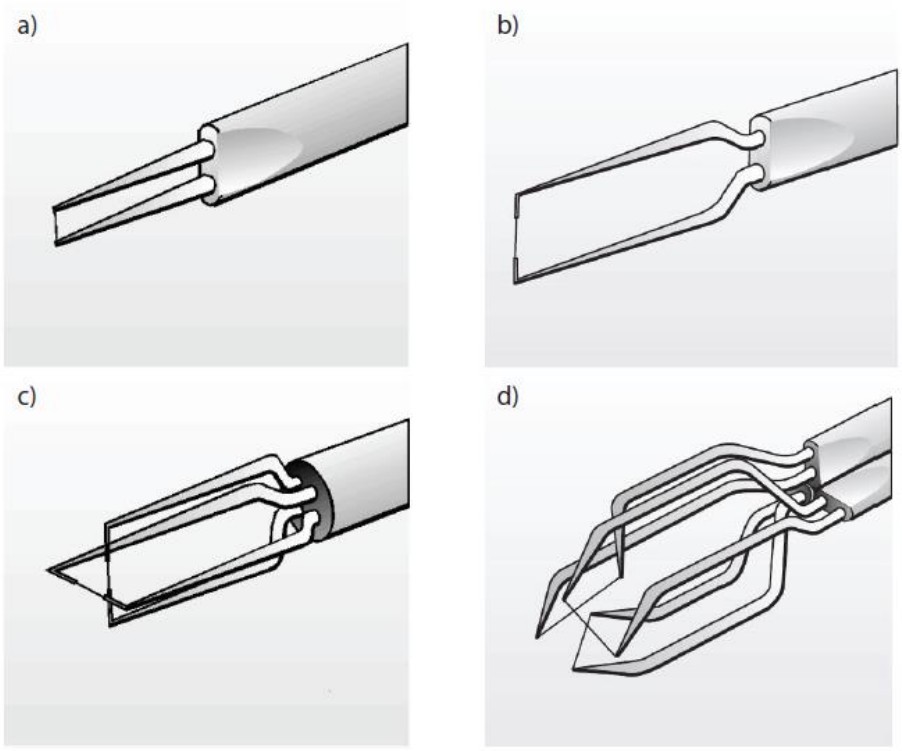

Figure 1 Different types of probes (Reprinted from Jorgensen (2002))

Calibration

We must note that the previous equations are practically never used to calculate the response of the hot-wire anemometry to the flow velocity. They are used only for approximate estimates of the effect of different factors on heat transfer between the wire and the flow.

The aim for the calibration procedure for a hot-wire sensor and its anemometer is to establish the relationship between the anemometer output voltage and the magnitude and direction of the incident velocity factor. Each hot-wire probe must be calibrated before measurements by exposing it to a set of known velocities. To obtain the transfer function that converts voltage data into velocities, a calibration curve must be fitted to the calibration points. Typical calibration curves include king's law,

$$E^2 = A + BU^n$$

But also, polynomial fitting might be used, being a very common one the fourth order polynomial relation.

$$U = C_0 + C_1E + C_2E^2 + C_3E^3 + C_4E^4$$

Despite not having any physical basis, polynomial fitting allows for a very high accuracy with a small linearization error. It works very well when high number of calibration points have been acquired but falls short when the velocities are outside of the calibration ones, i.e. low velocities. For this, King's law remains

a better solution, because it utilizes Newton's law of cooling that relates Joule heating and forced convection. But it also may lead to some error when forced convection is not the sole phenomenon causing cooling on the wire, for example, in very low velocities, where natural convection becomes relevant.

This is valid when the velocity vector is perpendicular to the wire and parallel to the prongs. If it's not the case because the probe is misaligned, or the calibration also covers when the probe has an angle respect to the velocity of the flow appears an effective velocity V_e that goes into the king's law.

$$E^2 = A + BV_e{}^n$$

This one is related to the velocity vector, V. The velocity vector can be expressed in terms of its magnitude $\bar{V}$, the yaw angle α, and the pitch angle β, or in terms of the corresponding three velocity components, U_N(normal and in plane with the prongs), U_T(tangencial to the wire) and U_B (binormal; normal to the sensor and the plane of the prongs). the wire doesn't have the same response to the three velocity components; if it has the same response the effective velocity would be equal to the magnitude of the velocity vector. However, this doesn't occur so because of that the effective velocity is defined with the Jorgensen's relation [3], which take these factors into account and is,

$$V_e^2 = U_N^2 + k^2U_T^2 + h^2U_B^2$$

Where k and h are referred as the sensor's yaw and pitch coefficients. And are experimentally determined weighing factors that depends mostly in the aspect ratio of the sensor.

Introducing the effective velocity in the King's law, it's obtained,

$$E^2 = A + B(U_N^2 + k^2U_T^2 + h^2U_B^2)^{n/2}$$

Which represents a hot wire response equation considering angles between the probe and the direction of the flow.

When calibrating X-probes an angular calibration of each wire with respect to its yaw angle is needed in addition to the velocity calibration. This is usually done by placing the probe in a rotating arm while keeping the hot-wires centered and in the same measurement area.

The result will be the calibration map of the probe, and from that can be obtained the calibration curve for each of the wires using the relations written before.

The aim of the calibration is to determine the values of the constants of the previous equation. The calibration is performed in a special calibration facility or in a flow field in which the magnitude and direction of the flow vector is known.

As a rule, whether which response equation is selected, it should provide a good approximation to the calibration data over the complete range, and if required, the yaw and pitch range.

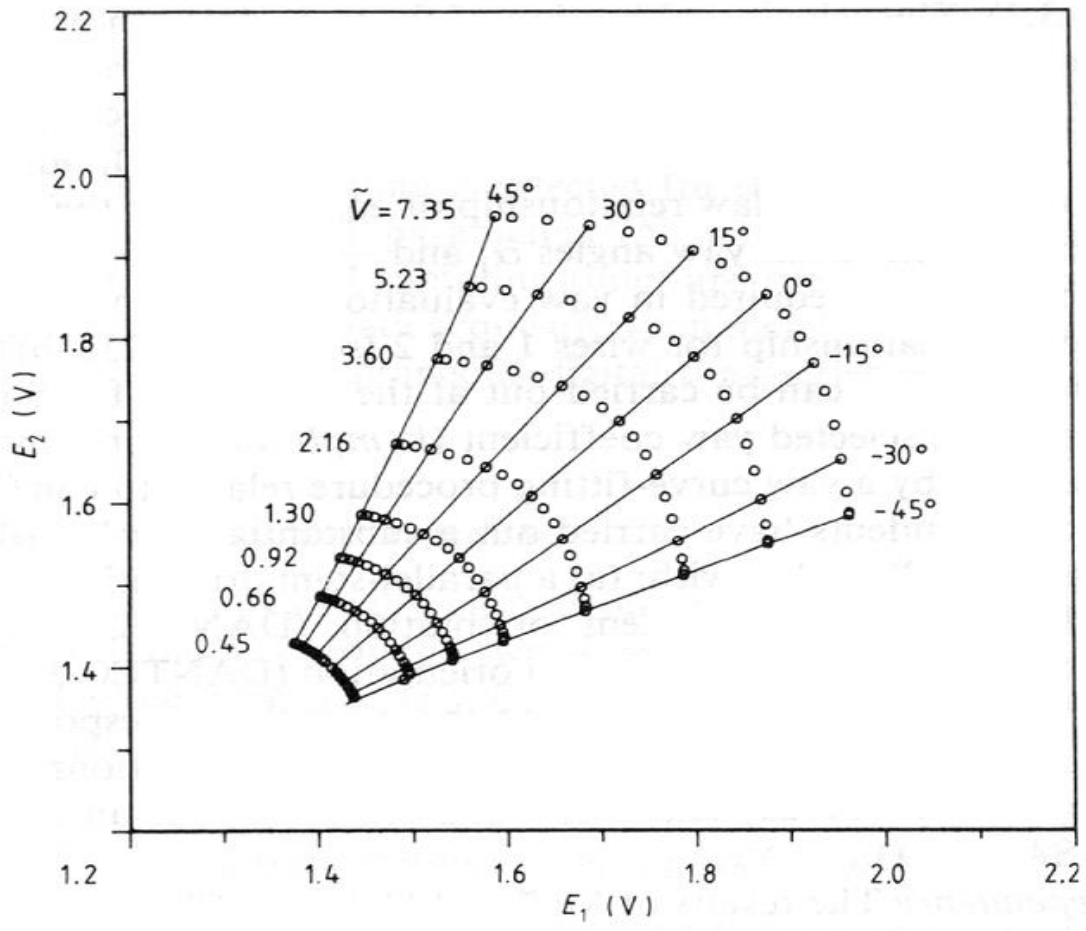

Figure 2 Example of a calibration plot for the X-wire probe (Reprinted from Orlu [9])

This way of calibrating the probes is preferred to computational procedures for the following reasons:

- The basic relationship for the Nusselt number is only an approximation to the experimental results, which always exhibit a certain spread.
- The Reynolds number is always subject to an error that cannot be controlled since the diameter of the wire is not known with absolute precision and may vary along its length.
- The physical properties of a thin metal wire are always some-what different from the properties of the corresponding material in bulk, so that tabulated data on the resistance as a function of temperature are also subject to some uncertainty.

Due to the nature of the physical principles upon which the hot-wire anemometer is based, it's clear that is very sensitive to the temperature of the ambient. The readings will be different for a given flow velocity if the temperature of the flowing material is different, therefore, the temperature of the flowing fluid must be kept constant during the calibration measurements, and it also needs to be noted in the calibration curve the temperature at which those measurements were taken.

If a hot-wire is used to measure velocity at a higher or lower flow temperature than its calibration, the heat dissipated via forced convection will be lower, and so will be the velocity reading. To retrieve the correct velocity a compensation for temperature variations must be required.

The calibration is made at a certain temperature (T_{ref}), and an analytical correction must be used to retrieve the correct voltage output at the operating flow temperature T_a,

$$E\left(T_{ref}\right)^2 = E(T_a)^2 \frac{T_w - T_{ref}}{T_w - T_a}$$

Where T_w is the wire's temperature and its fixed if the sensor is operating in constant temperature mode, $E(T_a)$ is the output voltage and $E(T_{ref})$ is the compensated output voltage. This can be rewritten by using the overheat ratio a_w, which is the relative difference in resistance between the wire at operating and ambient temperature, and the temperature coefficient of electrical resistivity α,

$$E\left(T_{ref}\right)^2 = E(T_a)^2 \left(1 - \frac{T_w - T_{ref}}{a_w/\alpha}\right)^{-1}$$

These parameters are known from the material properties and the anemometer's settings and are more easily to read and use than the wire's temperature. To employ this correction method is necessary to measure the flow temperature both during the calibration and the experiment. Since the measured average velocity always depends, at least to some extent, on the intensity of the turbulence fluctuations, the calibration measurement must be performed in a flow with the minimum possible level of turbulence, hence, the most laminar possible.

The most typical case of an increase in the air temperature in wind tunnel is connected with its heating due to the operation of the system producing the flow. For this reason, anemometer measurements on turbulence in wind tunnels must be performed only after a certain interval of time running the wind tunnel to achieve steady-state thermal conditions in the tunnel. During calibration, another probe; most of the time a Prandtl probe; is used to measure the velocity for reference.

Types

Mainly in hot-wire anemometry two types of circuits are used, constant current anemometer and constant temperature anemometer.

Constant current anemometer

It was the first mode of operation to be employed. The most practical and effective way to use this technique is to insert the sensor in a Wheatstone bridge, even though it's not necessary. After a specific overheat ratio has been selected, the wire resistance R_w can be retrieved when the bridge is in balance by the expression,

$$\frac{R_w + R_L}{R_1} = \frac{R_3}{R_2}$$

Where R_3 is the adjustable resistance and R_L is the cable resistance, which includes also connections and prongs resistance, with exception of the wire itself. During calibration, the current is kept at a constant value and the bridge is kept in balance by acting on the adjustable resistance; when is balanced, the R_w is calculated with the equation.

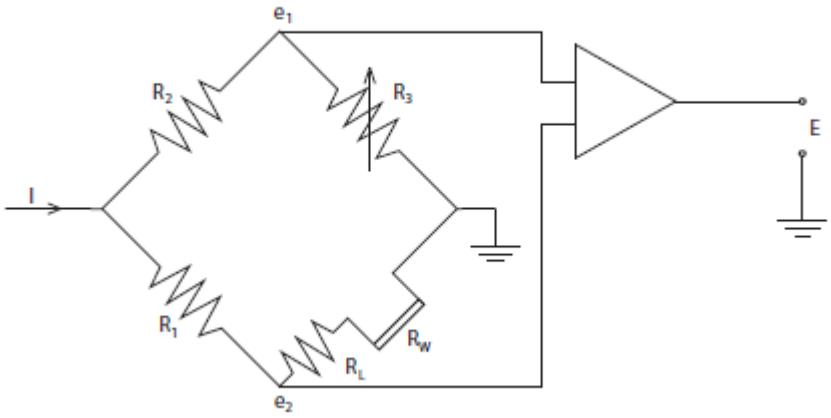

Figure 3 Example of a constant current anemometer circuit

Constant temperature anemometer

This mode has become more popular later than the previous, but it presents many advantages and is currently the method universally used for turbulent velocity measurements.

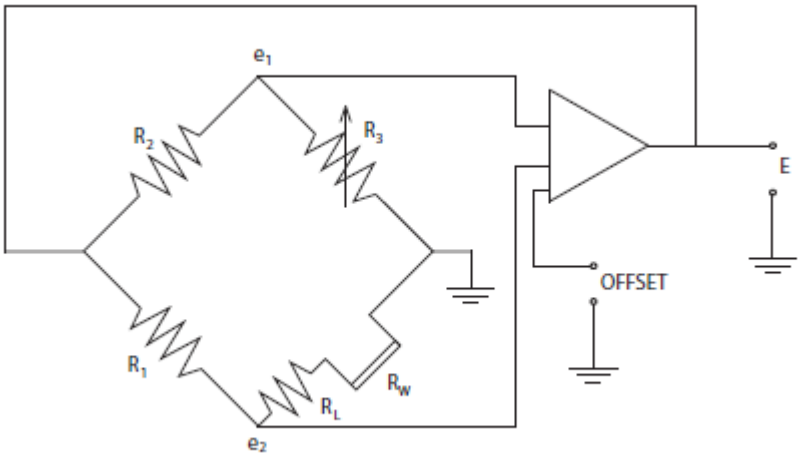

Figure 4 Example of a constant temperature anemometer circuit

Since the wire is kept at a constant temperature and therefore resistance, it's thermal inertia doesn't limit anymore the frequency response of the system, allowing for a much better tracking of the high frequency turbulent fluctuations. However, this requires a more complex circuit that allows for extremely fast variations in the heating current of the wire; it also requires a feedback mechanism. Even though it has been theorized since the 40s it wasn't until mid-60s when the progress in electronics allowed this mode of operation to be used. The hot-wire is placed in a Wheatstone bridge; as the flow velocity varies, the wire's temperature varies, and so does its resistance R_w. The voltages e_1 and e_2 are the inputs of the differential amplifier, and their difference is a measure of how much the wire's resistance has changed. The output current of the amplifier is inversely proportional to $e_2 - e_1$, and is fed on the top of the bridge, restoring the wire's nominal resistance (and temperature).

Wind tunnels

Introduction

Since the first days of aeronautics research and developments, all have been based in the latest technologies available at the moment and all pertinent sources. Three broad categories are commonly recognized: analytical computational and experimental.

The analytical approach plays a vital role in the background studies and in gaining knowledge and setting ground information and stablishing the laws that rules the natural phenomenon when it comes to researching in aeronautics, but it never suffices for a development program of any kind. All development from the first flight of the Wright brothers to the 1960s were based on a combination of analytical and experimental approaches.

In the 1960s the evolution of electronics and computers reached a point where it was possible to use these tools to approximate solutions for forms of fluid dynamic equations (Navier-Stokes) to vehiclelike geometries. This advance and the development of methods and computing machinery advancing rapidly led to the prediction that “computer will replace wind tunnels”. However, this was not certain due to the fact that the continuing development of computers, increase in velocity and processing power and even more optimized methods to solve the fluid dynamic equations, has only partially tamed the complexity of real flows. Mainly due to turbulence that in order to achieve good results, a “turbulence model” needs to the tailored for specific types of flow, there’s no general form that is accepted for all of them.

For increasing the effectiveness of applications of the computer, Hammond [1] gives three aspects of development as pacing items: central processing speed, size of memory available and turbulence models. The first two continue to advance at a rapid rate, and the last one has had many developments but there’s not a certainty that progress in achieving generality has been made. This is the Achilles heel of current efforts to extend applications of computational dynamics.

For these reasons, the experimental brand is still today a major tool to research and develop programs in aeronautics, specially wind tunnels with contribution of computers; these are used to manage data gathering and presentation and possibly provide control of the experiment. With computers, the time required to present the corrected data in the way needed is usually less than a second after the measurement is taken.

The availability of increased computing power has contributed in other ways to the effectiveness of wind tunnels programs; the process of model design and construction has been affected by the use of computer-design, which provides a way to make designs easily and in a fast way and the possibility of changes in them without losing time in the process. This can shorten the time required to prepare for an experiment or an eventually change of the purpose of the wind tunnel during the phase design.

Wind tunnels, especially low speed wind tunnels, are devices that enable researchers to study the flow over objects of interest, the forces acting on them and their interaction with the flow. Since the first days of aeronautics, these has been used to verify aerodynamic theories and facilitate the design of aircrafts;

nowadays, the use of wind tunnels has expanded to other fields such as automotive, architecture, environment, education, etc., making low speeds especially, more and more important. Although the use of computational fluid dynamics (CFD) has been going up in the last decades, thousands of hours of wind tunnel are still essential for the development of a new design, like an aircraft or a wind turbine, or in the case of this thesis as it was explained in the previous section, the calibration of probes due to the inexactitude of the equations. Consequently, due to the growing interest of other industries and process who can't be simulated in computer due to the incapability of achieving accurate solutions with numerical codes, low speed wind tunnels are essential and irreplaceable during research, design, and other processes.

Using this tool (wind tunnel), it is possible to measure global and local flow velocities, as well as pressure and temperature around the body; as well as optical tests using special insemination substances or wool wires can be performed to visualize flow motion.

A crucial characteristic of wind tunnels is the flow quality inside the test chamber, which knowing it's dimensions depends mainly in the type of testing. Three main criteria are commonly used to define them are: maximum achievable speed, flow uniformity and turbulence level. The purpose for what the wind tunnel is created for is also a very important parameter to define it, therefore, the design aim of a wind tunnel is to get a controlled flow in the test chamber, achieving the performances and quality parameters that were stablished during this phase.

In case of aeronautical wind tunnels, the requirements that are stablished during design are extremely strict, often substantially increasing the cost of the facilities. Low turbulence and high uniformity in the flow are only necessary in some applications, like the one this wind tunnel is being built for, because turbulence can change the lecture of the hot-wire anemometer, leading to an inaccurate calibration of the probe and an insertion of errors in procedures where it will be used. This leads to define the biggest parameter in the design of this wind tunnel which is high flow uniformity and close to inexistent turbulence.

As stated before, the design of a wind tunnel depends mainly in their final purpose. Most wind tunnels can be categorized into two basic groups: open and closed circuit. They can be further divided into open and closed test section, although these must be now considered as the two ends of a spectrum since slotted walls (for boundary layer suction, for example) are now in use.

In an open circuit wind tunnel, the air follows a straight path from the entrance, the convergent to the test section followed by a diffuser, a fan section and an exhaust of the air. In this configuration, the air is being pulled by fan the fan through the test section; the other configuration is when the air is being pushed by the fan to the test section through a settling chamber, to ensure low turbulence and flow uniformity, and the convergent, to ensure the required speed. The first configuration may have a test section with no solid boundaries (open jet of Eiffel type) or solid boundaries (closed jet); the second configuration mainly has an open test section.

The air flowing in a closed wind tunnel recirculates continuously with little or no exchange of air with the exterior. Most of the closed-circuit tunnels have a single return, although tunnels with both double and annular returns have been built. This type can have either an open or closed test section, depending the purpose of it. The main factor when choosing a type of tunnel is the funds available and purpose. As with every engineering design there are advantages and disadvantages with both types of circuits and test-sections.

With the open circuit wind tunnels the main advantages are:

- Construction costs are usually lower.
- The possibility of visualizing the flow using smoke without the need to purge the tunnel.

Opposed to the disadvantages which are:

- When located inside a room, depending on the dimensions of the wind tunnel and the room, it may require an extensive screening at the inlet to get high quality flow. The same goes if the inlet and/or exhaust is open to the atmosphere, where wind and cold weather can affect the operation.
- For a given size and speed the tunnel will require more energy to run. This is only a factor when the tunnel is going to be submitted to a high usage rate.
- This type of tunnel tends to be very noisy which may cause environmental problems.

Because of the low initial cost, this type of tunnel is ideal for schools and universities where it's used for academical purposes and research and high utilization it's not required.

In opposition to this, closed circuit tunnels have this advantages and disadvantages:

Advantages:

- Through the use of screens and corner turning vanes, the quality of the flow can be well controlled, and it will be independent of the environment because of the closure (no exchange of air).
- Less energy is required for a given test-section size and velocity. This is very important for wind tunnels with a high usage ratio.

Disadvantages:

- The initial cost is higher due to the return ducts and corner turning vanes
- If used for flow visualization with smoke, the smoke need to be purged, so there must be a way to do that. The purge is made so the smokes don't interfere with the operation of the fan.
- If the tunnel has high utilization, it may have an air exchanger some method of cooling because the air is constantly in friction with the walls and it's never changed, and this can cause changes in the desired velocity and Reynolds numbers to which it was built for.

After choosing an open or closed-circuit wind tunnel, the decision of what type of test section the wind tunnel will have is the next step. An open test-section with an open circuit tunnel will require an enclosure around the test section to prevent air drawn into the tunnel form the test section rather than the inlet when the fan is downstream; this is not a problem when the fan is upstream.

The most common geometry is a closed test section, but a wide range of tunnel geometries have provided good experimental conditions once the tunnel perks have become known to the operators and users. Slotted wall test sections are becoming more common for experiments where the size of the boundary layer needs to be controlled to a certain dimension.

Design criteria

The design criteria are strongly linked with specifications and requirements that must be in accordance with the wind tunnel applications. The building and operation costs are highly related to the specifications and these are just consequences of the application of the wind tunnel.

As said before, the requirements in research and development in aeronautics, the quality of the flow becomes very important, resulting in more expensive construction and higher operational costs.

The main specifications for a wind tunnel are the dimensions of the test section and the desired maximum operating speed. According with this the flow quality, in terms of uniformity and turbulence level, needs to go in accordance with the applications. At this point the elements of the wind tunnel that will help to get the specifications should be defined.

Flow quality, which is one of the main characteristics and a crucial one in this wind tunnel, is a result of the whole final design, and can only be verified during calibration tests. However, according to previous empirical knowledge, some rules can be followed to select adequate values of the variables that affect the associated quality parameters. In our case, the wind tunnel parts that have the greatest impact on the flow quality are the settling chamber (with screens and honeycombs) and the contraction nozzle.

Definition of the elements of the wind tunnel

In this section we will go through the design of each part that contributes to achieve the flow uniformity and turbulence level for the application this tunnel is meant for; addressing the general and particular requirements. Not only the design but the definition of each part will be treated and in the next section it will be reviewed everything related to the pressure losses for each element, including calculations of all the parameters needed; and the power associated to the flow speed and size of the test section.

Power plant

The main aim of the power plant is to maintain the flow running inside the wind tunnel at a constant speed, compensating for all the losses and the dissipation this means they provide a rise in pressure as the flow passes through the section. In wind tunnels, the power plant is always a fan whether it’s axial, centrifugal, etc.; and can also be multiples fan, in a matrix all at the same distance of the test section or sequential through the stream. The fan, specially the axial ones, introduce swirl in the flow they induce unless some combination of prerotation vanes and straightening vanes are provided.

The power plant needs to be strong enough to maintain the desired maximum speed in the test section accounting the pressure losses produced by the elements in the stream, the increase in pressure provided must be equal to these.

Honey Comb

When a high flow quality is required, this element is installed to increase the flow uniformity and to reduce the turbulence level at the entrance of the contraction nozzle. According to Prandlt [2] “a honey comb is a guiding device through which the individual air filaments are rendered parallel”; This specific element is very efficient at reducing the lateral turbulence, as the flow pass through long and narrow pipes. Nevertheless, it introduces axial turbulence of the size equal to its diameter, which restrains the thickness of the honeycomb.

The next figure shows streamwise views of typical implementations of honeycomb that encompass the majority of honeycomb types in use today.

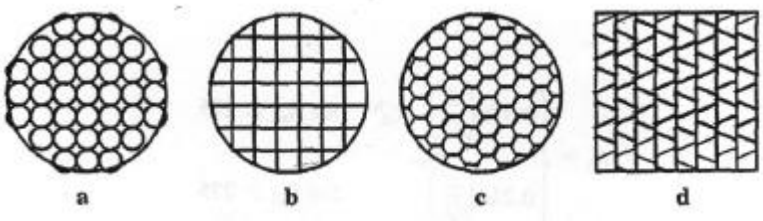

Figure 5 Different types of honeycombs designs (Reprinted from [2])

In the design procedure of a honeycomb, the key factors are its length (L_h), cell hydraulic diameter (D_h) and the porosity (β_h); this las one is defined as the ratio of actual flow cross-section area over the total cross-section area.

$$\beta_h = \frac{A_{flow}}{A_{tot}}$$

Two main criteria must be verified in the design of the honeycomb; these criteria are:

$$6 \leq \frac{L_h}{D_h} \leq 8$$

$$\beta_h \geq 0.8$$

Screens

They do not have significantly influence in the lateral turbulence, but they are very efficient at reducing the longitudinal turbulence. One screen can reduce very drastically the longitudinal turbulence level, however a series of screens, specially 2 or 3, can also attenuate turbulence in the two directions.

To achieve a better flow quality a combination of honeycombs and screens is the most recommended solution, with the honeycomb located upstream of the/or screens. Using only one screen is not recommended due to the fact that to achieve a good quality flow the porosity of the screen will be lower than recommended and it won’t create a uniform flow doing an effect called “overshoot”.

When using two of more screens, the pressure drop generated is the sum of the pressure drops pf each individual screen. Multiple screens must have a finite distance between them so that the turbulence induced by the previous decays to a significant degree before the next screen encountered. Spacing values based on mesh size of greater than 30 as well as spacing based on a wire diameter of about 500 are recommended. As honeycombs, porosity shouldn't be lower than 0.58 and a value in the vicinity of 0.8 is recommended; lower values leads to flow instability and higher values aren't suitable for good turbulence control. So,

$$0.58 \leq \beta_s \leq 0.8$$

Screens should be also installed on a removable frame for cleaning and maintenance, because screens have an amazing ability to accumulate dust. The dust always has a nonuniform distribution, so the screen's porosity and pressure drop will change, which will change the velocity and angularity distribution in the test section over time in an unpredictable way making it a big problem, especially in this wind tunnel design that we need the most uniform flow possible.

Contraction "cone" or nozzle

This takes the flow from the settling chamber to the test section while increasing the average speed. It has the highest impact on the test chamber flow quality further reducing flow turbulence and non-uniformities in this one. The flow acceleration and non-uniformity attenuations mainly depend on the contraction ratio N, between the entrance and exit section areas. This parameter should be as large as possible because it strongly influences the overall wind tunnel dimensions. Therefore, depending on the expected applications, a compromise for this parameter should be reached.

The effect of the contraction is also a reduction in stream-wise turbulence greater than that of the transverse fluctuations, which could also increase through the contraction if this one is long, due to the stretching and spin-up pf elementary longitudinal vortex lines.

When designing a contraction for a wind tunnel who will be used in civil or industrial applications as well as those for educational purposes, contractions ratios between 4 and 6 may be sufficient. With a good design of the shape, the flow turbulence and non-uniformities levels can reach the order of 2.0%, which is acceptable. Adding a screen in the settling chamber will reduce these values to 0.5%.

When dealing with aeronautical applications for research and development, where the flow quality must be better than 0.1% in non-uniformities of the average speed and longitudinal turbulence level, and better than 0.3% in vertical and lateral turbulence level, a contraction ratio between 8 and 9 is more desirable. This ratio also allows installing 2 or 3 screens in the settling chamber to ensure the target flow quality without high pressure losses through them, due to the low speed in the settling chamber because of the more accentuated contraction.

There are two aspects to concentrate when designing a contraction: maintaining a good flow exit uniformity (regarding both exit flow uniformity and exit boundary layer thickness) and avoidance of flow separation. The contraction is designed to, basically, search for the optimum wall shape leading to the minimum nozzle length required for a given purpose. The design usually aims to limit the nozzle length in

order to minimize its size and cost nut also avoiding making it too short which will produce an exit flow with inherent unsteadiness and thick boundary layers.

To achieve these aspects, the shape of the contraction needs to be defined. Considering that the contraction is rather smooth, a one-dimensional approach to the flow analysis would be adequate to determine the pressure gradient along it. Although this is right for the average values, the pressure distribution on the contraction walls has some regions with adverse pressure gradient, which may produce local boundary layer separation. When it happens, the turbulence level increases drastically, resulting in poor flow quality in the test chamber.

Until the advent of the digital computer there was no wholly satisfactory method of designing nozzles. The nozzle was designed either by eye or by adaptations of approximate methods. Experience has shown the radius of curvature should be less at the exit than at the entrance. Most of the early work on nozzles was based on potential theory. Once the wall shape was determined, the regions of adverse pressure gradient were checked to make sure that they were not too sharp.

So, resuming, the problem of contraction design is search for the optimum shape with minimum nozzle length for a desirable flow quality at the nozzle end. When the length is reduced, the contraction cost less and fits into a smaller space. Adding to this, the boundary layer will generally be thinner due to the combined effects of decreased length of boundary layer development and increased favorable pressure gradients in the contraction. However, the possibility of flow separation increases.

The design starts with the selection of a contraction ratio, then the nozzle shape and length are determined to satisfy predetermined design criteria; the flow quality in the test chamber, space available and cost. Considering that we are working in low speed the most direct way of engineering a contraction was suggested by Morel [4] which is based on a pair of cubic polynomials, and the parameter used to optimize the design for a fixed length and contraction ratio, is the location of the joining point (inflection point). Morel's design procedure starts by describing a level of velocity non-uniformity at the contraction exit section, which leads to a corresponding minimum wall pressure near the exit. After the Stratford criterion is applied to check for the possibility of separation, the final choice is the joining point that satisfies the design criteria for flow quality the better possible.

Because the contraction in this wind tunnel is only in the height of this, it's a two-dimensional contraction, so in order to simplify the design of the contraction, instead of using two matched cubic polynomials, we will use a six-order polynomial. The wall curvature at inlet and the location of the point of inflection in the wall profile were chosen as design parameters. This method was developed and tested by a group of engineers in Australia [5] and it's explained here.

First, the coordinate system for the contraction profile is defined with origin on the tunnel centerline at the contraction inlet plane, and x coordinate increasing in the downstream direction. The y coordinates define the contraction profile and z is in the spanwise direction. The six-order polynomial chosen to define the profile shape is:

$$y = ax^6 + bx^5 + cx^4 + dx^3 + ex^2 + fx + g$$

The chosen profile has 7 parameters (a-g). Five of these are specified by the inlet and outlet height, zero slope at the inlet and outlet and zero curvature at outlet. The remaining two parameters are available for optimization. These are specified by the inlet curvature and the axial position of the inflection point relative to the contraction length.

The 7 conditions defining the profile are:

$$y(x = 0) = h$$

$$y'(x = 0) = 0$$

$$y''(x = 0) = \alpha$$

$$y''(x = i) = 0$$

$$y(x = l) = 0$$

$$y'(x = l) = 0$$

$$y''(x = l) = 0$$

Where:

$h = inlet\ half\ height - exit\ half\ height$

$\alpha = inlet\ curvature$

$i = axial\ location\ of\ inflection\ point$

$l = length\ of\ the\ contraction$

The conditions specified directly provide the following constants for the polynomial chosen:

$$g = h$$

$$f = 0$$

$$e = \alpha/2$$

The other constants are defined by the equation:

$$Aw = B$$

Where, for $\alpha = 0$ for the standard case, which will be used (with no inlet curvature):

$$A = \begin{bmatrix} 30i^4 & 20i^3 & 12i^2 & 6i \\ l^6 & l^5 & l^4 & l^3 \\ 6l^5 & 5l^4 & 4l^3 & 3l^2 \\ 30l^4 & 20l^3 & 12l^2 & 6l \end{bmatrix}$$

$$B = \begin{bmatrix} 0 \\ -h \\ 0 \\ 0 \end{bmatrix}$$

$$w = \begin{bmatrix} a \\ b \\ c \\ d \end{bmatrix}$$

The range of the variable i, distance to the point of inflection which gives a sensible, monotonically decreasing curve is 0.4-0.6l; a higher or lower value gives the profile an under shape or it overshoots. This is deemed impractical for a contraction profile.

The chosen value of i in this case was 0.6 because it was proven that when the inflection point was located as far downstream as possible it produces the best result, giving the most uniform velocity profile at inlet to the working section, and preventing separation of the flow within the contraction [5].

Component energy losses

Introduction

In every component of the wind tunnel except the fan it's said that a loss of energy occurs, but it's an energy transformation from mechanical form to heat that results in a raise of the temperature of the flowing gas and the solid in contact. This transformation will be called a "loss".

Considering Bernoulli's equation:

$$P_{static} + \frac{1}{2}\,\rho\, V^2 = P_{total} = constant$$

When it's written between two locations in a duct it only applies if there's no losses between the sections. There are always losses, and one or the other of the two terms at the second section must show a diminution corresponding to the loss. The law of continuity for incompressible flow,

$$A_1 V_1 = A_2 V_2$$

Where A and V are area and velocity at the two stations, constrains the velocity, and hence the dynamic pressure down the flow cannot decrease. But there will be equal drops in static head corresponding to the friction loss. The losses that occur appear as successive pressure drops to be balanced by the pressure rise of the fan.

The loss in a section is defined as the mean loss of total pressure sustained by the stream in passing through the particular section. It's given in dimensionless form by the ratio of the pressure loss ΔH_l in the section to the dynamic pressure at the entrance of the section,

$$K_l = \frac{\Delta H_l}{\frac{1}{2}\,\rho_l V_l^2} = \frac{\Delta H_l}{q_l}$$

The time rate of energy loss in a section can be expressed as the product of the total pressure loss times the volume rate of flow through the section,

$$\Delta E_l = A_l V_l \Delta H_l$$

Where,

$$\Delta H_l = K_l q_l$$

So, it gives,

$$\Delta E_l = A_l V_l K_l q_l$$

And finally,

$$\Delta E_l = K_l \left(\frac{1}{2}\dot{m}_l\, V_l^2\right)$$

Shows that the loss coefficient defined based on total pressure loss and dynamic pressure is also the ratio of the rate of energy loss to the rate of flow of kinetic energy to the section.

This is the local loss coefficient and they must be referred to the test-section dynamic pressure, defining the coefficient of loss of the local section referred to the test-section dynamic pressure as,

$$K_{lt} = \frac{\Delta H_l}{q_l}\frac{q_l}{q_t} = \frac{K_l q_l}{q_l}\frac{q_l}{q_t}$$

So,

$$K_{lt} = K_l \frac{q_l}{q_t}$$

Knowing that $q = \frac{1}{2}\rho V^2$ and using the law of continuity, the loss coefficient can be expressed as,

$$K_{lt} = K_l \left(\frac{A_t}{A_l}\right)^2$$

And using the nomenclature for this actual wind tunnel the equation is,

$$K_{lt} = K_l \left(\frac{A_{ts}}{A_{sc}}\right)^2$$

Using the definition of power and using the equations stated above, the total rate of loss in the circuit is obtained by summing the rate of section losses for each of the individual sections,

$$P_c = \sum_l K_{lt}\, P_t$$

Where P_t is the power needed to maintain a certain speed in the test section and P_c is the net power that the tunnel drive device must deliver to maintain steady conditions and K_{lt} are the loss coefficients referred to the test section.

In this wind tunnel we will use screens and honeycombs, so we will calculate the loss coefficient for these items. The losses of the convergent as well as the one for the skin will not be considered because both are caused by friction of the air with the skin and this is a short tunnel, so they don't bring a significant loss of pressure and they can be negligible

Screens

The basic design parameters to characterize a screen are: the "porosity" β_s and the wire Reynolds number, based on the wire's diameter, $R_{ew} \equiv {\rho V d_w}/{\mu}$. A third parameter, the "mesh factor" K_{mesh} is used to differentiate among smooth and rough wire.

The Reynolds number and the mesh factor comes determined by the mesh that will be used for the screen, while the porosity needs to be calculated with the wire diameter and the weave density; it also depends on geometric factors, in this case, we will use a square one, so we calculate the weave density as:

$$\rho = {}^{1}/_{w_m}$$

With w_m the width of one square cell. With the weave density calculated now we can calculate the porosity,

$$\beta_s = (1 - d_w \rho_m)^2$$

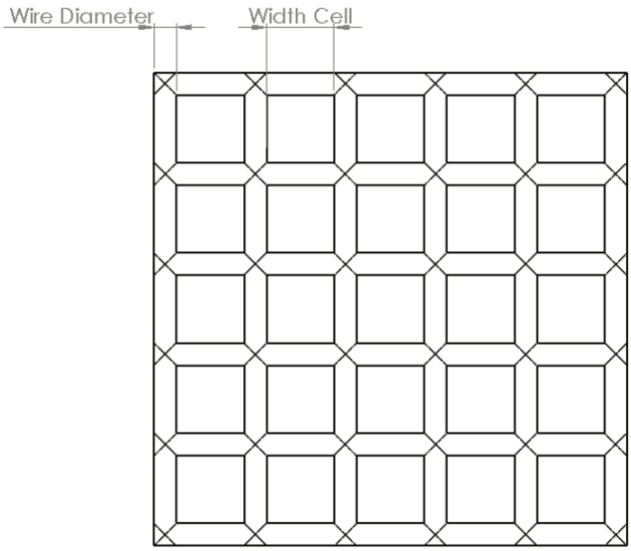

Figure 6 Mesh example

The compliment of the porosity is the screen solidity, which is the ratio between the cross-section area occupied by the metal sheet and the total cross-section area,

$$\sigma_s = 1 - \beta_s$$

Mesh factors are given by Idel'chik [6] and these are: 1.0 for new metal wire, 1.3 for average circular metal wire and 2.1 for silk thread.

Once these parameters are calculated, we can determine the coefficient loss by the next expression,

$$K_m = K_{mesh} K_{Rn} \sigma_s + \left(\frac{\sigma_s}{\beta_s}\right)^2$$

Where K_{Rn} is: for $0 \leq R_{ew} < 400$

$$K_{Rn} = \left[0.785 \left(1 - \frac{R_{ew}}{354}\right) + 1.01\right]$$

And, for $R_{ew} > 400$,

$$K_{Rn} = 1.0$$

Honeycombs

As stated in the previous section, the design parameters are: length (L_h), cell hydraulic diameter (D_h) and the porosity (β_h).

The length usually comes determined by the fabricant of the honeycomb mesh; but if it's possible to choose it, the length needs to be long enough to rendered parallel the flow, eliminating the transverse turbulence but not long enough to generate a boundary layer capable of disrupting the flow (turbulent) and introducing new turbulence.

The porosity of the honeycomb mesh is calculated the same way as the screen with the difference that now the wire diameter is replaced with the thickness of the cell (s_{honey}) and the width of the mesh with the cell size (d_{honey}); knowing that the density is $\rho = {}^{1}/_{d_{honey}}$, introducing it into the equation for the porosity, this one now is,

$$\beta_s = \left(1 - {}^{s_{honey}}/_{d_{honey}}\right)^2$$

The hydraulic diameter is a term used when handling flow in non-circular tubes and channels; with this term, one can calculate many things in the same way as for a round tube as for example, the Reynolds number. This can be calculated with the generic equation:

$$D_h = \frac{4A}{P}$$

Where:

$$A = cross - section\ area\ of\ the\ flow$$

$$P = wetted\ perimeter\ of\ the\ cross - section$$

In our case, being the shape a regular hexagon, because we are talking about a honeycomb, we can calculate the perimeter and area with the equations for this shape; being a regular hexagon, all the angles are 120°. And the center angle, which is the angle formed between the center of the hexagon and two lines that join this one with two consecutive vertex is,

$$\alpha = \frac{360°}{N} = \frac{360°}{6} = 60°$$

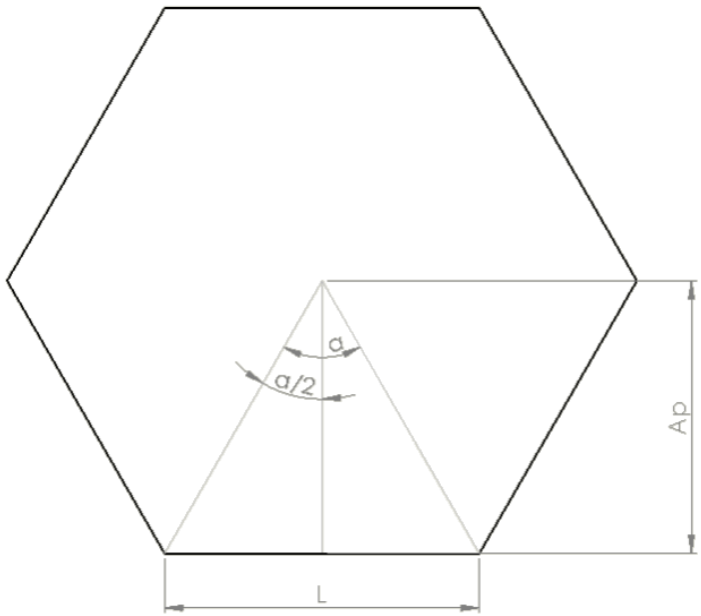

Figure 7 Hexagon example

In this case, we have the cell size, which is two times the apothem, and the tangent of the half of the center angle, we can calculate the length of the side of the honeycomb.

$$ap = \frac{d_{honey}}{2}$$

$$ap = \frac{d_{honey}}{2} = \frac{l_{honey}}{2\ \tan(\frac{\alpha}{2})} =>$$

$$l_{honey} = d_{honey}\ \tan(\frac{\alpha}{2}) = d_{honey}\ \tan(30°)$$

Once we know the length of the side of the hexagon we can calculate both the perimeter and the area of the hexagon. The perimeter is the sum of the length of the six sides of the hexagon; in this case is a regular one so the perimeter is,

$$perimeter_{honey} = 6 * l_{honey}$$

The area is calculated as half the product between the perimeter and the apothem. Because the perimeter is six times the length of the side, the area is,

$$Area_{honey} = 3 * l_{honey} * Ap$$

$$Area_{honey} = 3 * l_{honey} * \frac{l_{honey}}{2\ \tan\left(\frac{\alpha}{2}\right)}$$

$$Area_{honey} = 3 * \frac{{l_{honey}}^2}{2\ \tan\left(\frac{\alpha}{2}\right)}$$

Calculated the area and perimeter of the hexagon we can calculate its hydraulic diameter; once we have this and the other two parameters, we can calculate the Reynolds number through the cell size and then the losses through the honeycomb. The expression for this is,

$$K_h = \lambda_h \left(\frac{L_h}{D_h} + 3\right)\left(\frac{1}{\beta_h}\right)^2 + \left(\frac{1}{\beta_h} - 1\right)^2$$

Where

$$\lambda_h = \begin{cases} 0.375 \left(\frac{S_{honey}}{D_h}\right)^{0.4} R_{e\Delta}^{-0.1} & for\ R_{e\Delta} \leq 275 \\ 0.214 \left(\frac{S_{honey}}{D_h}\right)^{0.4} & for\ R_{e\Delta} > 275 \end{cases}$$

The parameters in these expressions are hydraulic diameter of a honeycomb cell, D_h; Reynolds number based on honeycomb material roughness and incoming flow speed, $R_{e\Delta}$; honeycomb porosity, β_h; and honeycomb thickness in flow direction, L_h.

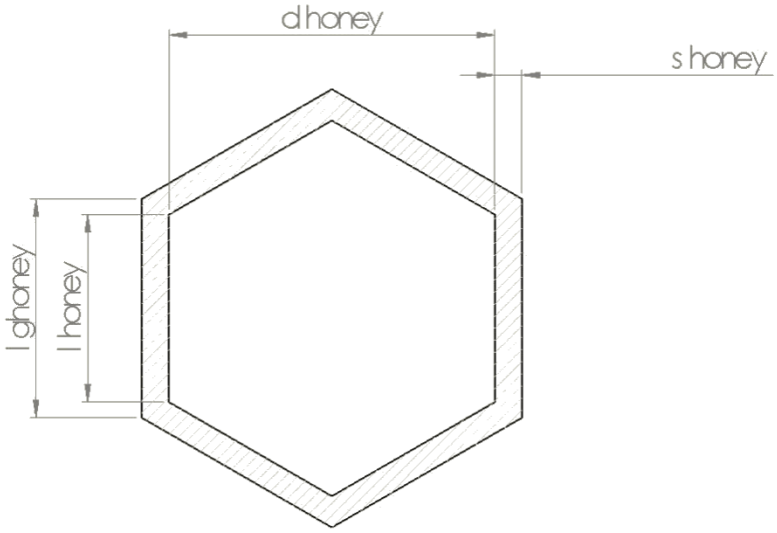

Figure 8 Example of a honeycomb cell

Jet power

Even though this component doesn't present energy losses, it's the one that provides the energy to the wind tunnel, that's why it is introduce in this section. This is the component that will provide the pressure to maintain the speed in the test section and also the pressure rises to equilibrate the drops the previous components will introduce.

The parameters that specify this are the pressure increment (ΔP), the volumetric flow (Q), the desired cross-section surface in the test section ($A_{test-section}$) and the velocity ($V_{test-section}$) in it. Once we have these values by design we can calculate the power needed to maintain the speed in the test-section.

$$P = \Delta P * Q$$

Where,

$$Q = V_{test-section} * A_{test-section}$$

$$\Delta P = \frac{1}{2} \rho V_{test-section}^2$$

So, the equation for power remains:

$$P = \frac{1}{2} \rho A_{test-section} V_{test-section}^3$$

This equation will tell the power needed in the fan to maintain the desired speed in the test section; in our case, the maximum speed desired given that this wind tunnel will have variable speed for the calibration of the probes, this will be shown in a graphic of pressure at a certain speed versus the flow rate at that speed in the next section.

Calculation of the coefficient losses.

In this section the calculation of the coefficient losses will be performed with the methods illustrated in the previous section. As stated in the introduction, our wind tunnel is going to have in the test-section a width of $500\ mm$ and $10\ mm$ tall. The settling chamber where all the components that uniform the flow are will have a length of approximately $70\ cm$ and the cross-section is going to have $50\ mm$ tall and a width of $500\ mm$. It will be powered by a centrifugal fan and the connection between these and the settling chamber is yet to be discussed.

Power in the test section

First its calculated the amount of power needed to maintain the maximum speed achievable in the test section. This power will be the base to calculate the actual amount of power the fan will need to supply.

The maximum speed is $75\ m/s$ and the test section is,

$$A_{test-section} = Height_{test-section} * Width_{test-section}$$

$$A_{test-section} = 10\ mm * 500\ mm$$

$$A_{test-section} = 5000\ mm^2 = 0.005\ m^2$$

The density in the hangar laboratory, the same as the Forli airport (30 meters over sea level) where is located is, according to the standard atmosphere (ISA),

$$\rho = 1.22159\ \frac{Kg}{m^3}$$

So, the power needed is,

$$P = \frac{1}{2} * 1.22159 \frac{Kg}{m^3} * 0.005\ m^2 * (75 \frac{m}{s})^3$$

$$P = 1288.4\ [W]$$

This would be the power if the losses in the screen and honeycomb didn't exist.

Velocity in the section of the settling chamber

The elements that uniform the flow are introduce in the settling chamber, the speed of the flow where they will work isn't the same as in the test section, so it's necessary to calculate it. To do this, the equation of continuity is used.

$$A_{sc}V_{sc} = A_{ts}V_{ts}$$

Where,

$$A_{sc} = Area\ of\ settling\ chamber$$

$$V_{st} = Velocity\ in\ settling\ chamber$$

$$A_{ts} = Area\ of\ test\ section$$

$$V_{ts} = Velocity\ of\ test\ section$$

Both areas are defined by the design of the wind tunnel and the velocity in the test section is set to maximum needed. With these values is simple to find the velocity in the settling chamber.

$$A_{ts} = 10\ mm * 500\ mm = 0.005\ m^2$$

$$A_{sc} = 50\ mm * 500\ mm = 0.025\ m^2$$

$$V_{sc} = V_{ts}\left(\frac{A_{ts}}{A_{sc}}\right)$$

$$V_{sc} = 75\ {}^{m}/_{s}\left(\frac{0.005\ m^2}{0.025\ m^2}\right)$$

$$V_{sc} = 75\ {}^{m}/_{s}\ (0.2)$$

$$V_{sc} = 15\ {}^{m}/_{s}$$

This is speed that will be used to calculate all the coefficient losses of the different elements. The lower speed will allow us to minimize the losses the elements produce, and it won't introduce high pressure drops.

Screen losses

We will use three screens, who continuously gets smaller, for the reasons stated in the previous section and also because by researches made in other wind tunnels it's clear that is used between three and five screens, so for costs and practicality when building the wind tunnel, we will use three. It's also a compromise between flow uniformity and power needed to move the fan, consequently adding to the reasons why three screens are used.

The three screens are shown in the next table,

Screen	Width Mesh [mm]	Wire Diameter [mm]
1st	3.2	0.71
2nd	2.4	0.56
3rd	0.7	0.16

Table 1 Specifications of screens used

With this data we can calculate the porosity of each screen to check if they are in the parameters of the porosity ($0.58 \leq \beta_s \leq 0.8$) resulting in,

Screen	Porosity
1st	0.6055
2nd	0.5878
3rd	0.5951

Table 2 Porosity for each screen

As is shown the porosity values for each of the screens are inside the parameters, meaning that these screens can be used, and they will fulfill their purpose of uniform the flow. With this parameter calculated and the equation stated in the previous section, we calculate the Reynolds number ($R_{ew} \equiv {\rho V d_w}/{\mu}$), with this the factor $K_{rn}$and then the loss coefficient with $\rho = 1.22159$ and $\mu = 1.81 * 10^{-5}$.

This process is shown in the next two tables,

Screen	Diameter Wire [mm]	Reynolds Number	K_{rn}
1st	0.71	718.78	1
2nd	0.56	566.92	1
3rd	0.16	161.97	1.4358

Table 3 Values for calculation of coefficient loss

Then,

Screen	Loss coefficient
1st	0.8191
2nd	0.9041
3rd	1.0443

Table 4 Coefficient loss for each screen

These coefficients are not referred to the test-section, step that is performed after we get all the coefficient losses for all the parameters.

Honeycomb Losses

The honeycomb used will be placed before the screens and the one used has these dimensions given by the manufacturer,

Length of the Honeycomb (L_{honey})	50 mm
Thickness of the cell (s_{honey})	0.1 mm
Size of the cell (d_{honey})	6.35 mm

Table 5 Specifications for the honeycomb used

First, it's calculated the porosity of the honeycomb with the formula stated in the previous section,

$$\beta_s = \left(1 - {s_{honey}}/{d_{honey}}\right)^2$$

$$\beta_s = \left(1 - {0.1\ mm}/{6.35\ mm}\right)^2 = 0.9688$$

With the previous data of the hexagon cell that compose the honeycomb shown in the table, we can calculate the length of the side of the cell and with that the area and perimeter to calculate the hydraulic diameter,

$$d_{honey} = Size\ of\ the\ cell = 6.35\ mm$$

$$l_{honey} = d_{honey} \tan(30°) = 6.35\ mm * 0.5774$$

$$l_{honey} = 3.7\ mm = 0.0037\ m$$

With this value we can calculate both the perimeter and area,

$$perimeter_{honey} = 6 * l_{honey} = 6 * 0.0037\ m = 0.0220$$

$$Area_{honey} = 3 * \frac{{l_{honey}}^2}{2 \tan\left(\frac{\alpha}{2}\right)} = 3 * \frac{(0.0037\ m)^2}{2 \tan\left(\frac{30°}{2}\right)} = 0.0000349250\ m^2$$

Now the hydraulic diameter is calculated,

$$D_h = \frac{4 * 0.000034925\ m^2}{0.0220\ m} = 0.0064\ m$$

Now the Reynolds number($R_{ew} \equiv {\rho V d_{honey}}/{\mu}$) is calculated and with that the coefficient landa,

Reynolds Number	λ
6428,5	0.0407

Table 6 Reynolds number and landa coefficient

With all the values, the coefficient loss is calculated,

$$K_{honeycomb} = 0.4723$$

This coefficient is not referred to the test section, procedure that is shown in the next part.

Coefficient losses referred to test section

Once the coefficient losses are calculated, these needs to be referred to the test section to obtain the actual factor that will yield the pressure drops we will have to overcome with the fan. The equation was obtained and explained in previous section and it's,

$$K_{lt} = K_l \left(\frac{A_{ts}}{A_{sc}}\right)^2$$

$$K_{lt} = K_l \left(\frac{0.005\ m^2}{0.025\ m^2}\right)^2$$

$$K_{lt} = K_l (0.2)^2$$

$$K_{lt} = K_l * 0.04$$

With this factor the coefficient losses of each component referred to the test-section are calculated,

Element	Local coefficient loss	Test-section coefficient loss
1st screen	0.8191	0.0328
2nd screen	0.9041	0.0362
3rd screen	1.0443	0.0418
Honeycomb	0.4723	0.0189

Table 7 loss coefficient for each component (local and test section)

Power Needed

With the loss coefficients calculated it's possible to calculate the power needed in the fan to maintain the speed ($75\ ^{m}/_{S}$) in the test section. To account for the power that needs to arrive in the test-section the loss coefficient of the test-section its equal to 1. This is because all the pressure rise built by the fan is used here in the test-section to maintain this speed. Taking this into account the power needed (P_c) is,

$$P_c = \sum_{l} K_{lt}\, P_t$$

$$P_c = (1 + 0.0328 + 0.0362 + 0.0418 + 0.0189) * 1288.4\ [W]$$

$$P_c = \ 1455.4\ [W]$$

This is the power the fan will need to have to supply the pressure rise to maintain the desired speed in the test-section, accounting for all the losses.

The power factor is the sum of all the coefficient losses and in this case is,

$$P_{factor} = 1 + 0.0328 + 0.0362 + 0.0418 + 0.0189 = 1.1296$$

The energy ratio is the ratio of power in the test-section flow to the rate of losses around the circuit. This is a measure of the energy efficiency of the wind tunnel, it can be expressed in many ways; mechanical, as the ratio between the power of the motor and the power in the shaft of the fan, and many mores. In this case, we will focus as stated in the definition of the energy ratio in the aerodynamic aspect of it. According to this, the energy ratio is,

$$E_R = \frac{P_t}{P_c}$$

$$E_R = \frac{1288.4\ [W]}{1455.4\ [W]} = \ 0{,}89$$

This can be interpreted that we need more power to drive the entire tunnel than we need power in the test section, so this type of wind tunnel is inefficient, that's why there are no big tunnels with this configuration. Although this inefficiency this type of tunnel is the best one for the application is being used here and the amount of power needed is not significantly bigger, so we can make this compromise and spend more in energy to achieve the flow we need for the application and the uniformity that it carries.

Map of fan usage

The number obtained before is the maximum amount of power the power plant will use during its operation, it's an important value to start deciding which fan, especially which motor, will move the air in the wind tunnel to create the flow. The motor must be able to provide at least this amount of power or more to be in the safe zone. Higher power motors are better in case the design of the tunnel is changed, and we need more power to maintain the same flow. This can be caused by a change in the elements that uniform the flow or adding more of these.

The fan that the motor will power translate that power into the pressure rise needed to maintain the flow and the flow rate at speed in the test section. This tunnel varies the speed, so it will be a curve that determines where the fan will work. This curve is helpful in choosing the appropriate fan for the application. It shows the pressure needed at a certain speed and the flow rate it needs to maintain. The expressions for these parameters are,

$$\Delta P = \frac{1}{2}\,\rho\, {V_{ts}}^2 P_{factor}$$

$$\dot{m} = A_{ts} V_{ts}$$

Where

$$\Delta P = pressure\ rise\ at\ certain\ speed\ [PA]$$

$$\dot{m} = flow\ rate\ at\ certain\ speed\ \left[{}^{m^3}/_{s}\right]$$

The tunnel works in the range of 0 m/s to 75 m/s, and with the equations for the parameters and the values, a graph can be made which will tell us the range of the usage of the fan and simplifies the search for it.

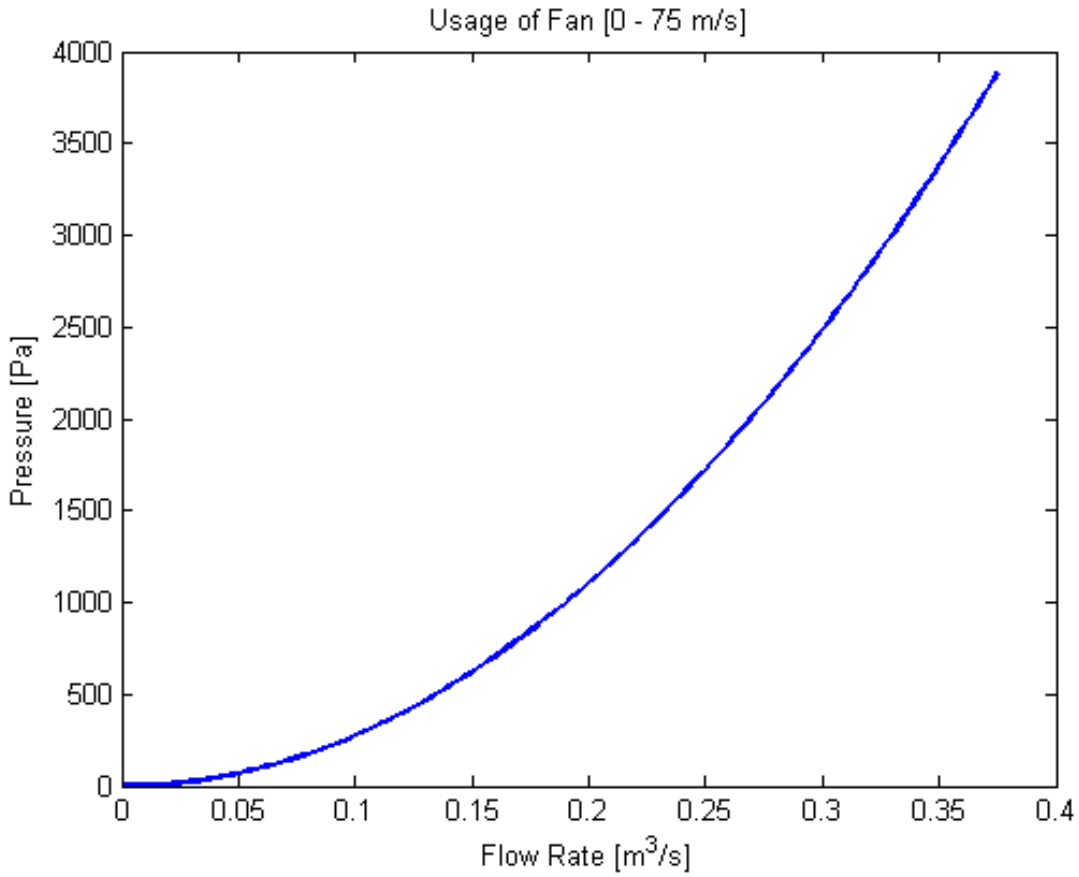

Figure 9 Curve of usage of the fan

The graph shows that we need a fan capable of achieving high pressures at low flow rates, so the fan of choice needs to be centrifugal type who can achieve the type of curve we need.

After the calculation and design of all the components, a model of the wind tunnel is going to be presented and with that a choice for the fan.

Convergent

This is one of the most critical parts in the wind tunnel and one of the most difficult to design. This part is key in the shape of the distribution of the flow in the test section; a sharp contraction will create a non-uniform distribution of the parallel speed in the test-section and a long contraction with a small angle will help in the enlarging of the boundary layer and disturbing the flow uniformity, making it not suitable for this application.

To this application due to the low longitude of the wind tunnel and the contraction ratio being small, a straight contraction at a determined angle can be suitable for it. It needs to be proved that it won't create a non-uniform distribution of the speed and also won't create a separation of flow due to the adverse pressure that the contraction can generate.

A straight contraction can or can't satisfied the flow uniformity needed for the wind tunnel, because of this, the design theory for the convergent is used and tested as well as two straight contractions; one with an angle of 25° and one of 40°. For this tunnel a contraction in the height of the section will be used, resulting in a one-dimension contraction of the section, not in the width only in the height.

In this section, the straight convergent will be called contractions and the convergent made by the convergent design theory will be called convergent.

Designs of the convergent

Contractions

As stated in the introduction the three contractions used are 25 Degrees, 40 Degrees and a convergent design; now will be introduced both straight contractions and then the convergent will be designed. Now these are shown, and all dimensions are in [mm]. First the 25 Degrees contraction which is a lower angle and can be give really good results.

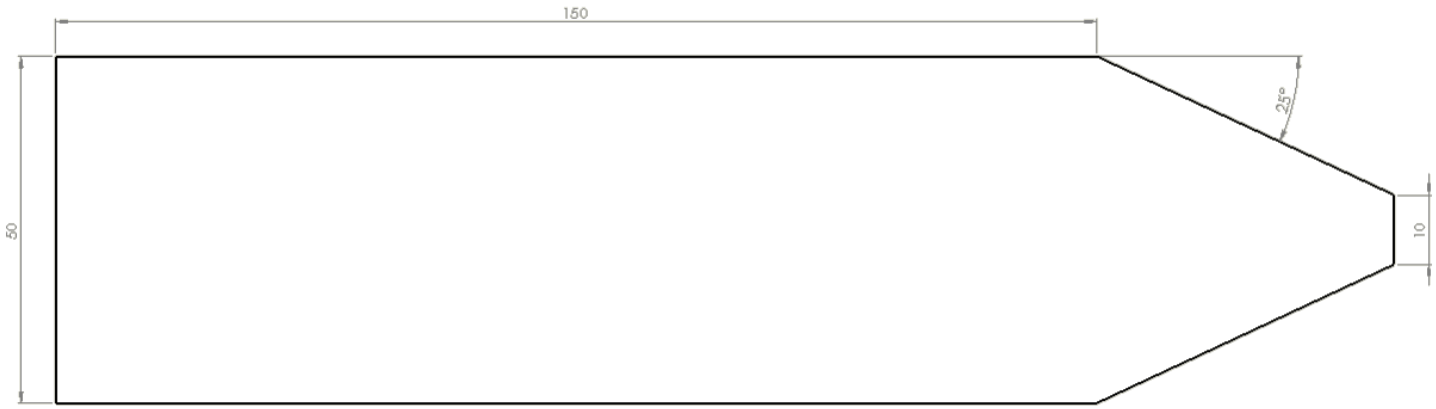

Figure 10 25 Degrees contraction model

The first part is the settling chamber after the last screen, which is this long to allow the flow to stabilize before entering the contraction to get accelerated. This is a 2D model showing the transversal section of the wind tunnel. Now the 40 Degrees contraction is shown.

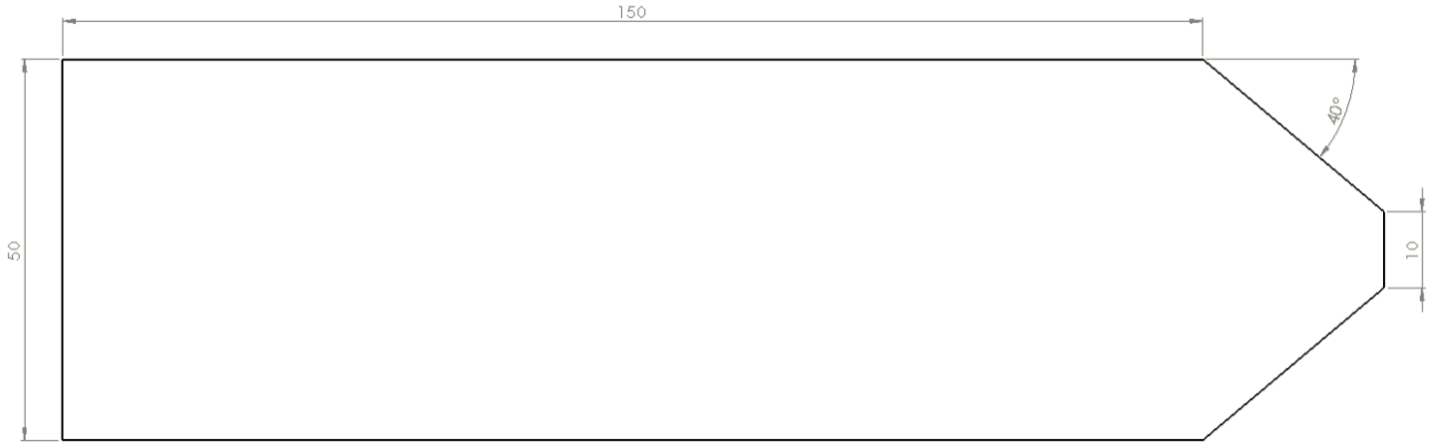

Figure 11 40 Degrees Contraction model

As before this is the 2D model showing the transversal section of the wind tunnel with the last part of the settling chamber. In this both designs the test section is at the end of the contraction, this could cause problems with the stability and uniformity of the flow so two alternate designs are presented with an extension of the contraction in a constant section with the dimensions of the test section to help stabilize the flow; this will also be tested. The addition of this extension is based in the convergent design theory that states that the end of the convergent should be a constant section to allow the flow to stabilize after the contraction and stabilize. The length of this extension it's initially 10 [mm] but it can change according to the results of the simulations. Both are presented now.

Figure 12 25 Degrees contraction with extension model

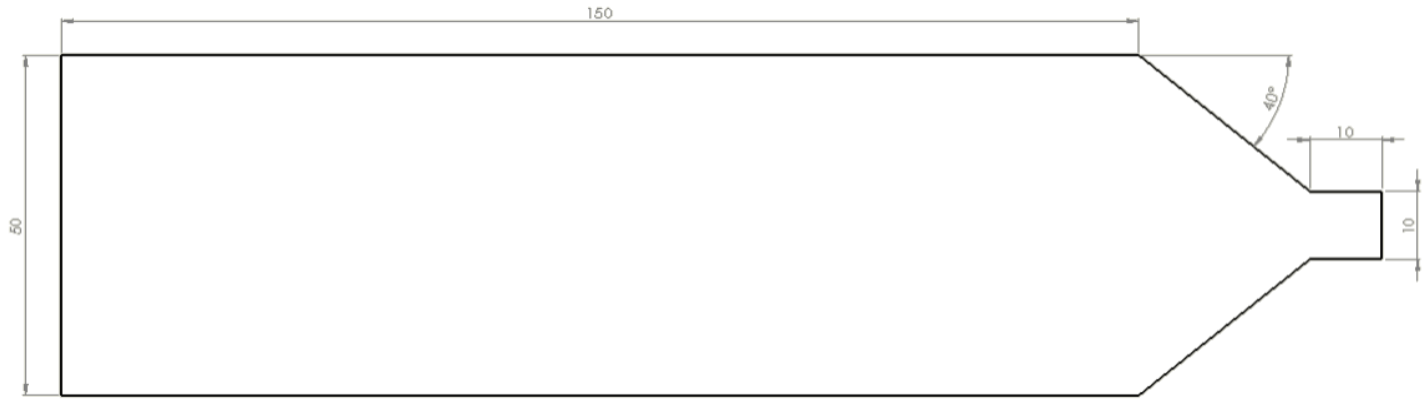

Figure 13 40 Degrees contraction with extension model

Convergent

The other option is the convergent designed by the theory presented in the previous section. To design it some parameters are needed like the length it will have, the axial location of the inflection point, the inlet curvature and the height at the inlet and outlet of the contraction.

The heights are determined by the height of the settling chamber and the test-section which have been determined beforehand. The inlet curvature is 0 Degrees, so the flow can enter smoothly to the convergent; The axial location of the inflection point (in percentage since the length haven't been selected) was determined when the process was explained, and its value is 60%. The length of the contraction is the same as a straight contraction with an angle of 12 Degrees because this give a reasonable length and a good behavior of the fluid. This value of angle is extracted from the Ahmed book [7].

To calculate the length, we need the angle (12 Degrees) and the height of the difference between the settling chamber and the test section and apply trigonometry.

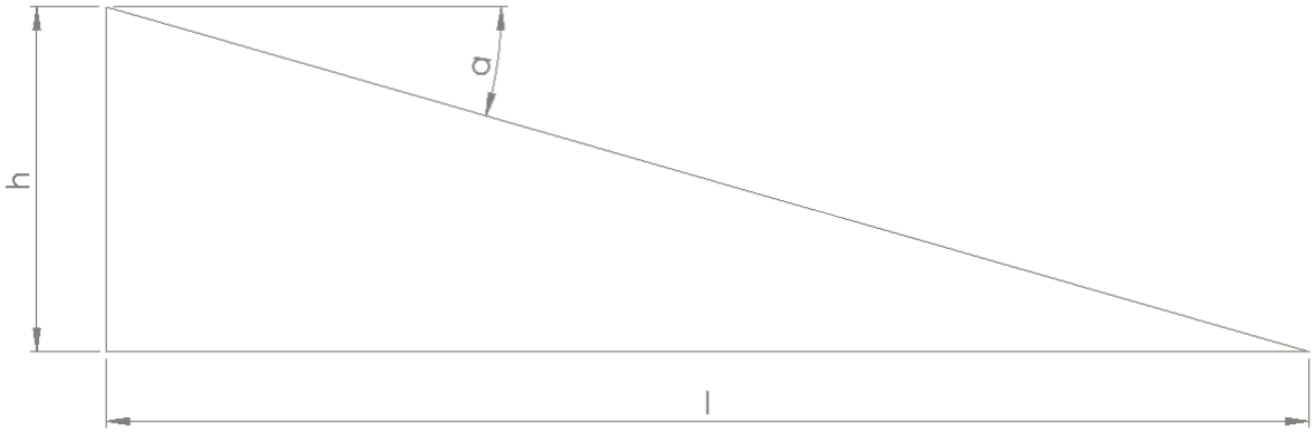

Figure 14 Example to calculate length of contraction

Where,

$$h = inlet\ half\ heigth - outlet\ half\ height$$

$$h = 25 - 5 = 20\ [mm]$$

$$a = \ angle = 12\ [Degrees]$$

With these values it's possible to calculate the length of the contraction,

$$\tan a = \frac{h}{l}$$

$$l = \frac{h}{\tan a} = \frac{20}{\tan 12}$$

$$l = 94.09\ \approx 94\ [mm]$$

All the parameters values are:

$$h = inlet\ half\ height - exit\ half\ height = \ 25 - 5 = 20\ [mm]$$

$$\alpha = inlet\ curvature = 0\ [Degrees]$$

$$i = axial\ location\ of\ inflection\ point = 60\%l = 0.6 * 94 = 56.4\ [mm]$$

$$l = length\ of\ the\ contraction = 94\ [mm]$$

Having all these values, the seven parameters for the polynomial equation can be calculated. Three of them are defined by these parameters and the others are calculated. The three defined are,

$$g = h = 20$$

$$f = 0$$

$$e = {}^{\alpha}/_{2} = \ {}^{0}/_{2} = 0$$

Both matrixes are defined, and the equation is solved,

$$A = \begin{bmatrix} 30i^4 & 20i^3 & 12i^2 & 6i \\ l^6 & l^5 & l^4 & l^3 \\ 6l^5 & 5l^4 & 4l^3 & 3l^2 \\ 30l^4 & 20l^3 & 12l^2 & 6l \end{bmatrix} = \begin{bmatrix} 303555195.6 & 3588122.88 & 38171.52 & 338.4 \\ 6.8987e11 & 7339040224 & 78074896 & 830584 \\ 44034241344 & 390374480 & 3322336 & 26508 \\ 2342246880 & 16611680 & 106032 & 564 \end{bmatrix}$$

$$B = \begin{bmatrix} 0 \\ -h \\ 0 \\ 0 \end{bmatrix} = \begin{bmatrix} 0 \\ -20 \\ 0 \\ 0 \end{bmatrix}$$

And,

$$w = \begin{bmatrix} a \\ b \\ c \\ d \end{bmatrix}$$

The equation is,

$$Aw = B$$

$$A^{-1}Aw = A^{-1}B$$

$$w = A^{-1}B$$

Solved the equation the resulting vector with the four parameters is,

$$w = \begin{bmatrix} a \\ b \\ c \\ d \end{bmatrix} = \begin{bmatrix} -2.8991e-10 \\ 6.54036e-8 \\ -3.84246e-6 \\ -4.00488e-18 \end{bmatrix}$$

The polynomial that give the shape of the convergent is:

$$y = ax^6 + bx^5 + cx^4 + dx^3 + ex^2 + fx + g$$

$$y = -2.8991e-10 * x^6 + 6.54036e-8 * x^5 - 3.84246e-6x^4 - 4.00488e-18 * x^3 + 20$$

And the shape plotted is,

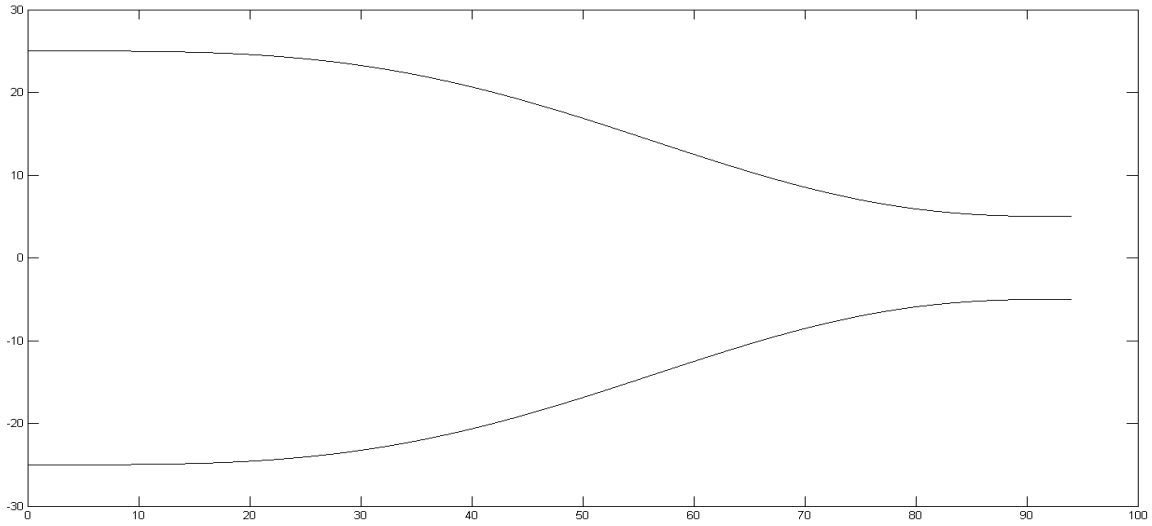

Figure 15 Shape of the convergent

Resulting the 2D transverse section of the wind tunnel with the last part of the settling chamber,

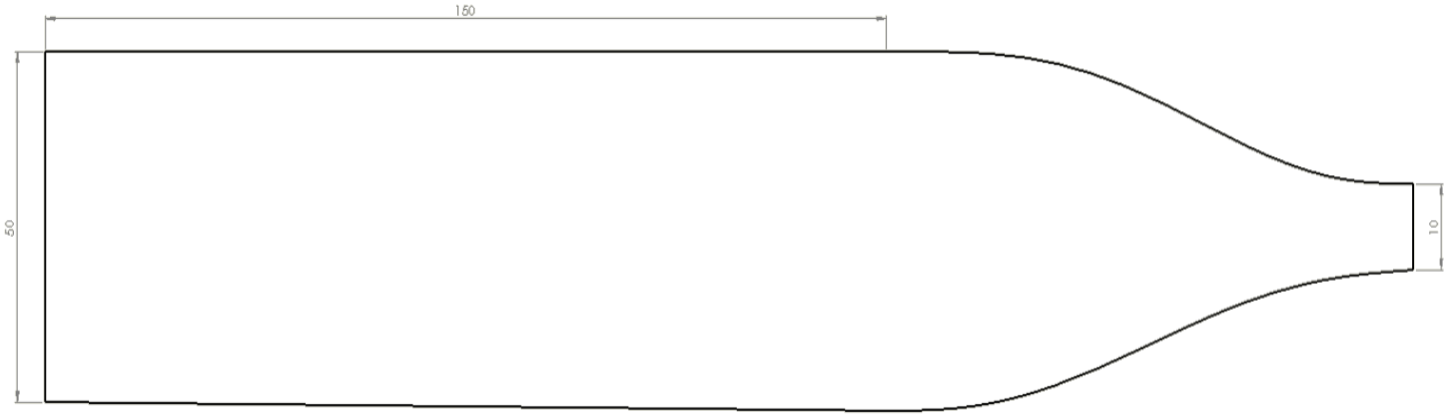

Figure 16 Convergent model

These are the options for the convergent in the wind tunnel; these are going to be tested in CFD to find the most suitable and best option for this wind tunnel and application.

Simulations

Introduction

To find the most suitable option for the wind tunnel, an analysis of all the options must be made to choose the fittest one. Back, when there were no computers, all the options would have been built and then tested to find the best. Nowadays with the technology, specially computers, this analysis can be made in them saving money and reducing the costs of the design. To perform these analyses the program ANSYS is used, specifically its module FLUENT which is the one for flow simulations.

ANSYS is a general-purpose software, used to simulate interactions of all disciplines of physics, structural, vibration, fluid dynamics and more for engineers. It enables to simulate tests of working conditions, this case, in a virtual environment before manufacturing prototypes or products. It also allows for determing and improving weak points, foreseeing probable problems and computing situations.

It can import CAD and has its own “preprocessing” abilities; which allows to compile the cad, and in our case that the module FLUENT, which uses finite volume models, is used, it can generate the mesh required for computation. After defining the conditions for the simulation and being carried out, results can be viewed as numerical and graphical. It also can carry out advanced engineering analyses quickly, safely and practically, making it the proper tool for this application.

The FLUENT module is used in a 2D model to verify the uniformity of the distribution of the velocity in the test-section and to verify that the pressure along the wall of the settling chamber and the contraction gradually decrease and there’s no sudden rise that could indicate separation of the flow and the creation of vortex that disturb the flow. The model used for the simulation is an inviscid laminar.

The reason a 2D model is used, is due to the small dimensions of the settling chamber and test-section, who allow to simplify the model into a 2D, ensuring that the results obtained will be applicable in the reality. The laminar model is used also to simplify the calculations and relying that the elements used to uniform the flow in the settling chamber are working properly and at the end of this one, a practically laminar stationary flow is obtained, that will remain this way during the operation of the wind tunnel; also, the flow in a laminar mode carries less energy than a turbulent one so if there’s no separation in the wall it’s really difficult that this will happen in a turbulent flow.

The five options designed for the convergent will be tested; the pressure along the wall and the distribution of velocity in the test-section will be obtained to define which option in the best. The simulations will be performed at low speed ($0.2\ m/s$ at settling chamber) and a normal/high speed ($10\ m/s$ at settling chamber) to ensure the proper functioning in the entire range of speeds the wind tunnel will work. Because the version used is the student version, the program its limited to 512.000 elements in the messing, the models will be optimized to the maximum within this limit concentrating the elements in the walls of the model and in the test-section represented by the outlet of the convergent in each model to ensure the best results possible.

All the results will be presented and a comparation between the options will be performed to find the solution who yields the best performance for this application. Both the contractions with the extension

will present the distribution of velocity in the test-section at various points starting with the end of the contraction so in this way it's possible to control if the length of the extension is the correct or needs to be larger or shorter if it's selected.

Results

In this section, for each model, graphs representing the pressure along the wall and the velocity distribution in the test section will be presented and then an analysis will be performed to decide in the best option.

25 Degrees Contraction

For $0.2\ m/s$:

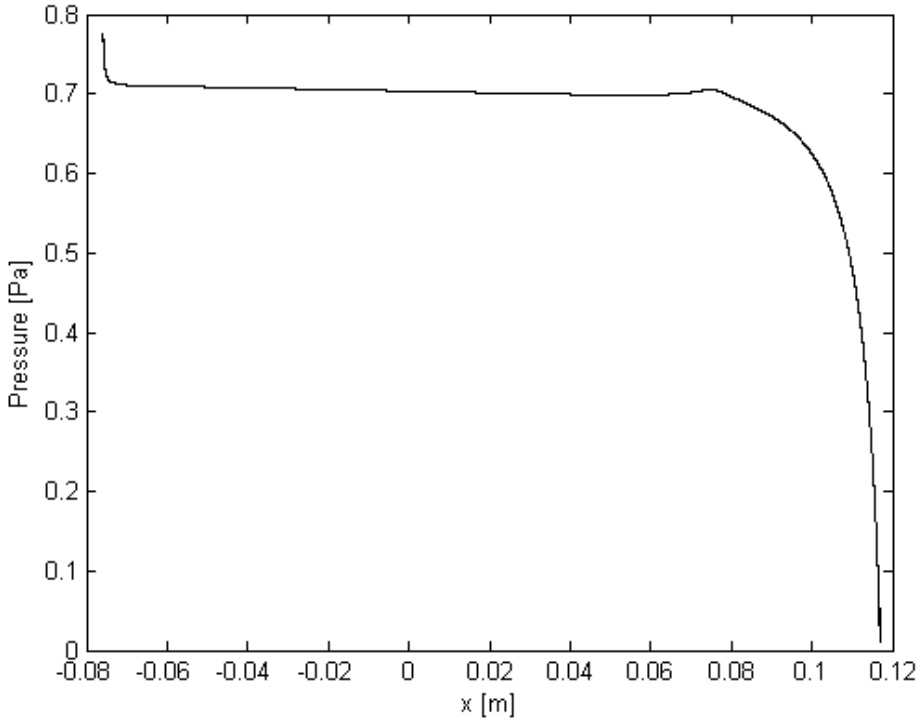

Figure 17 Graph of pressure for 0.2 m/s for the 25 Degrees contraction with the pressure in the y axis in [PA] and the position in the contraction in [m] along the x-axis for the wall (values of position given by ANSYS due to the positioning of the model).

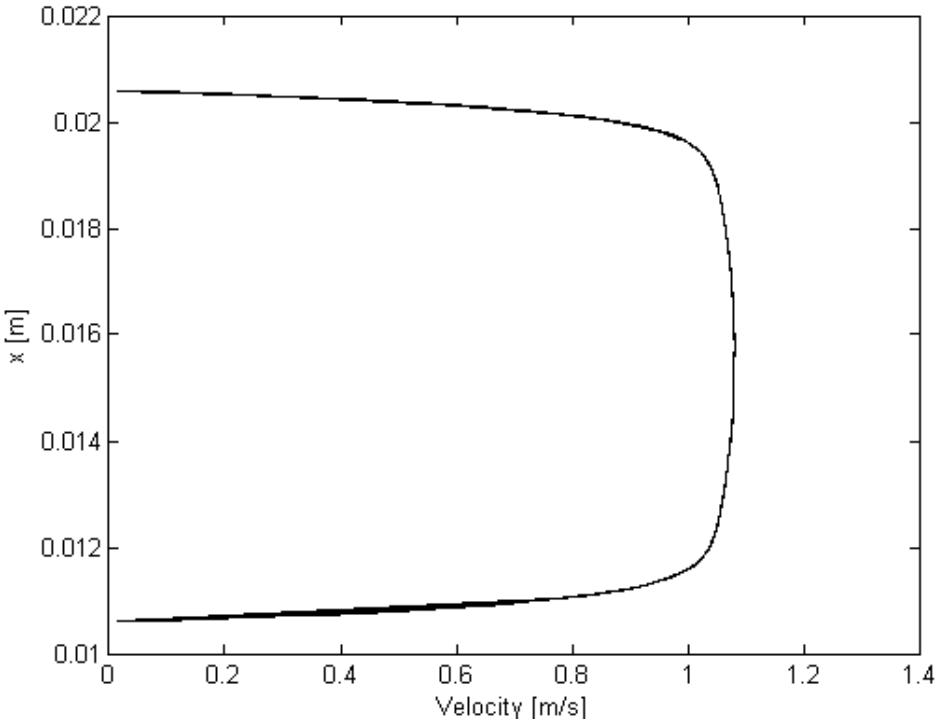

Figure 18 Graph of velocity for 0.2 m/s for the 25 Degrees contraction with the position in the test-section in the y axis in [m] and the velocity of each point in the x axis in [m/s]. (Values of position given by ANSYS due to the positioning of the model)

For 10 m/s:

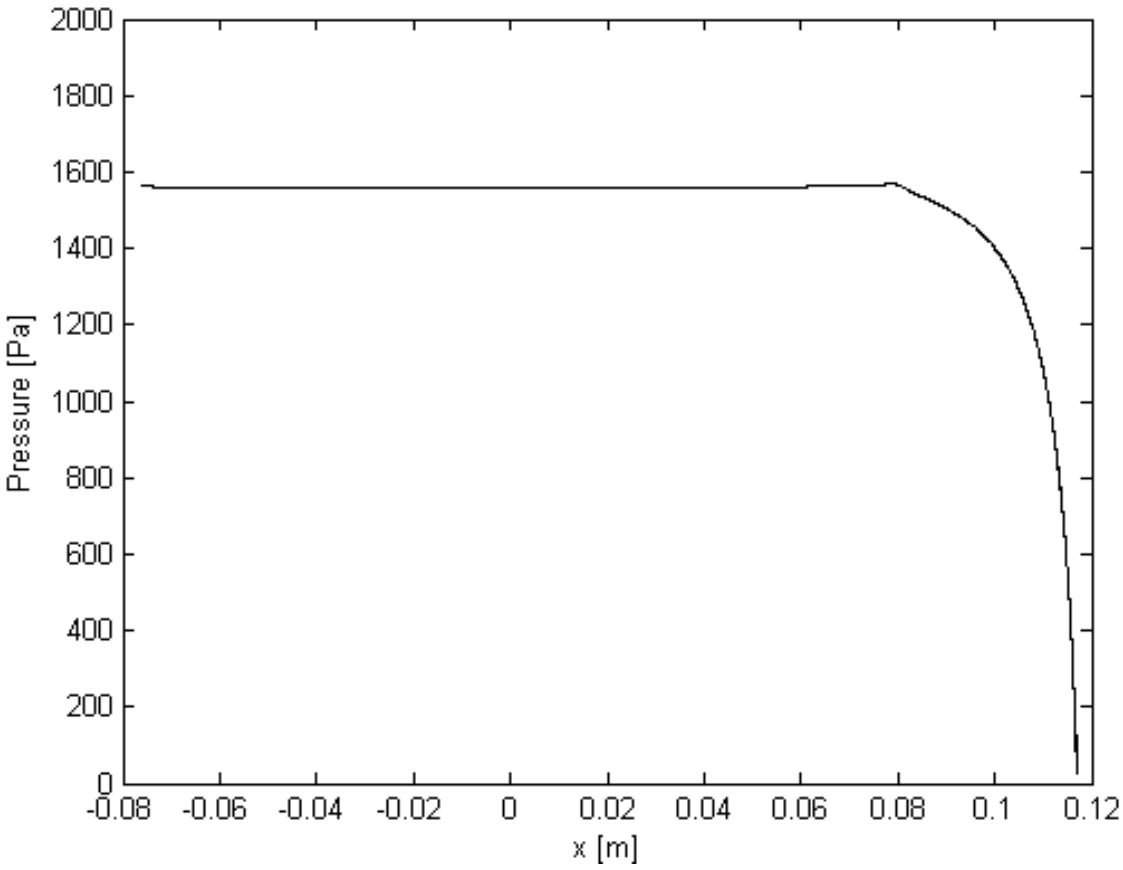

Figure 19 Graph of pressure for 10 m/s for the 25 Degrees contraction with the pressure in the y axis in [PA] and the position in the contraction in [m] along the x-axis for the wall (values of position given by ANSYS due to the positioning of the model).

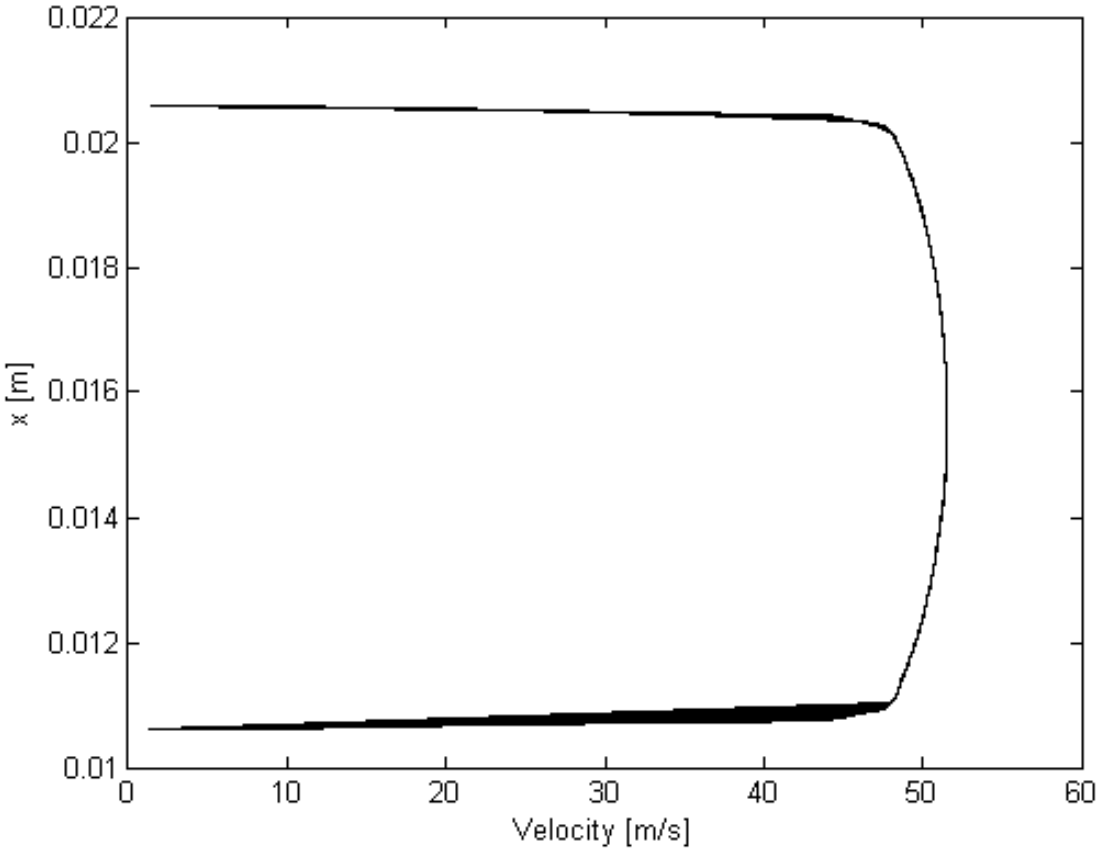

Figure 20 Graph of velocity for 0.2 m/s for the 25 Degrees contraction with the position in the test-section in the y axis in [m] and the velocity of each point in the x axis in [m/s]. (Values of position given by ANSYS due to the positioning of the model)

40 Degrees Contraction

For $0.2\ m/s$:

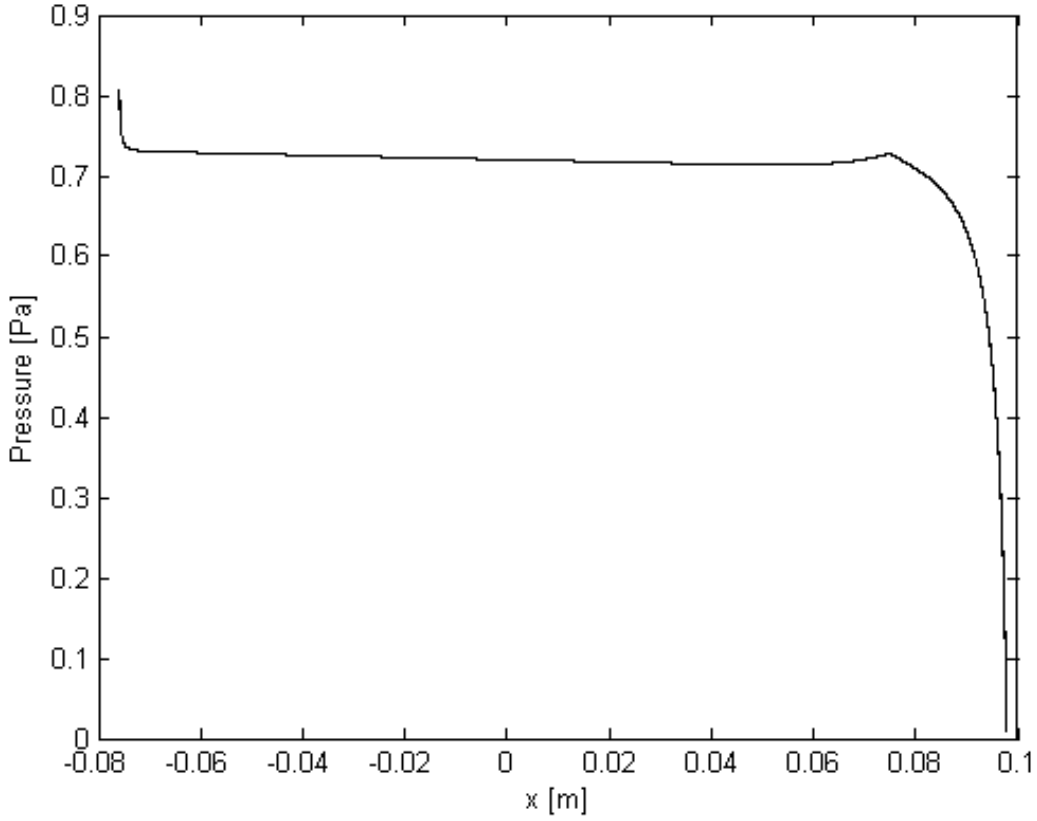

Figure 21 Graph of pressure for 0.2 m/s for the 40 Degrees contraction with the pressure in the y axis in [PA] and the position in the contraction in [m] along the x-axis for the wall (values of position given by ANSYS due to the positioning of the model).

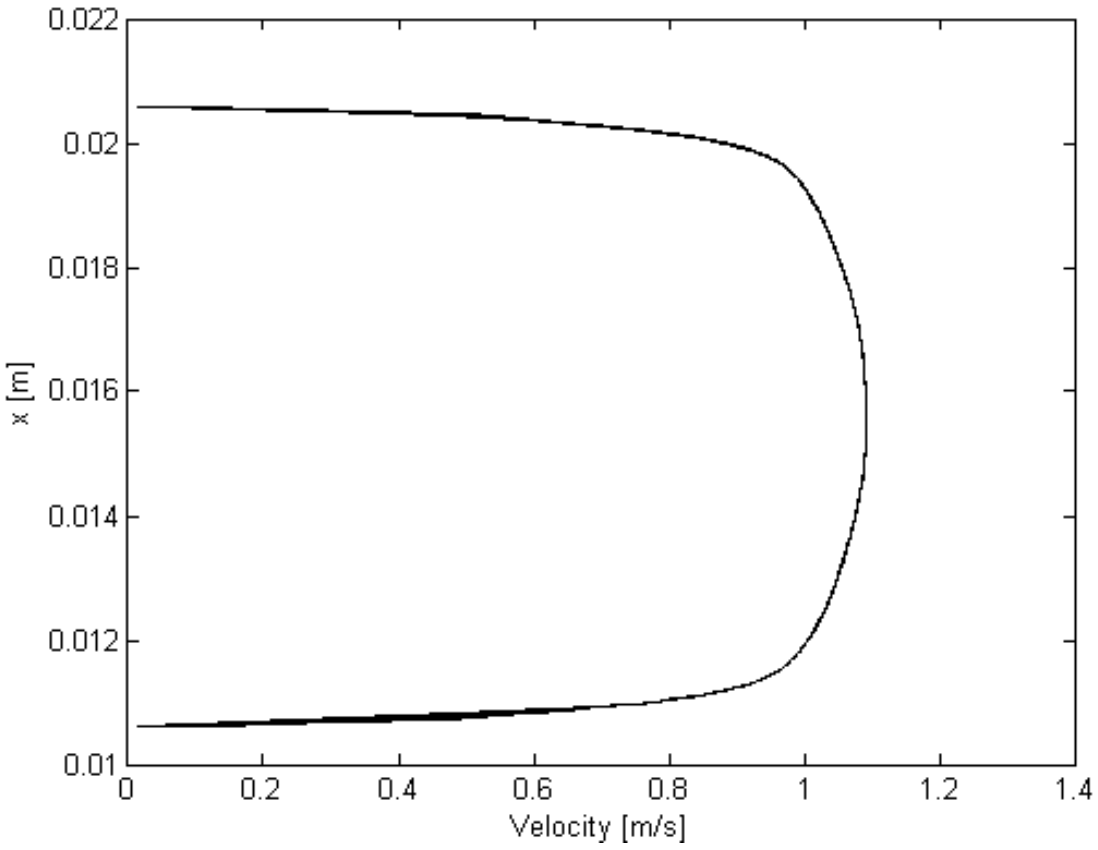

Figure 22 Graph of velocity for 0.2 m/s for the 40 Degrees contraction with the position in the test-section in the y axis in [m] and the velocity of each point in the x axis in [m/s]. (Values of position given by ANSYS due to the positioning of the model)

For 10 m/s:

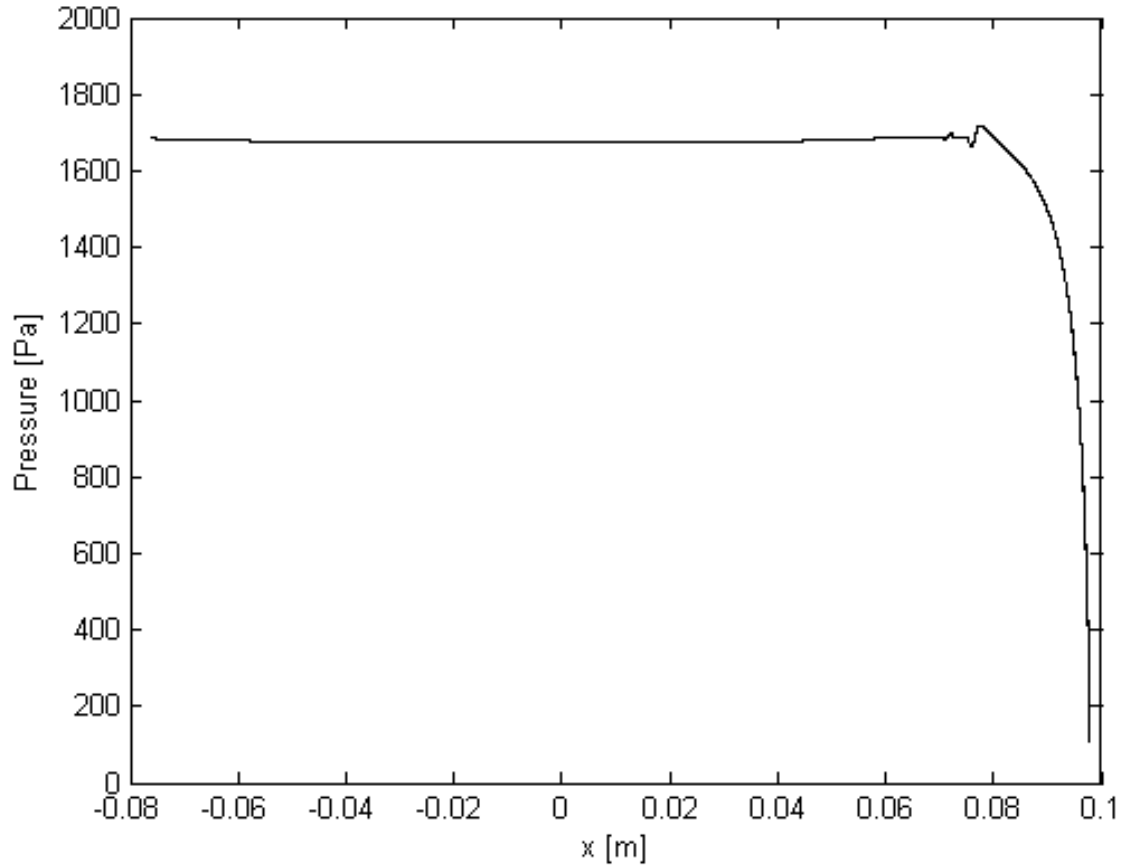

Figure 23 Graph of pressure for 10 m/s for the 40 Degrees contraction with the pressure in the y axis in [PA] and the position in the contraction in [m] along the x-axis for the wall (values of position given by ANSYS due to the positioning of the model).

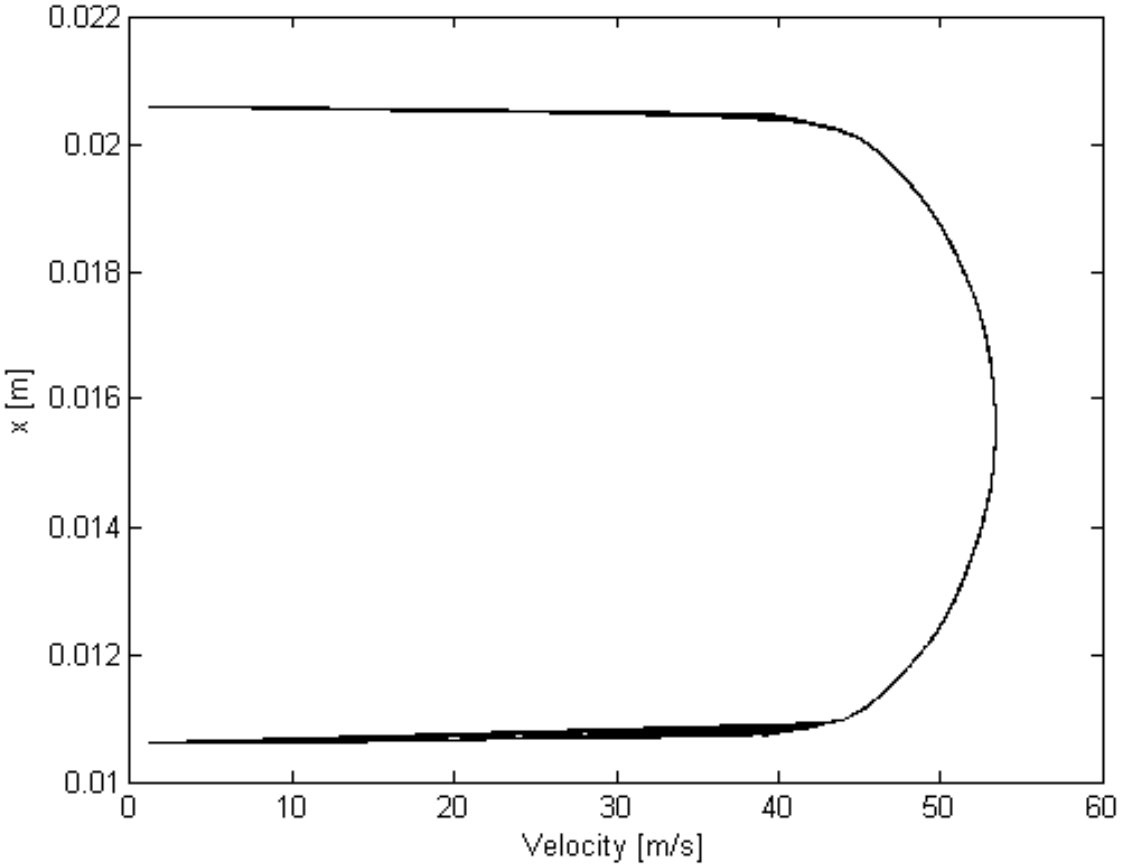

Figure 24 Graph of velocity for 10 m/s for the 40 Degrees contraction with the position in the test-section in the y axis in [m] and the velocity of each point in the x axis in [m/s]. (Values of position given by ANSYS due to the positioning of the model)

Convergent Design

For $0.2\ m/s$:

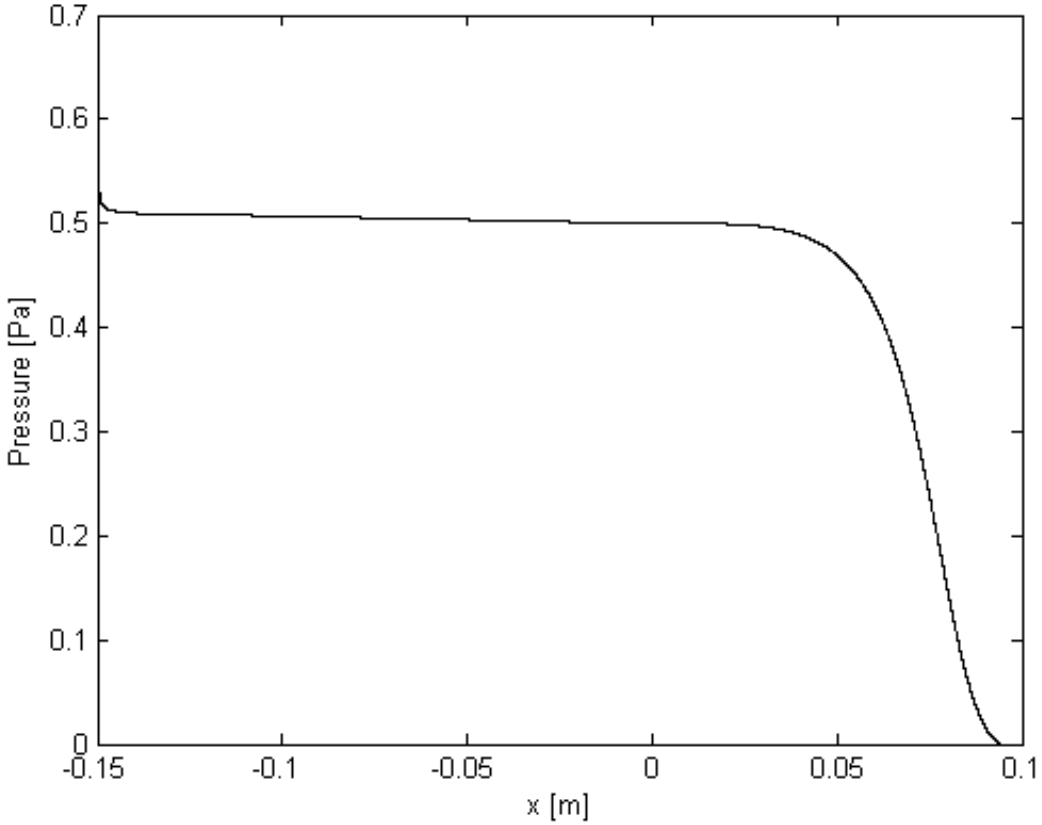

Figure 25 Graph of pressure for 0.2 m/s for the Convergent design with the pressure in the y axis in [PA] and the position in the contraction in [m] along the x-axis for the wall (values of position given by ANSYS due to the positioning of the model).

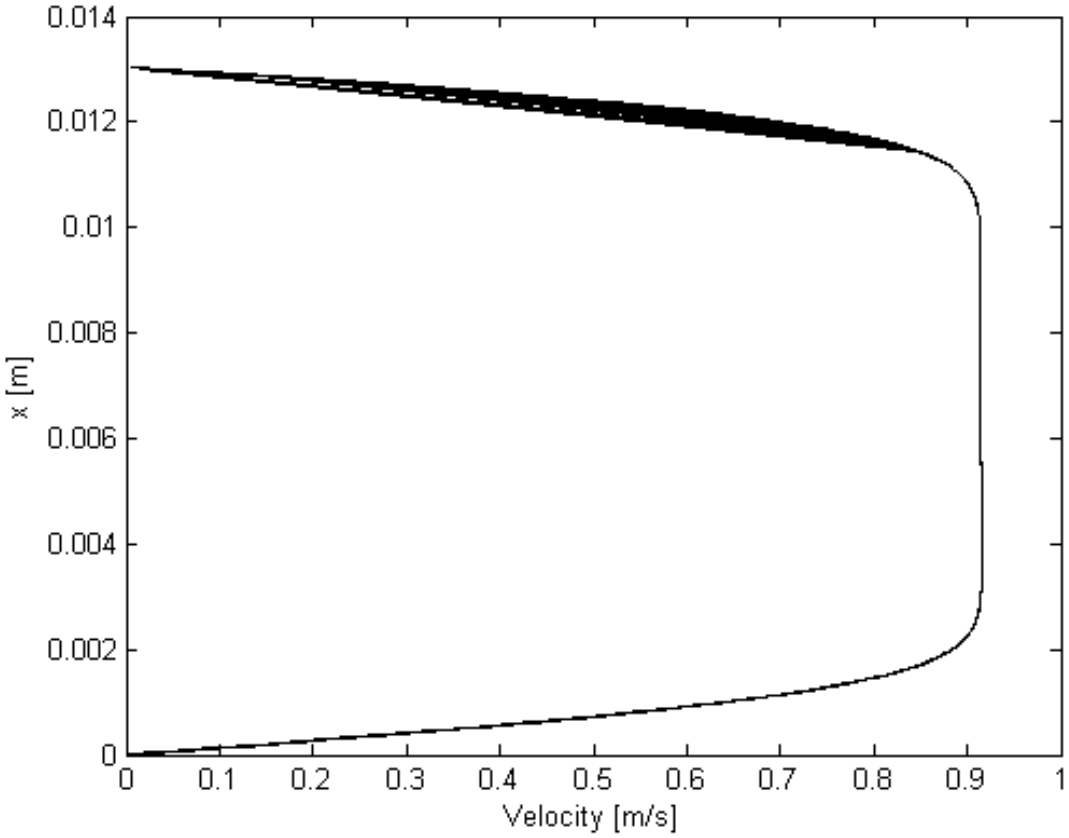

Figure 26 Graph of velocity for 0.2 m/s for the Convergent design with the position in the test-section in the y axis in [m] and the velocity of each point in the x axis in [m/s]. (Values of position given by ANSYS due to the positioning of the model)

For 10 m/s:

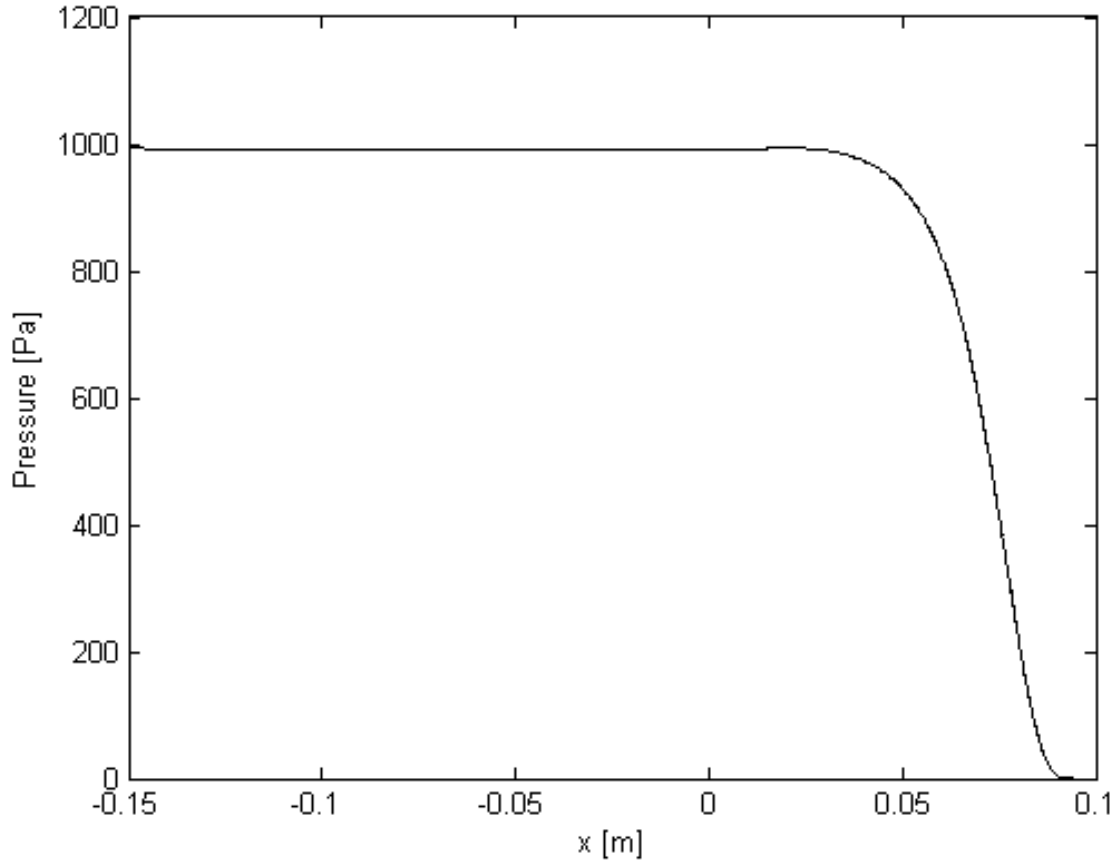

Figure 27 Graph of pressure for 10 m/s for the Convergent design with the pressure in the y axis in [PA] and the position in the contraction in [m] along the x-axis for the wall (values of position given by ANSYS due to the positioning of the model).

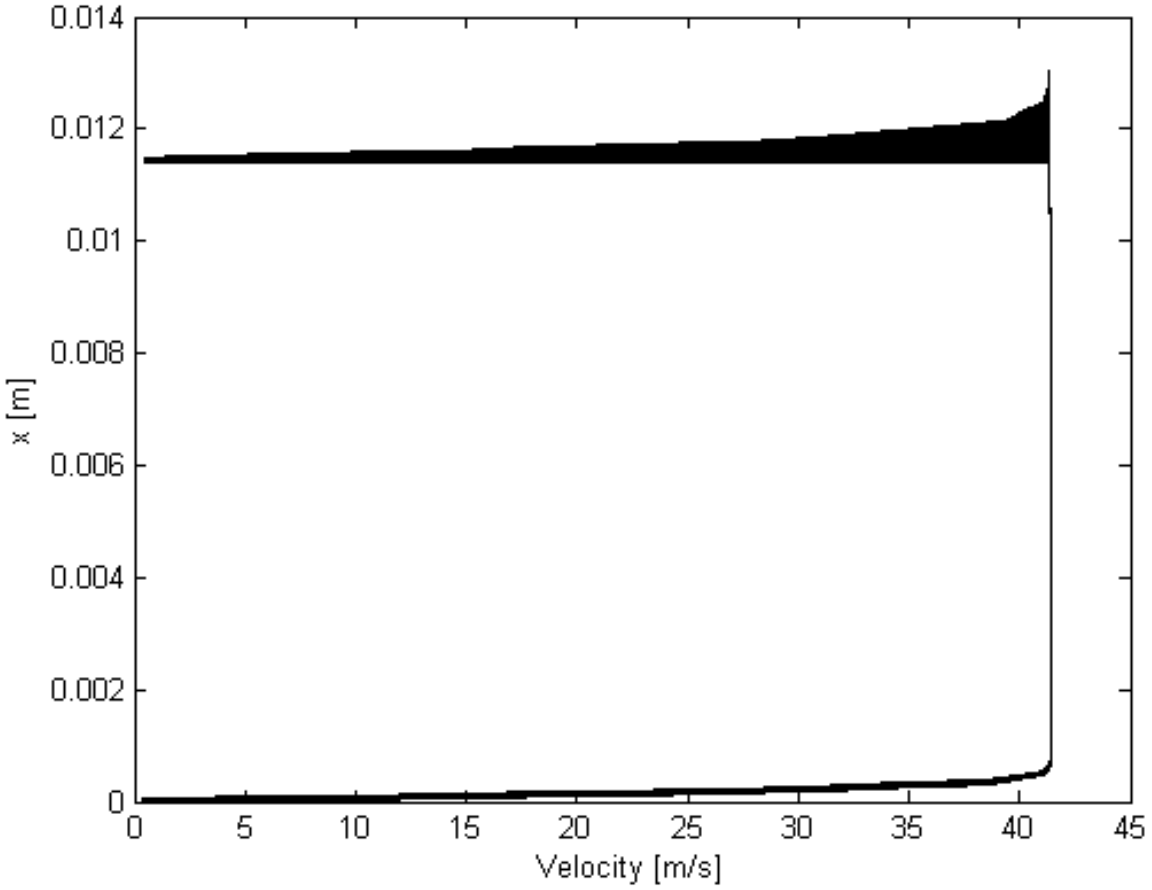

Figure 28 Graph of velocity for 10 m/s for the Convergent design with the position in the test-section in the y axis in [m] and the velocity of each point in the x axis in [m/s]. (Values of position given by ANSYS due to the positioning of the model)

25 Degrees Contraction with Extension

For $0.2\ m/s$:

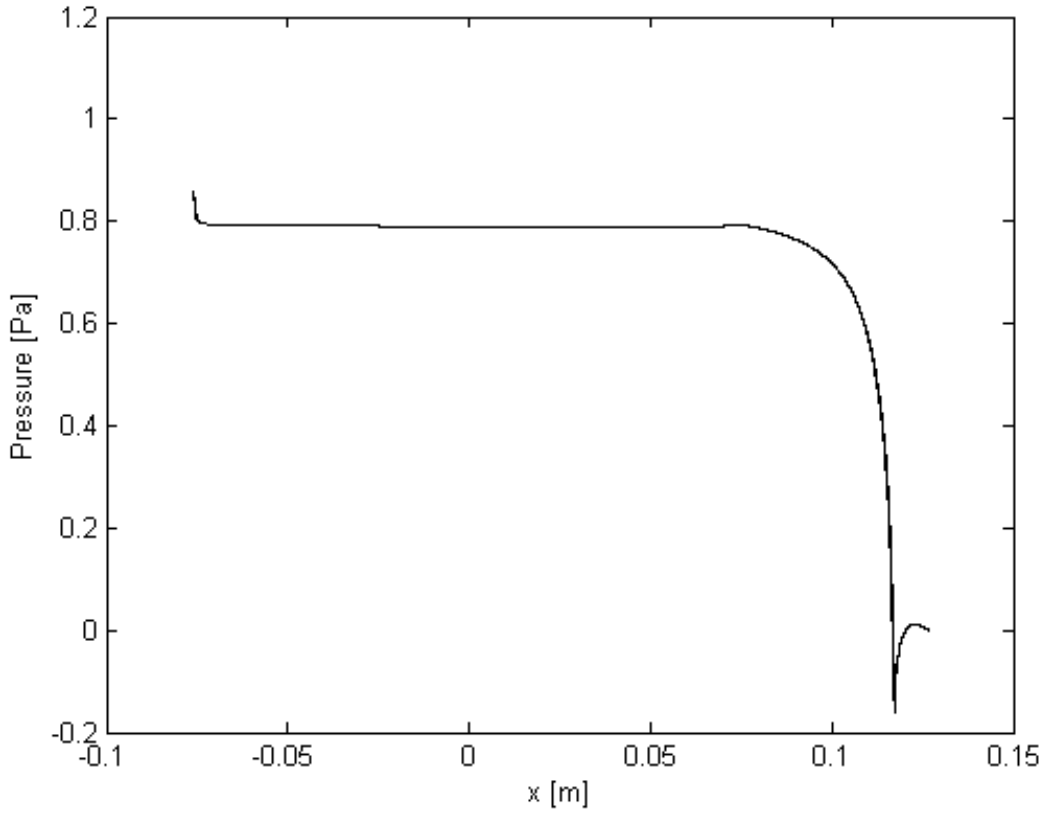

Figure 29 Graph of pressure for 0.2 m/s for the 25 Degrees contraction with the extension with the pressure in the y axis in [PA] and the position in the contraction in [m] along the x-axis for the wall (values of position given by ANSYS due to the positioning of the model).

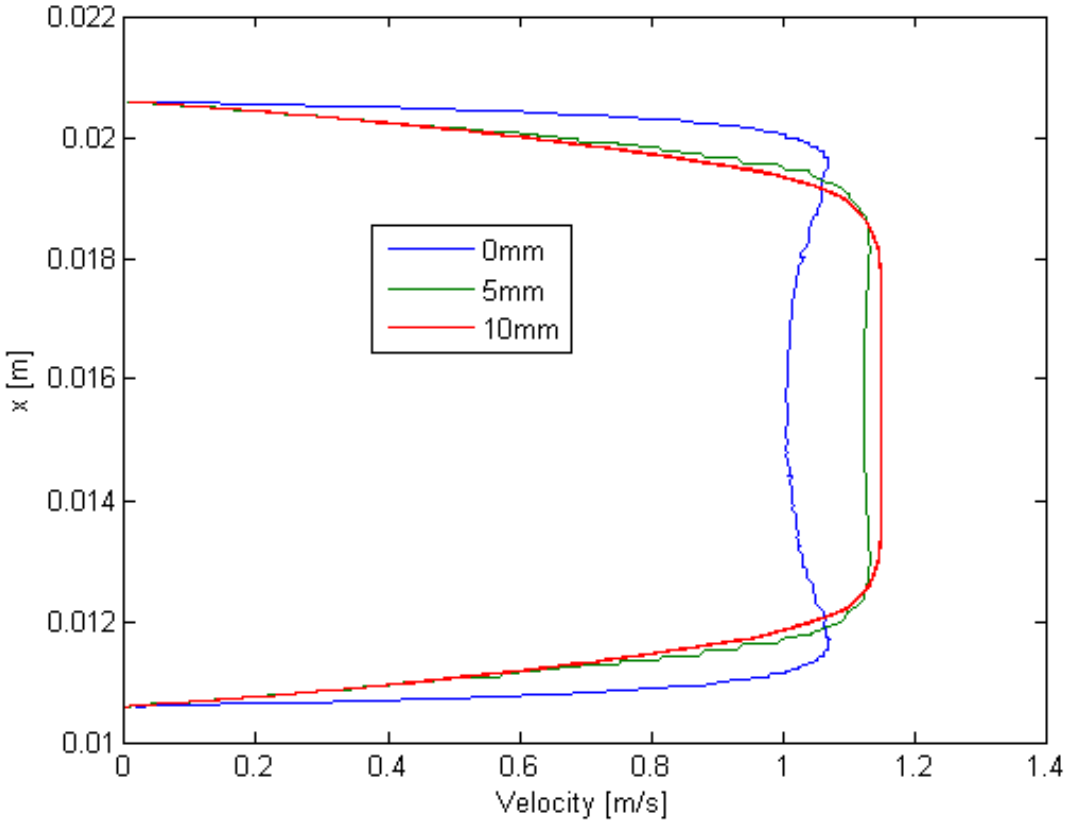

Figure 30 Graph of velocity for 0.2 m/s for the 25 Degrees contraction with the extension with the position in the test-section in the y axis in [m] and the velocity of each point in the x axis in [m/s]. (Values of position given by ANSYS due to the positioning of the model). The velocity is shown in different sections of the extension (beginning, middle and end).

For 10 m/s:

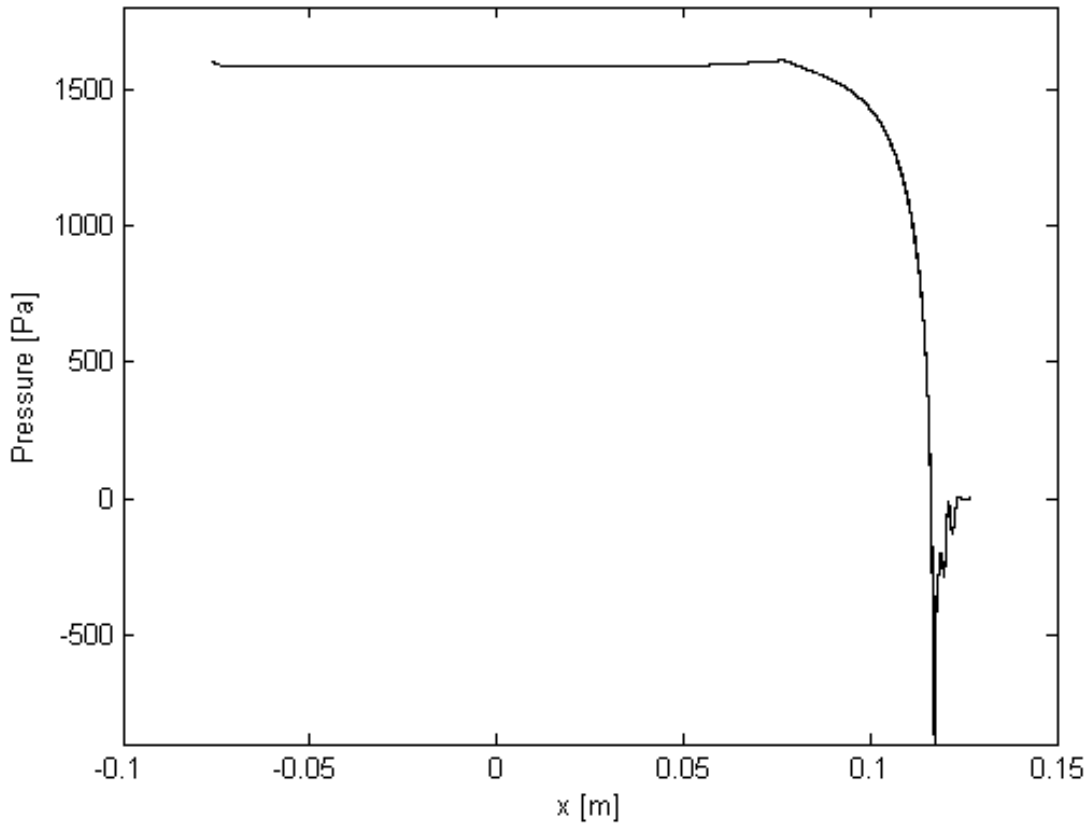

Figure 31 Graph of pressure for 10 m/s for the 25 Degrees contraction with the extension with the pressure in the y axis in [PA] and the position in the contraction in [m] along the x-axis for the wall (values of position given by ANSYS due to the positioning of the model).

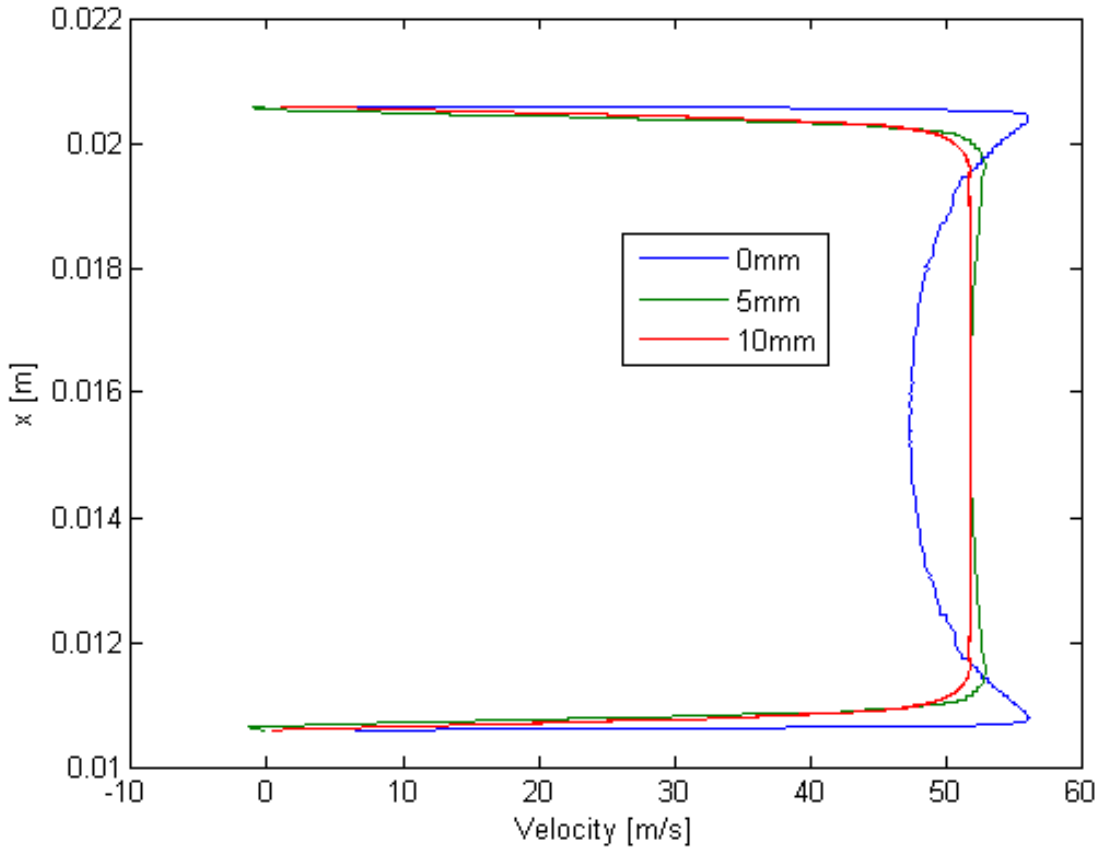

Figure 32 Graph of velocity for 10 m/s for the 25 Degrees contraction with the extension with the position in the test-section in the y axis in [m] and the velocity of each point in the x axis in [m/s]. (Values of position given by ANSYS due to the positioning of the model). The velocity is shown in different sections of the extension (beginning, middle and end).

40 Degrees with extension

For $0.2\ m/s$:

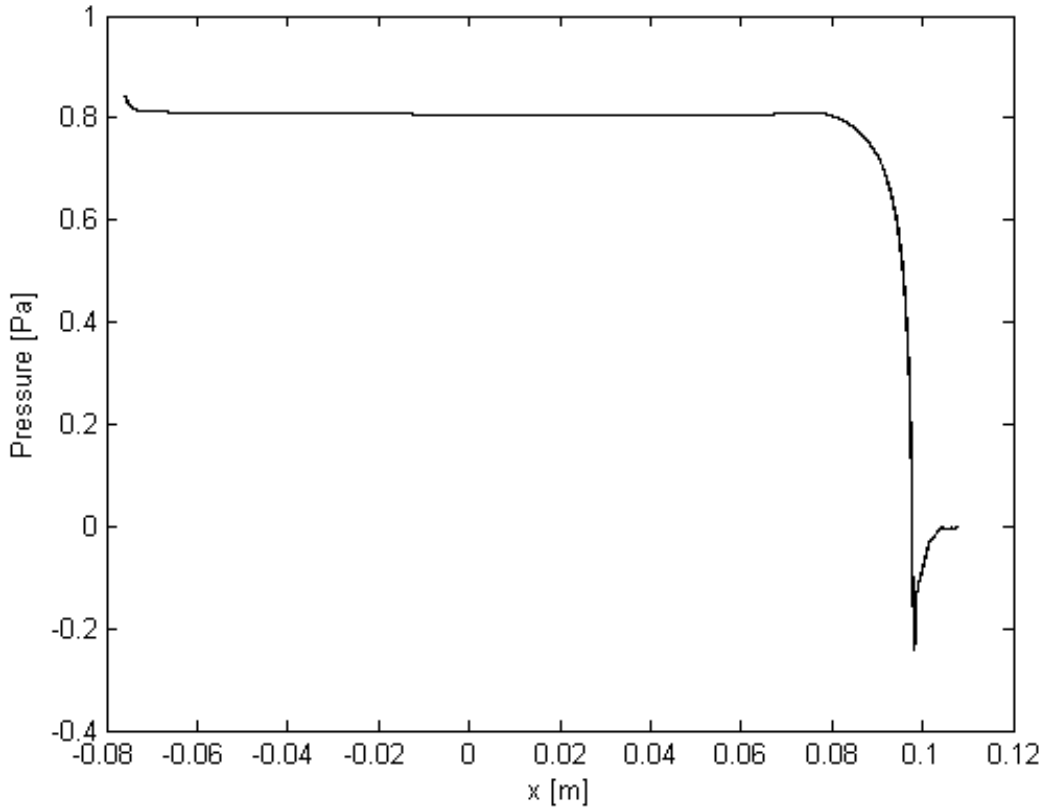

Figure 33 Graph of pressure for 0.2 m/s for the 40 Degrees contraction with the extension with the pressure in the y axis in [PA] and the position in the contraction in [m] along the x-axis for the wall (values of position given by ANSYS due to the positioning of the model).

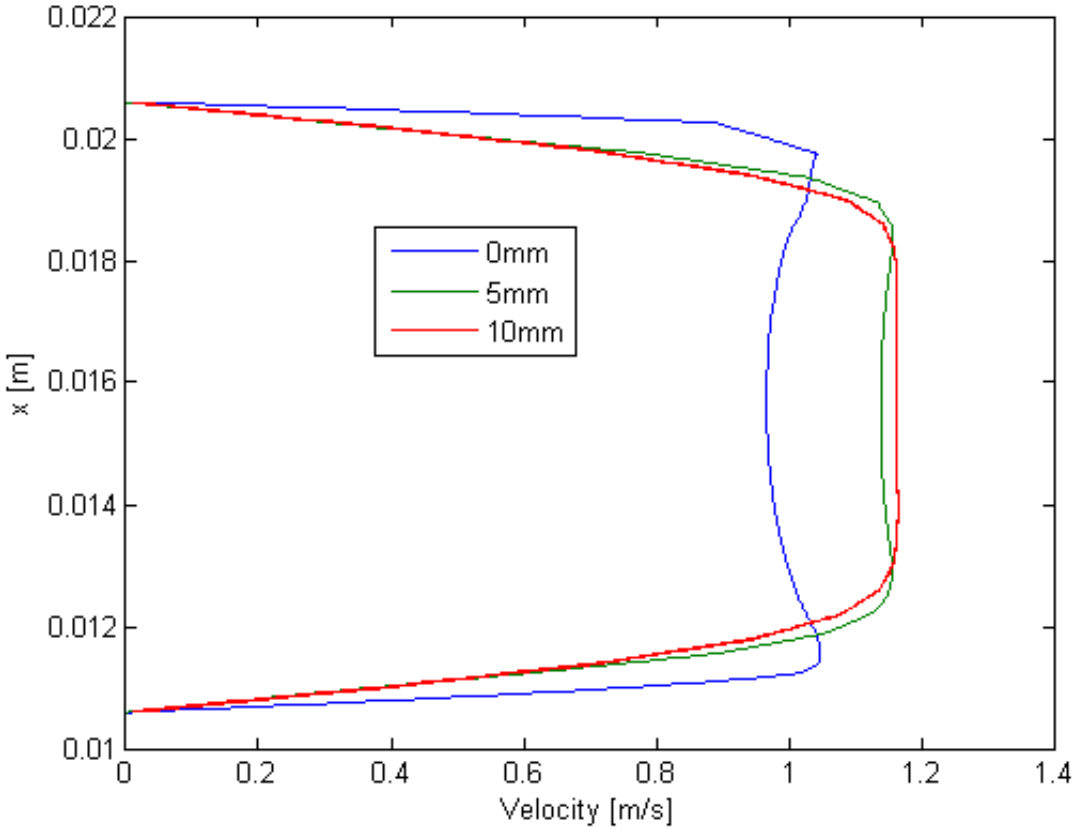

Figure 34 Graph of velocity for 0.2 m/s for the 40 Degrees contraction with the extension with the position in the test-section in the y axis in [m] and the velocity of each point in the x axis in [m/s]. (Values of position given by ANSYS due to the positioning of the model). The velocity is shown in different sections of the extension (beginning, middle and end).

For 10 m/s:

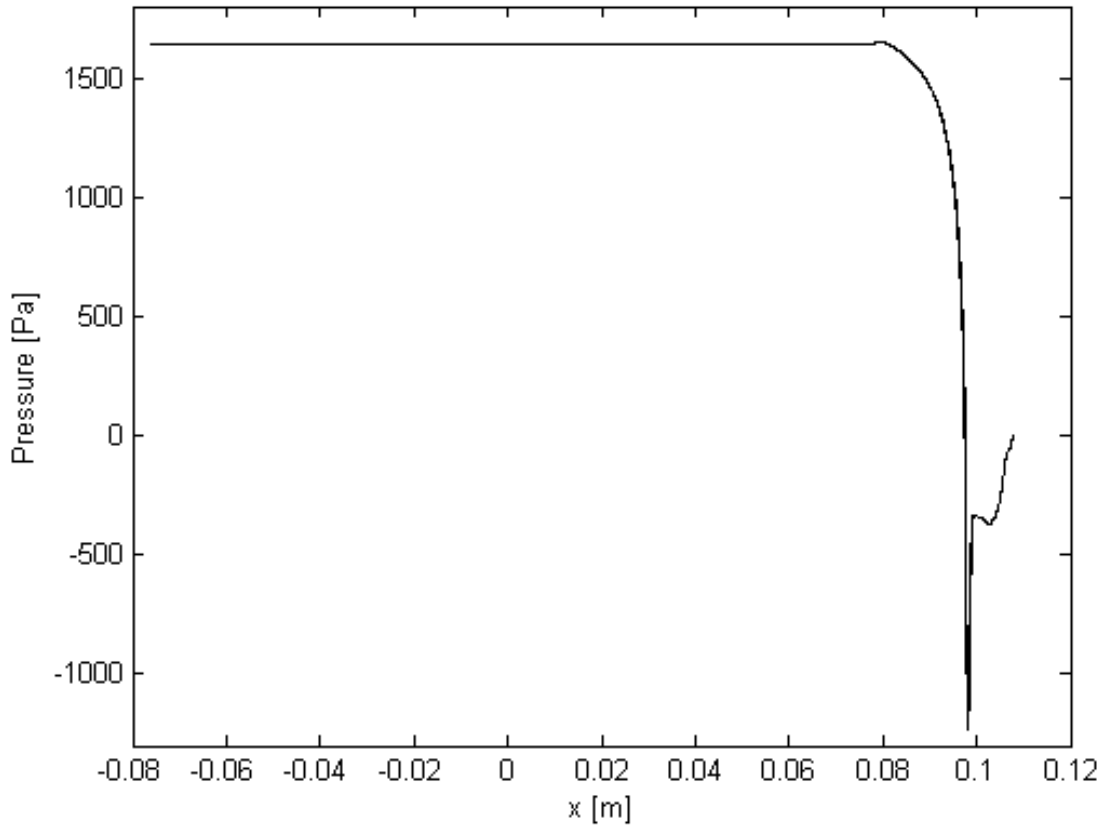

Figure 35 Graph of pressure for 10 m/s for the 40 Degrees contraction with the extension with the pressure in the y axis in [PA] and the position in the contraction in [m] along the x-axis for the wall (values of position given by ANSYS due to the positioning of the model).

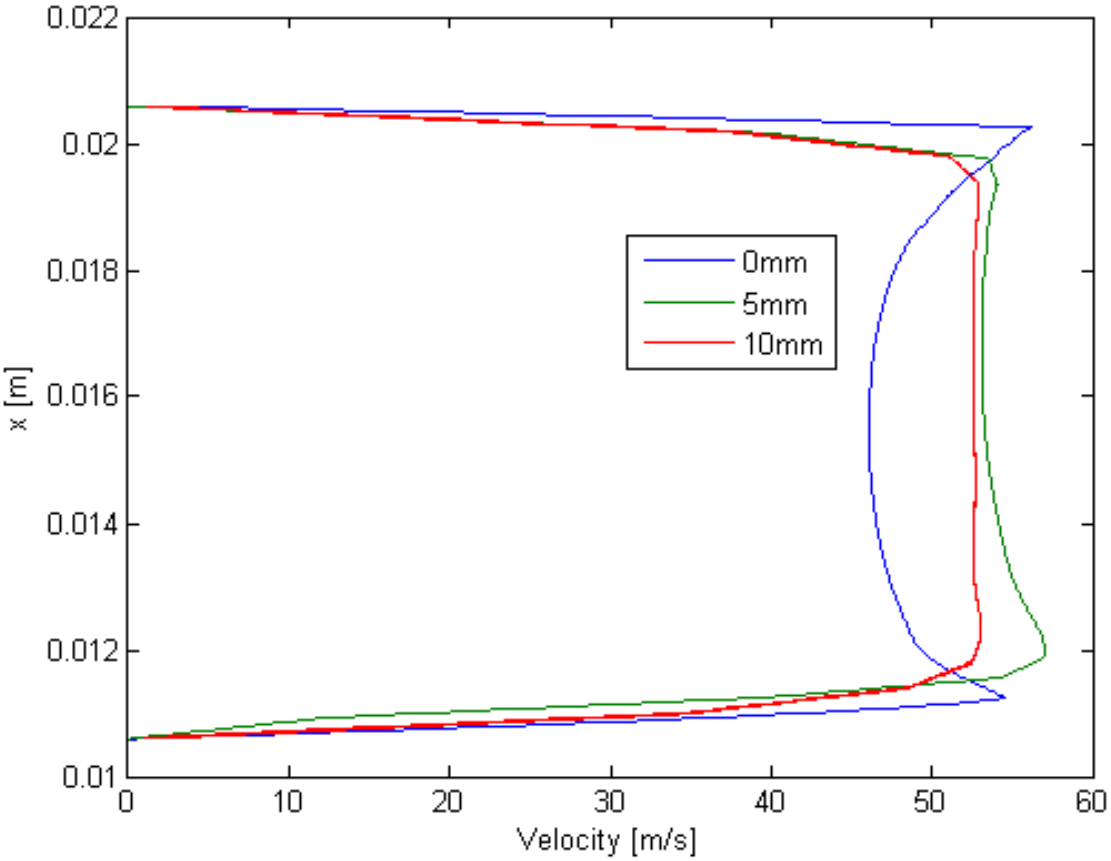

Figure 36 Graph of velocity for 10 m/s for the 40 Degrees contraction with the extension with the position in the test-section in the y axis in [m] and the velocity of each point in the x axis in [m/s]. (Values of position given by ANSYS due to the positioning of the model). The velocity is shown in different sections of the extension (beginning, middle and end).

Analysis

As it can be seen in the results obtained with the simulations, made with the most number of elements possible and the best mesh refinements possible, every option yields an acceptable outcome in both pressure and velocity distribution, with the convergent raising as the best in both categories, making it the most suitable option for the application. The drawback is the complexity in his construction compared with the other options, so these will be compared against each other and with the convergent to decide the most suitable option accounting also the complexity and construction of it.

Another outcome of these results is that the length selected for the extensions is the correct one; giving a proper velocity distribution in the test-section.

The drawback of the simulations is that the number of elements is restricted due to the use of a version student. This creates the problem of the amount of points we can obtain to produce the graphs, giving graphs that are very noisy even though the data is exported to a software (Matlab) to create the graphs. Also, the distribution of the points along the variables is not uniform, giving concentration of points that difficult the graph process and reading of the data. This is the reason the graphs are noisy even with the attempts of improving them with the software (Matlab).

To make this comparation the values of the simulations are adimensionalized to make a proper comparison; both in pressure and velocity distribution, where the graph is limited between [0.9 1] to better show the uniformity of this one. These graphs are presented next along with an explanation for the selection of the best option.

Comparison

Comparison of the pressure along the wall for the options

For $0.2\ m/s$:

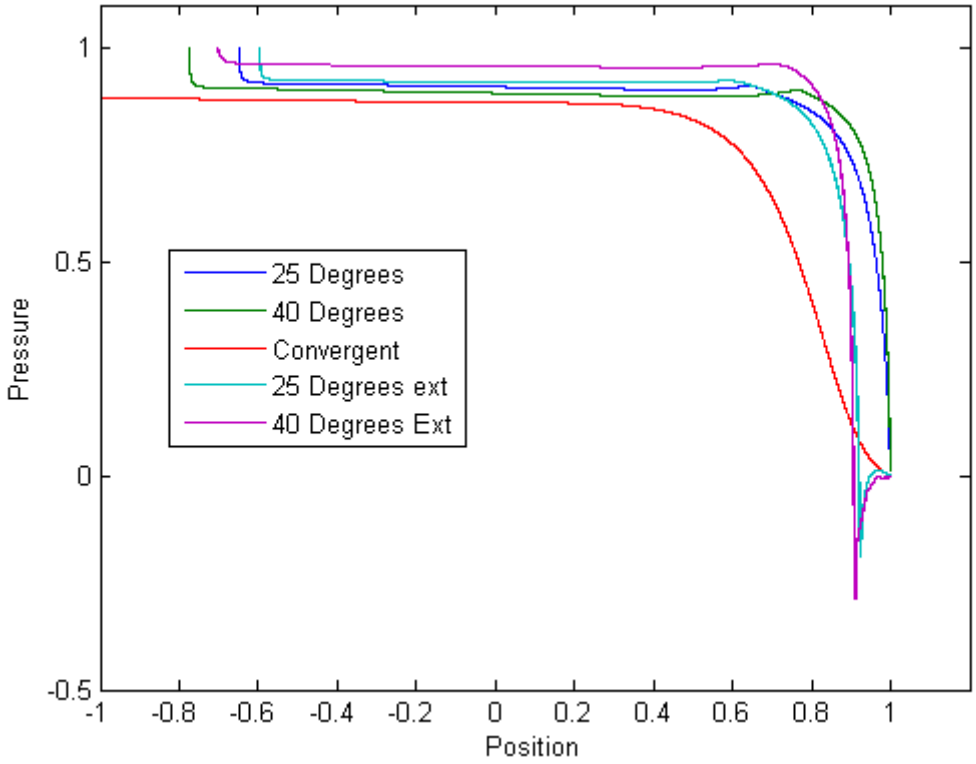

Figure 37 Comparison between the different options in pressure for 0.2 m/s. Each pressure graph was adimensionalized respect to the last point in the x-axis and respect to the highest pressure in the y-axis for each model.

For $10\ m/s$:

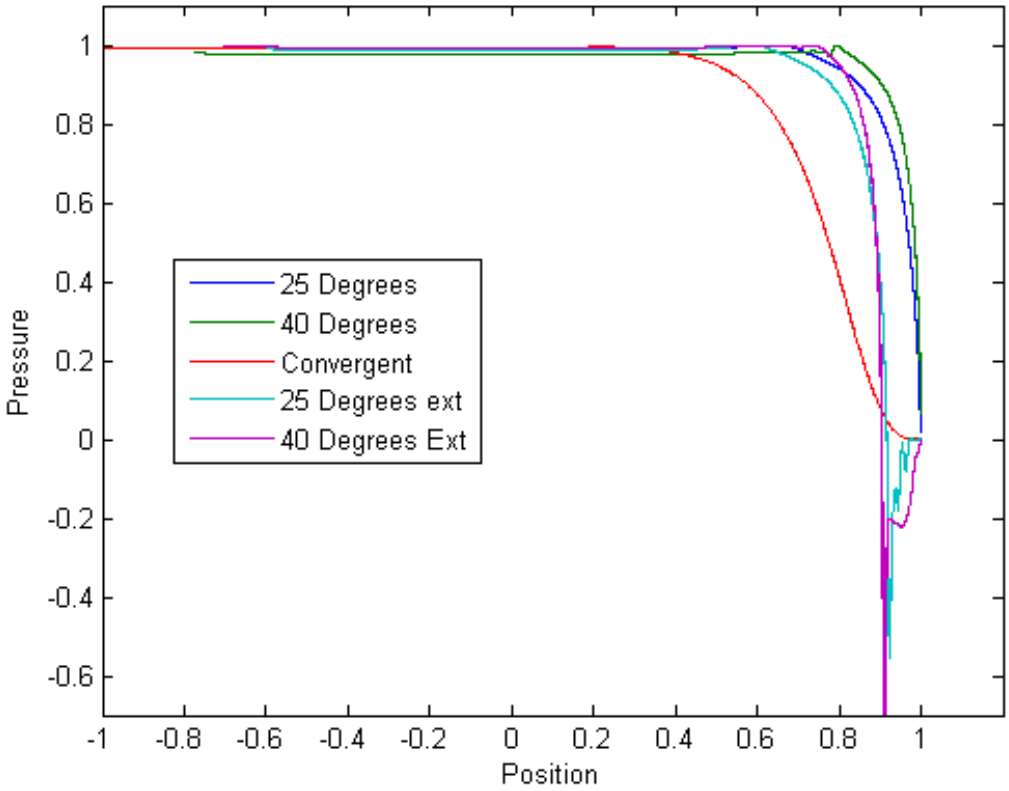

Figure 38 Comparison between the different options in pressure for 10 m/s. Each pressure graph was adimensionalized respect to the last point in the x-axis and respect to the highest pressure in the y-axis for each model.

Velocity distribution in test-section

For $0.2\ m/s$:

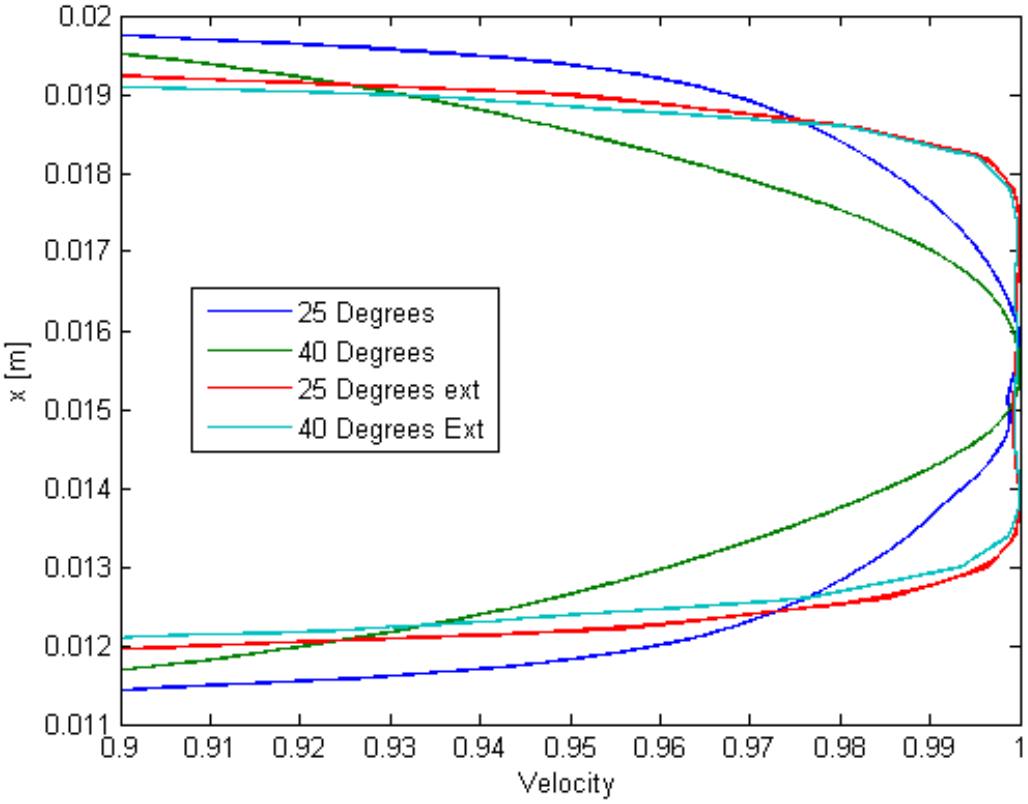

Figure 39 Comparison between the different options of velocity for 0.2 m/s. Each velocity graph is adimensionalized in the velocity (x-axis) respect to the highest velocity encountered in the middle of the test-section. Position is not adimensionalized since every graph has the same one.

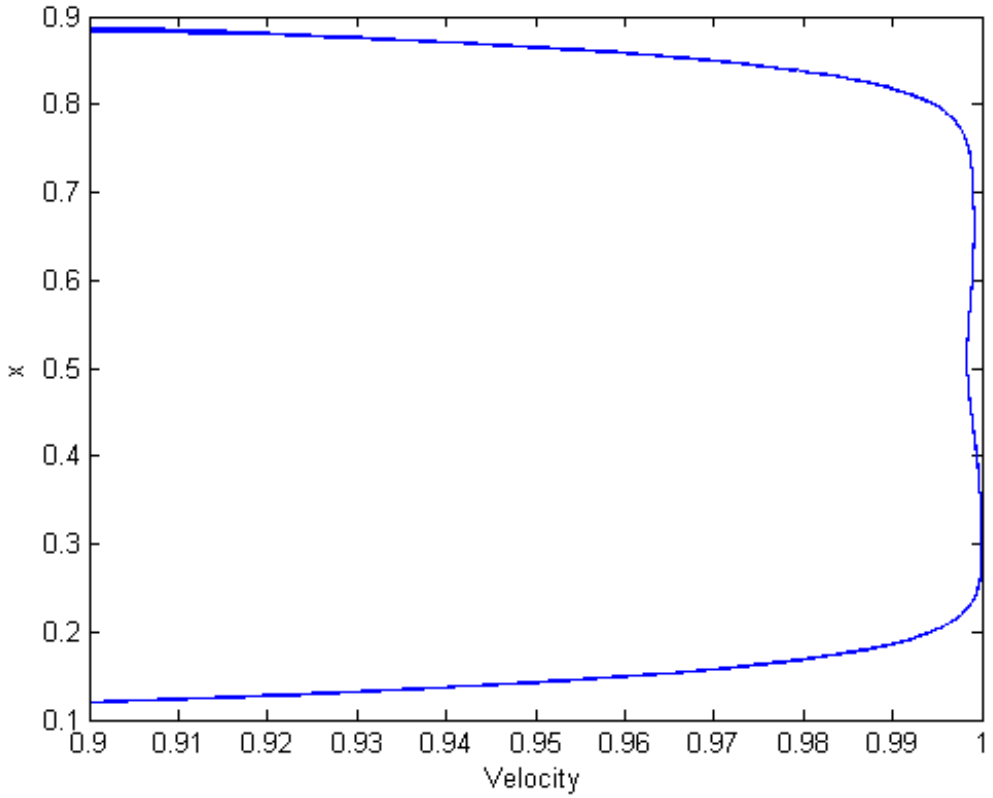

Figure 40 Graph of velocity for 0.2 m/s of the convergent for comparison. Velocity in the x-axis is adimensionalized respect of the highest velocity encountered in the middle of the test-section. Position in the y-axis is adimensionalized respect the highest position of the test-section. (Given by ANSYS by the positioning of the model).

For 10 m/s:

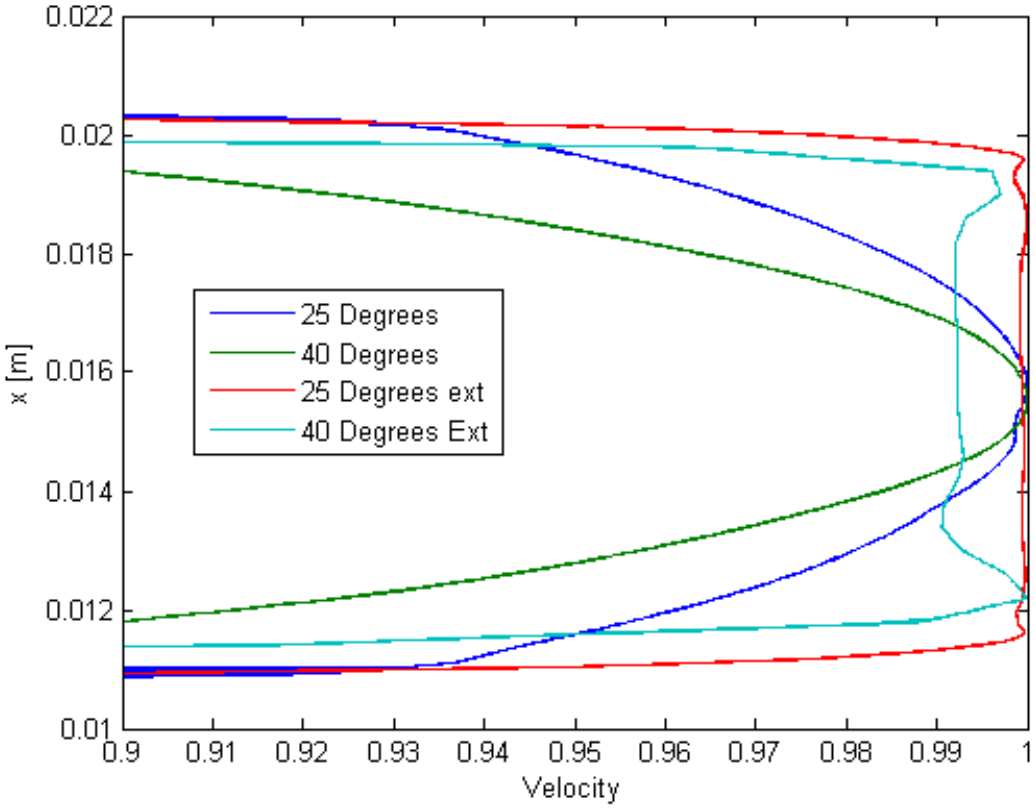

Figure 41 Comparison between the different options of velocity for 10 m/s. Each velocity graph is adimensionalized in the velocity (x-axis) respect to the highest velocity encountered in the middle of the test-section. Position is not adimensionalized since every graph has the same one.

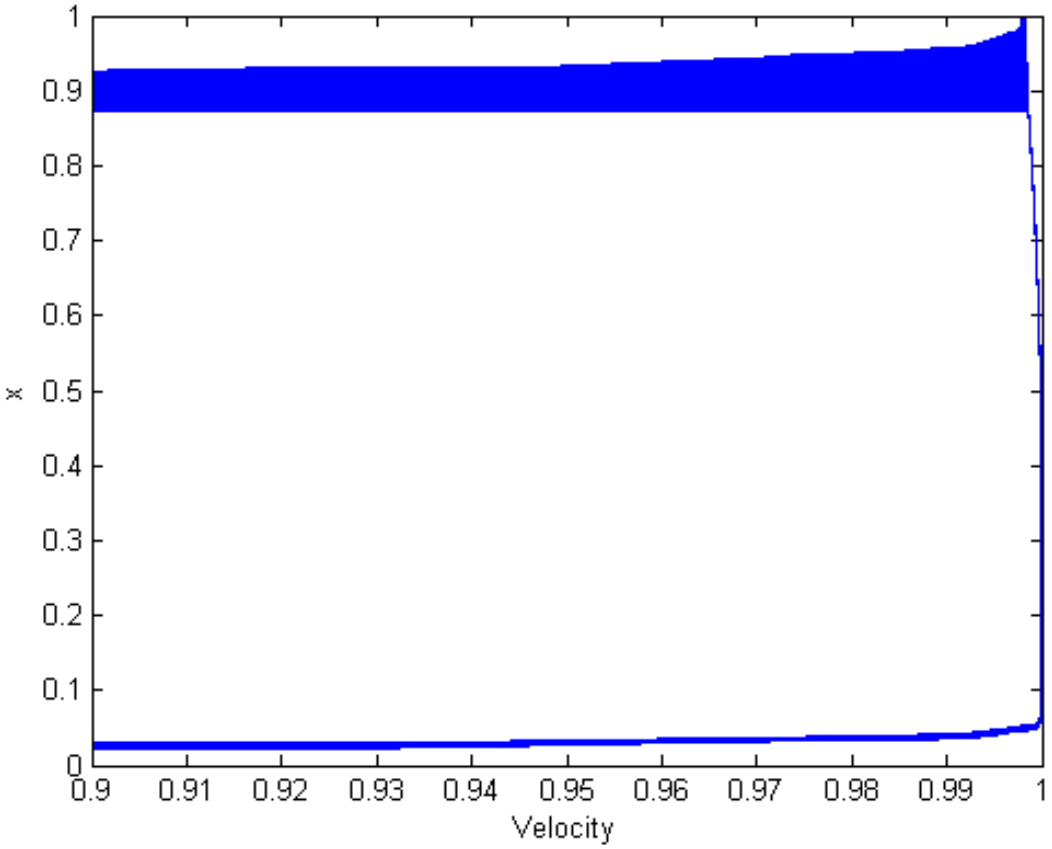

Figure 42 Graph of velocity for 10 m/s of the convergent for comparison. Velocity in the x-axis is adimensionalized respect of the highest velocity encountered in the middle of the test-section. Position in the y-axis is adimensionalized respect the highest position of the test-section. (Given by ANSYS by the positioning of the model).

Analysis

Looking at the options it shows that both contractions with extension have a rise of pressure during the contraction, both at low speeds and high speeds, especially in the beginning of the extension making them unsuitable for the application because this can mean that the flow is separated and disturbs the uniformity of the flow and in consequence the uniformity of the distribution of velocity in the test-section. The contraction of 40 Degrees has a small rise of pressure in the beginning of the contraction that, like before, can potentially be a separation that disturbs the flow.

Looking at the uniformity distribution of these three options, both with contractions have a suitable uniformity in the velocity distribution for the application, but the possibility of the disturbance caused by the separation of the flow leads to not taking them into account for this wind tunnel. Not like the 40 Degrees contraction where the distribution of velocity is uniform in the levels we need for this application in a relatively small height in the middle of the test-section, meaning that a small error when placing the probe can cause errors in the measurements and hence in the calibration.

These three options for the reasons stated above are discarded for the wind tunnel, leaving only the 25 Degrees contraction and the convergent. These will be compared again to make the decision and select the most suitable convergent, as before velocity distribution is limited to [0.9 1] and they are presented separated for better viewing.

Comparison between the best options

Pressure

For 0.2 m/s:

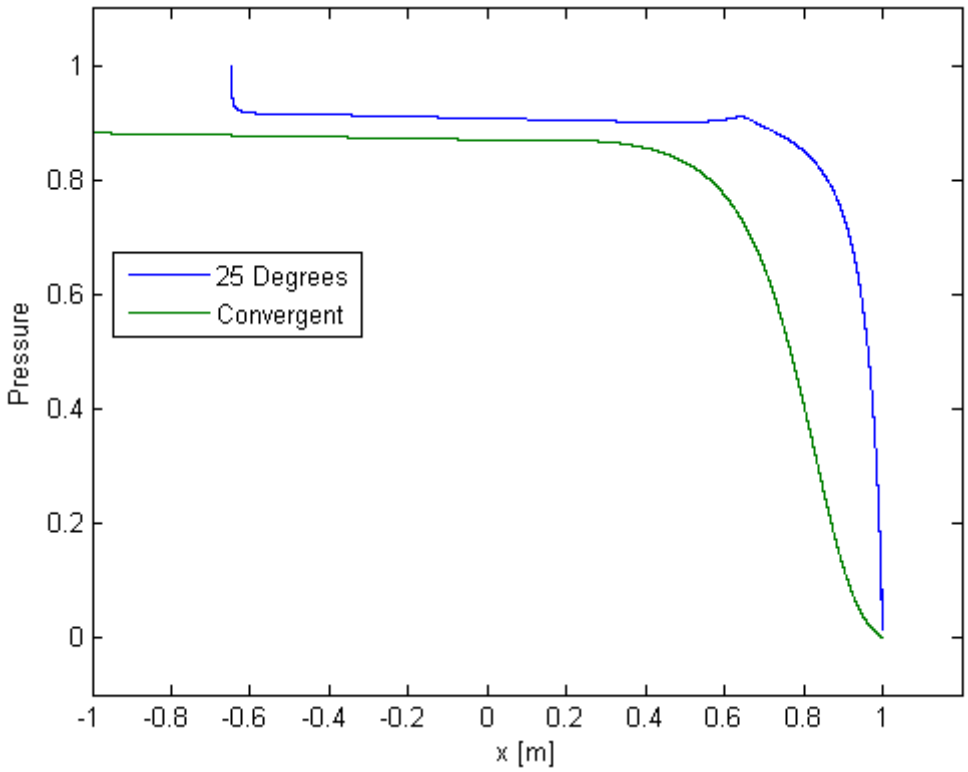

Figure 43 Comparison between the best two options in pressure for 0.2 m/s. Each pressure graph was adimensionalized respect to the last point in the x-axis and respect to the highest pressure in the y-axis for each model.

For 10 m/s:

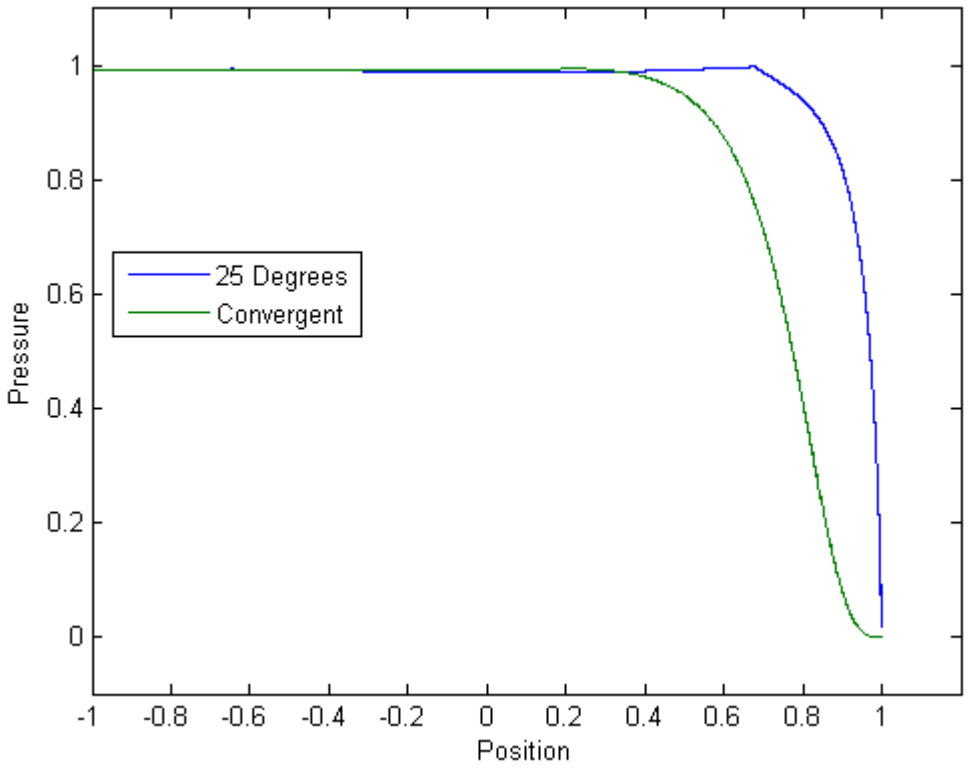

Figure 44 Comparison between the best two options in pressure for 10 m/s. Each pressure graph was adimensionalized respect to the last point in the x-axis and respect to the highest pressure in the y-axis for each model.

Velocity Distribution

For $0.2\ m/s$:

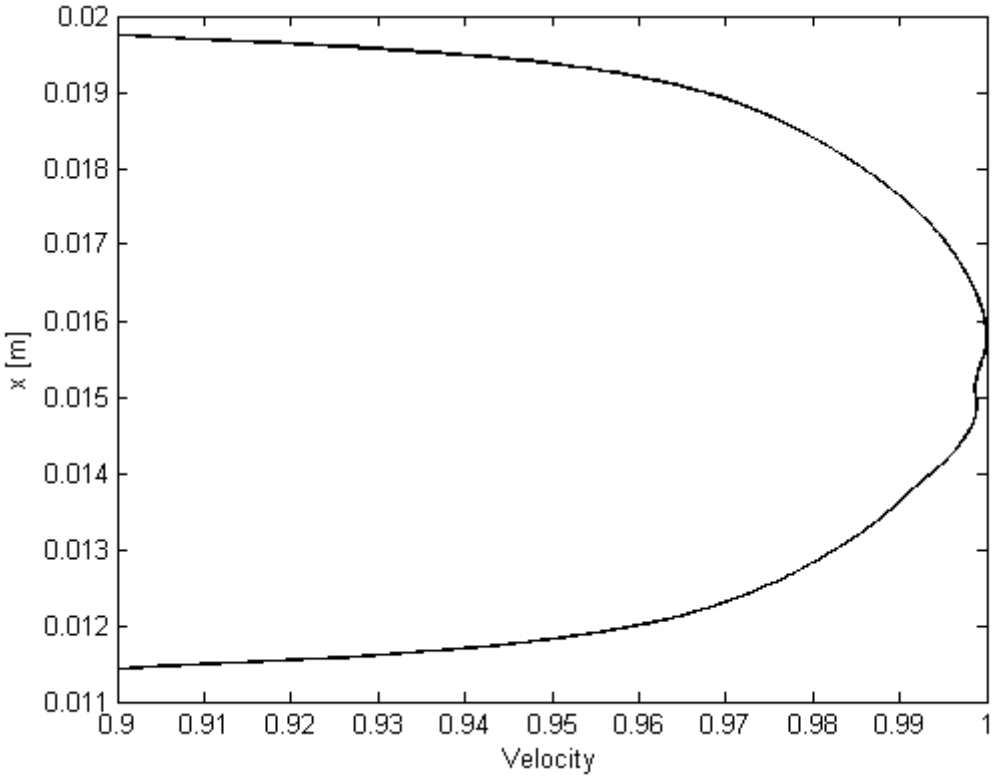

Figure 45 Graph for comparison of velocity for 0.2 m/s for the 25 Degrees contraction (1st best option). the graph is adimensionalized in the velocity (x-axis) respect to the highest velocity encountered in the middle of the test-section. Position is not adimensionalized since it's not needed.

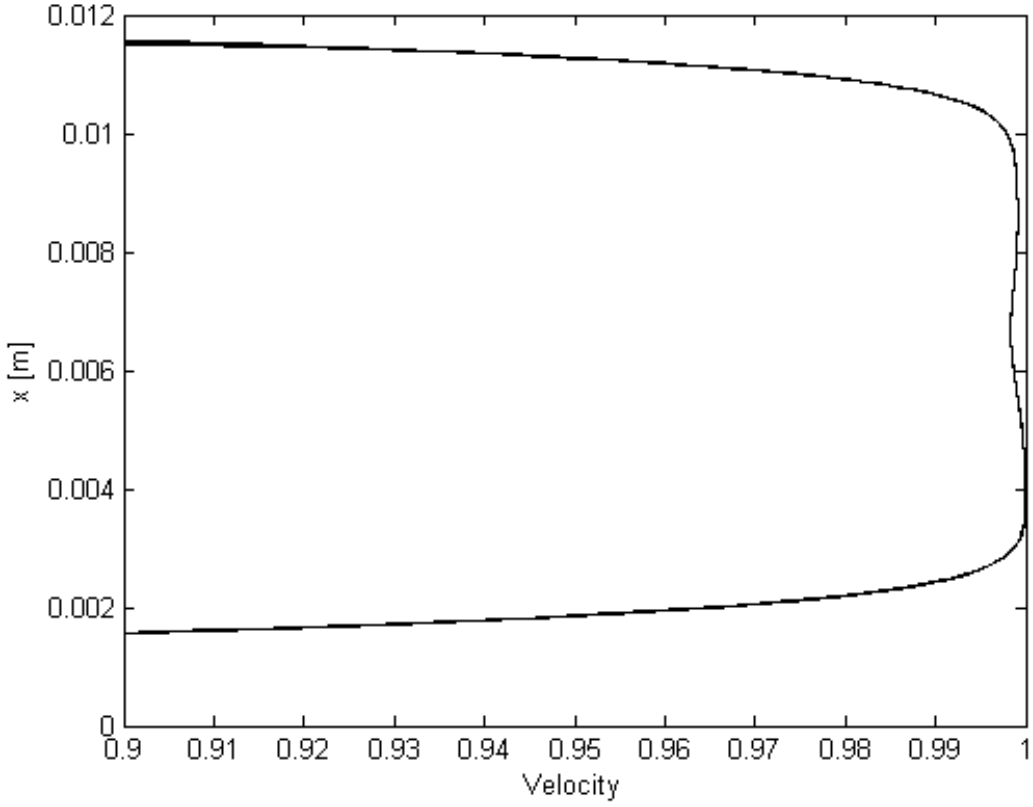

Figure 46 Graph of velocity for 0.2 m/s of the convergent for comparison (2nd best option. Velocity in the x-axis is adimensionalized respect of the highest velocity encountered in the middle of the test-section. Position in the y-axis is adimensionalized respect the highest position of the test-section. (Given by ANSYS by the positioning of the model).

For 10 m/s:

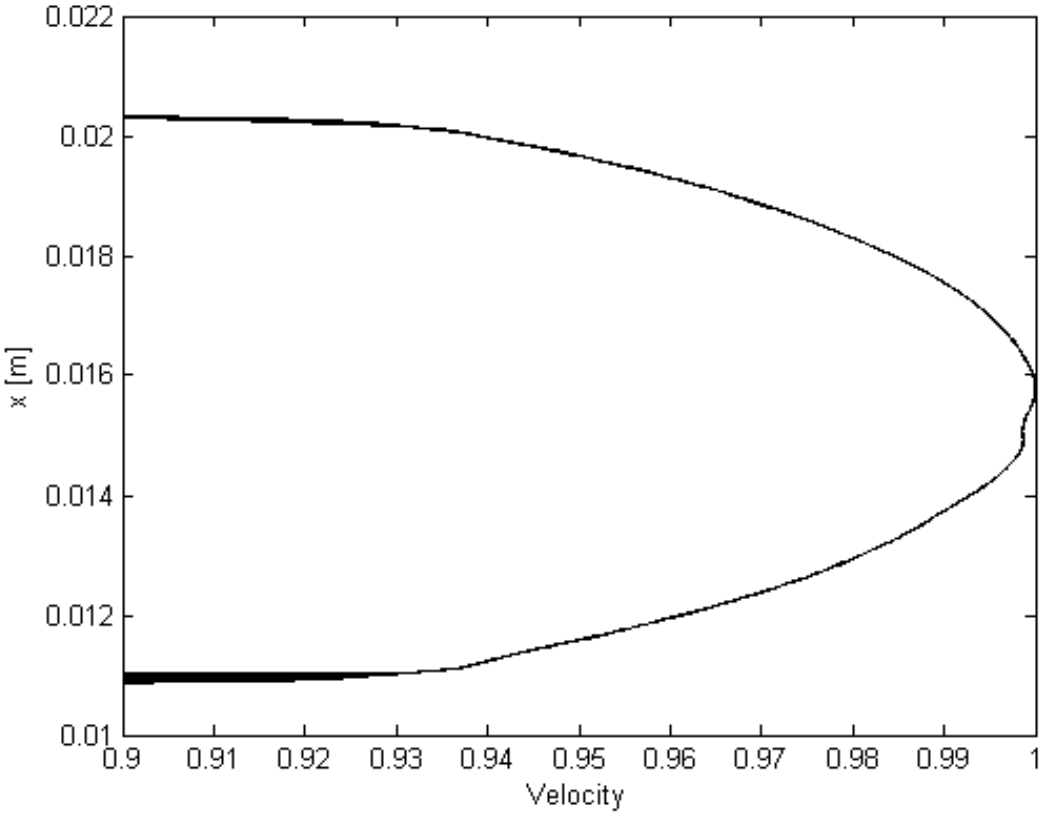

Figure 47 Graph for comparison of velocity for 10 m/s for the 25 Degrees contraction (1st best option). the graph is adimensionalized in the velocity (x-axis) respect to the highest velocity encountered in the middle of the test-section. Position is not adimensionalized since it's not needed.

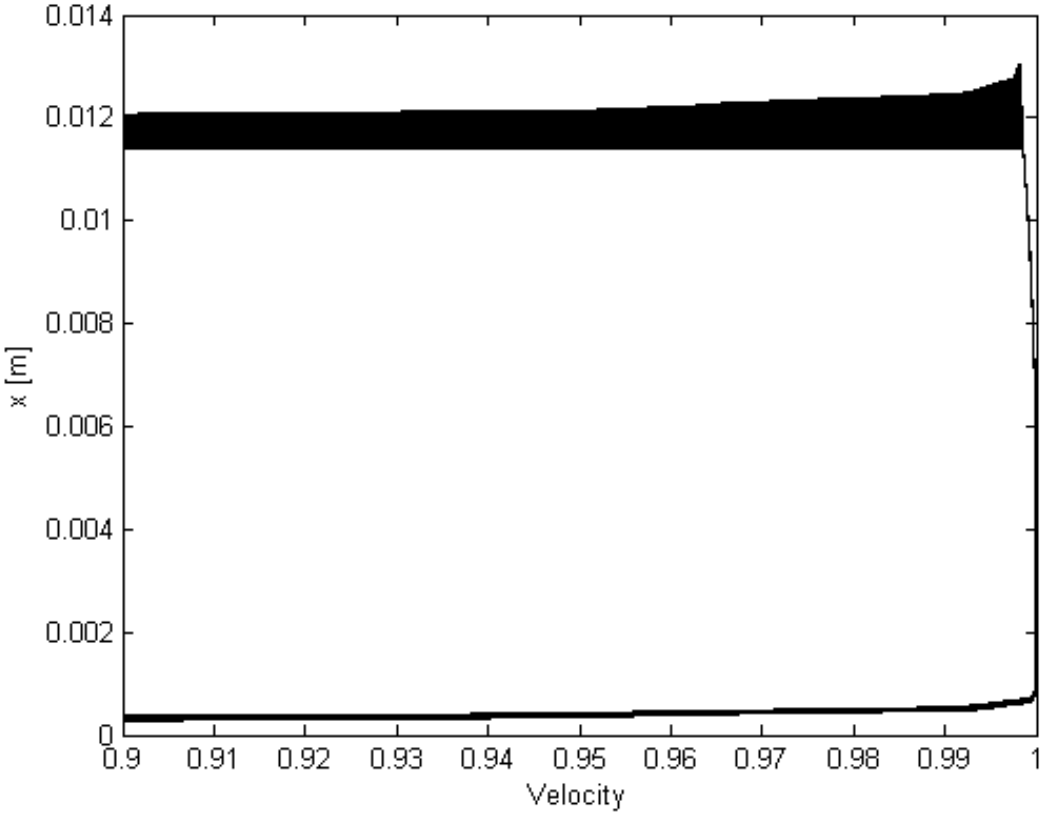

Figure 48 Graph of velocity for 10 m/s of the convergent for comparison (2nd best option. Velocity in the x-axis is adimensionalized respect of the highest velocity encountered in the middle of the test-section. Position in the y-axis is adimensionalized respect the highest position of the test-section. (Given by ANSYS by the positioning of the model).

looking at both graphs of pressure it's visible that there's a small pressure rise in the 25 Degrees contraction that could cause separation, but this is minimum in percentage making it unlikely to happen but still there's the possibility. The same doesn't occur with the convergent where the pressure descend smoothly to the minimum in the test-section accelerating the flow, working as it was intended in the design. Based on this comparison only the 25 Degrees can be used, it's a suitable option and the construction complexity is less than the convergent, meaning we don't need any special tools like a CNC to make it.

But if we look at the graphs of velocity distribution the 25 Degrees contraction has a variation that can cause problems with the calibration. Considering that a difference less than 0.5% is appropriate for this application the height of the test-section where we have less than this variation is a small region, acceptable for the calibration but making the position of the probe in the test-section a key factor for the calibration. Positioning it outside this zone will yield a bad calibration and as a result a bad measurement of the probe when working. The convergent design has almost no difference in velocity in the height of the test-section, making the positioning of the probe a minor problem, the probe just need to be in the test-section relatively close to the middle of it.

The disadvantage with the convergent design is in the building process which involves a specialized machine (CNC) to create the shape in two different pieces of material, then joined by metal sheets in each side creating the convergent. It will also be more expensive due to the use of material and the CNC time spend creating the shapes; while in the straight contraction the disadvantage doesn't come in the building process but in the calibration itself with the correct positioning of the probe. Due to the small size of probes and test-section an accurate method will need to be created to place it, losing time and introducing a possible error if the probe it's not well-placed ruining all the purpose of the calibrator.

Knowing that these probes will be used for research purposes, these calibrations needs to be the most accurate possible that's why the convergent selected it's the one designed by the convergent theory. Even though it's more difficult and more expensive to build it eliminates the possibility of the bad-placement of the probe that will lead to possible errors in the calibration, hence making the calibrations as accurate as possible. Although the disadvantage mentioned for the convergent design, the University of Bologna has a Hangar Laboratory with a CNC machine that is suitable for the creation of this one and because of the small dimensions of the two parts that needs to be built they can be made with unused materials or rests of other works making it less expensive. It will only require as an additional work the smoothness of the surface and joining both part together and to the wind tunnel.

For the reasons stated above is why the convergent designed with the design theory of convergent is the selected one. Having all the components selected, a fan will be proposed and a model of the wind tunnel.

Model of the Wind tunnel

Once all the components are selected and specified a model for the wind tunnel can be presented. This will consist of a settling chamber where all the elements to uniformize the flow will be placed and the convergent to the test-section. The attachment to the fan that will be selected next it's not decided yet. One option is to connect the settling chamber to a tank where the air will enter from the bottom from the fan and reach the wind tunnel itself in the top part of the tank.

The wind tunnel will be composed of a part of the settling chamber that will be attached, in case the tank option is selected, to the tank and to this part will be attached all the components, beginning with the honeycomb and then a part with a separation and at the end of this, a screen and so on until reaching to the last screen that will be attached to the final part of the settling chamber and this to the convergent. These separations are to ensure the stabilization of the flow before reaching a new component. All the components until the convergent are then joined together by screws pressing on them to maintain the sealing inside the wind tunnel to allow a proper functioning. The screws are attached to the corners and tighten to keep the sealing, in case there's flexion in the corners because of the screws, some nerves can be added to stiffen the components and avoid this. A CAD model is presented here illustrating the model proposed. Dimensions aren't defined, and the elements are not shown in the model, but the specifications are attached at the end.

First, an exploded model is shown with specifications to where each component is placed.

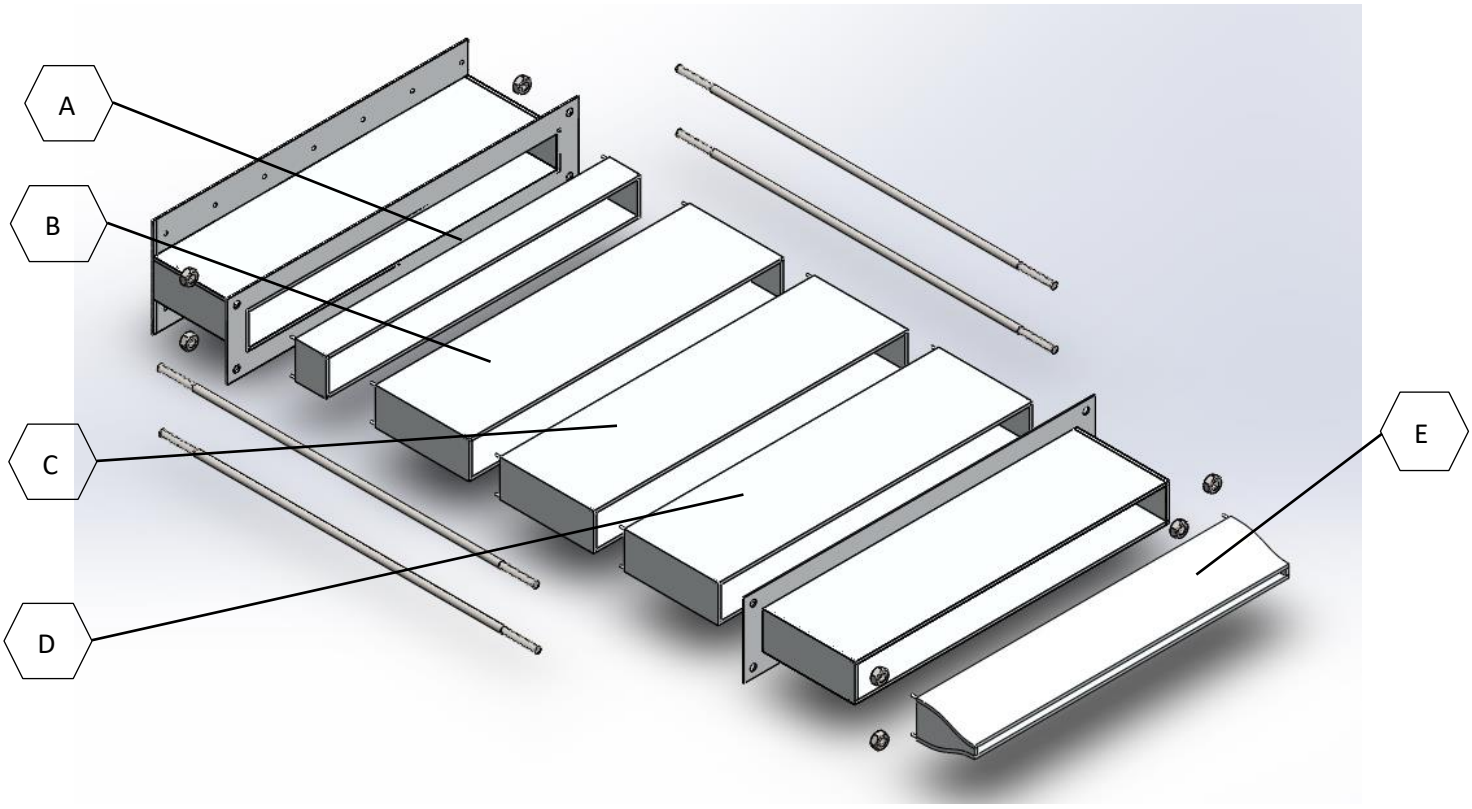

Figure 49 Exploded model of wind tunnel

As we can see in the picture, the honeycomb (A) is the first component placed, then comes a section of the settling chamber (B) to stabilize the flow and at the end of this one the first screen is screwed in place and add a rubber all around for the sealing. Same happens with parts (C) and (D) where the last one is attached to the last part of the settling chamber, where on the other side the convergent (E) is glued and

sealed to obtain our model for the wind tunnel. In every separation a rubber of glue is included to maintain the proper sealing. The model of the wind tunnel as it should look is,

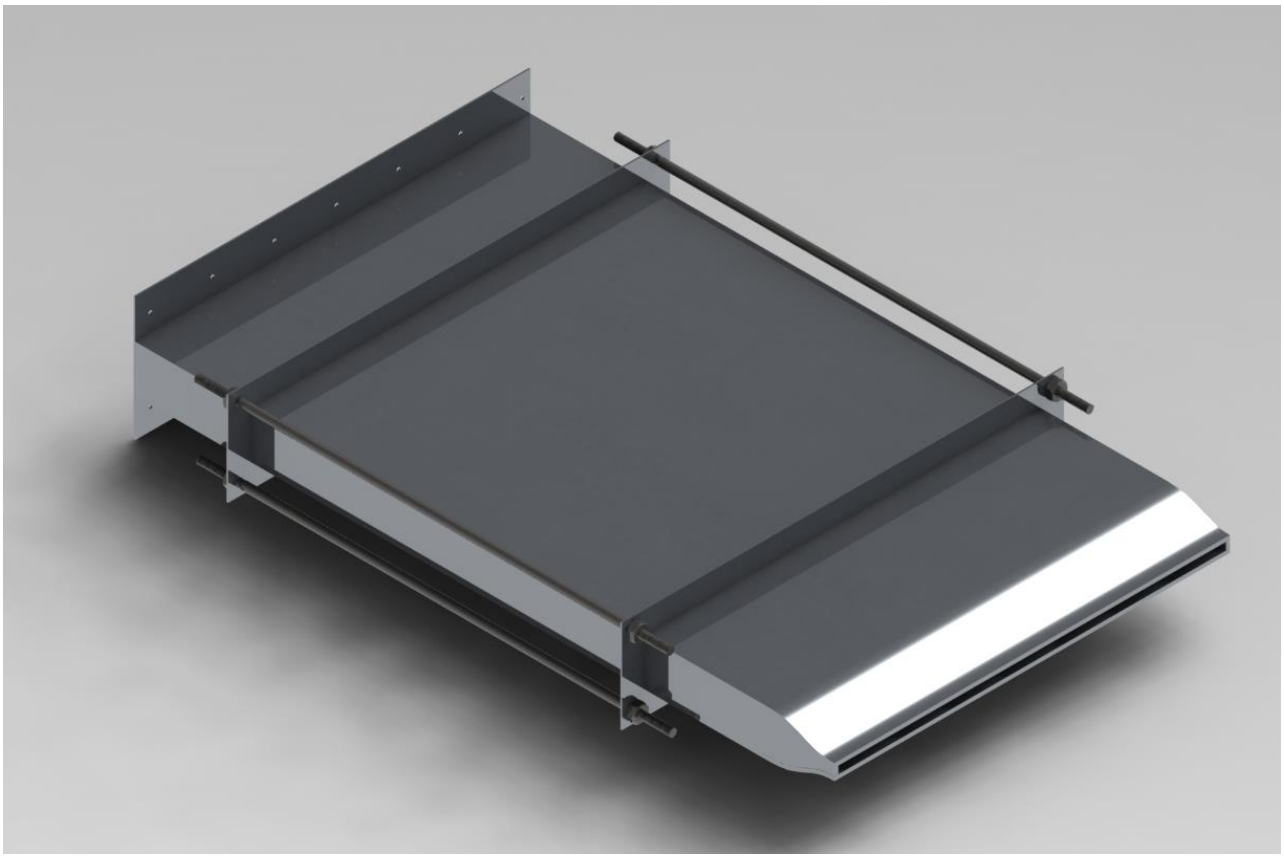

Figure 50 Model of Wind tunnel

Fan Selection

Once with the model presented, the selection of the fan, in this case, a centrifugal fan, is carried out. The attachment to the wind tunnel it's not defined but it's not important to the moment. Looking at the curve of usage of the fan obtained earlier, this was used to look through different curves of fan to find the one most suitable to it. Different manufacturers were consulted and two options from different ones are presented that can fit the wind tunnel and power it to the application.

Both options are centrifugal fans for medium to high pressure and low flow rates and the selected ones are: the centrifugal fan from the series VP/P (400) from MZ aspiratori and the centrifugal fan KA-451-PA from the manufacturer FERRARI ventilatori. Both curves and dimensions from these fans are attached to the end of this thesis. These fans don't match perfectly the curve of usage of the fan but are the two that are the closest to this one, that's why are selected. They fulfill the flow rate requirement but the pressure at what they deliver it's a little higher, needing more power than what was obtained before.

Conclusion

After concluding this thesis, a proper model of a wind tunnel is presented for the calibration of hot-wire probes, along with the specifications of each components and the power plant, and the selection of these for future construction of the wind tunnel.

The component selected are the proper ones that will ensure the requirements described in the introduction meaning that this part of the design is complete. The component who represented the most difficulty to select was the convergent, due to the fact it needed a simulation to ensure it proper functioning and the correct selection of this.

After performing the simulations and comparing the results as it was made in the relative chapter, the decision to go with the convergent design was based in the function of the wind tunnel. Having this convergent assure us the calibration will be the most accurate possible and will allow the future research made with the probes calibrated by this tunnel to obtain accurate and reliable readings from these.

Even though a convergent is more difficult to manufacture and require a specialized process, the value of having a tool properly calibrated outweighs these costs. The distribution and uniformity obtained with it make it more reliable and accurate against easier and cheaper contractions tested. Generally, a compromise is made when selecting between two options that has both advantages and disadvantages; in this case, the advantage of the uniformity of the flow was more important in the decision than the cost of building it.

The selection of the power plant was another difficult part in the analysis, the curve of usage obtained for the fan of the wind tunnel wouldn’t match exactly with any fan available commercially even though a lot of manufacturers were asked and an extensive search through catalogs of fans was performed.

Both options suggested don’t match the curve exactly but are the closest to it. When building the tunnel, a more extensive search can be made to find a fan that can fit better or ask for a tailor-made fan for it.

The model presented is a model made by looking at different wind tunnels in service in the hangar and considering the needs for the components to be inspected and cleaned to maintain proper functioning of the tunnel. It can be upgraded and optimized, this is a suggestion of how can be made. When the decision to make the tunnel is made, this can serve as a base for the design of the wind tunnel or as the design itself.

Bibliography

[1] Hammond, D., AIAA Conference on Multidisciplinary Optimization, Panama City, FL, Sept. 1994.

[2] Jewel B. Barlow, William H. Rae, Alan Pope, Low-Speed Wind Tunnel Testing, Wiley-Interscience; Third Edition.

[3] F. E. Jorgensen. Directional sensitivity of wire and fiber-film probes. DISA information, 11:31-37,1971

[4] Morel T., Design of two-dimensional wind tunnel contractions, Journal of Fluids Engineering, pp. 371-378, (June 1977).

[5] J.E. Sargison, G.J. Walker, R. Rossi. Design and calibration of a wind tunnel with a two-dimensional contraction. School of Engineering, University of Tasmania, TAS, 7001, AUSTRALIA, Ecole Polytechnique de l'Universite de Nantes, FRANCE, 2004.

[6] Idel'chik, I. E., Handbook of Hydraulic Resistance, The Israel Program for Scientific Translations, Tel Aviv, 1966, AEC-TR-6630.

[7] N. A. Ahmed (editor). Wind tunnel designs and their diverse engineering applications. Intech, 2013.

[8] F. E. Jorgensen. How to measure turbulence with hot-wire anemometers -a practical guide. Dantec Dynamics, 2002.

[9] R. Orlu. Experimental study of passive scalar mixing in swirling jet flows. Licenciate (TeknL) thesis, Royal Institute of Technology, Stockholm, Sweden,2006.

H.H. Bruun. Hot-wire anemometry, principles and signal analysis. Oxford Science Publications, 1995.

Justin D. Pereira (editor). Wind tunnels: aerodynamics, models and experiments. Nova Publishers, 2011.

V. Smol'yakov, V. M. Tkachenko (auth.), P. Bradshaw (eds.). The Measurement of Turbulent Fluctuations. An Introduction to Hot-Wire Anemometry and Related Transducers. Springer-Verlag, berlin, 1983.

Appendix

Appendix A: Components Dimensions

Screens (Dimensions may vary in decimals)

Screen	Width Mesh [mm]	Wire Diameter [mm]
1st	3.2	0.71
2nd	2.4	0.56
3rd	0.7	0.16

1st Screen

	Filo Ø *Wire Ø* [mm]	Luce maglia *Mesh opening* [mm]	Vuoto su pieno *Open area* in %	Peso *Weight* [kg/mq]*
N° 7 (poll.franc.) mesh 6,4 nit 12,6	0,55	3,42	74,3 %	0,95
	0,60	3,37	72,1 %	1,13
	0,70	3,27	67,9 %	1,54
	0,80	3,17	63,8 %	2,02
	0,90	3,07	59,9 %	2,55
	1	2,97	56,0 %	3,15
	1,1	2,87	53,2 %	3,81
	1,2	2,77	48,7 %	4,54
	1,3	2,67	45,3 %	5,32
	1,4	2,57	41,9 %	6,17
	1,5	2,47	38,7 %	7,09
	1,6	2,37	35,7 %	8,03
	1,8	2,17	29,9 %	10,21

2nd Screen

	Filo Ø *Wire Ø* [mm]	Luce maglia *Mesh opening* [mm]	Vuoto su pieno *Open area* in %	Peso *Weight* [kg/mq]*
N° 9 (poll.franc.) mesh 8,2 nit 16,2	0,45	2,64	72,5 %	0,82
	0,50	2,59	69,9 %	1,01
	0,55	2,54	67,2 %	1,22
	0,60	2,49	64,6 %	1,46
	0,70	2,39	59,5 %	1,98
	0,80	2,29	54,6 %	2,59
	0,90	2,19	49,9 %	3,28
	1	2,09	45,4 %	4,05
	1,1	1,99	41,6 %	4,90
	1,2	1,89	37,1 %	5,83
	1,3	1,79	33,3 %	6,84

3rd Screen

	Filo Ø *Wire Ø* [mm]	Luce maglia *Mesh opening* [mm]	Vuoto su pieno *Open area* in %	Peso *Weight* [kg/mq]*
N° 30 (poll.franc.) mesh 27,4 nit 54	0,16	0,77	69,0 %	0,35
	0,18	0,75	65,6 %	0,44
	0,20	0,73	62,2 %	0,54
	0,22	0,71	58,8 %	0,65
	0,24	0,69	55,5 %	0,78
	0,28	0,65	49,3 %	1,06
	0,30	0,63	45,9 %	1,21
	0,32	0,61	43,4 %	1,38
	0,35	0,58	38,9 %	1,65
	0,40	0,53	32,8 %	2,16
	0,45	0,48	26,9 %	2,74

Honeycomb

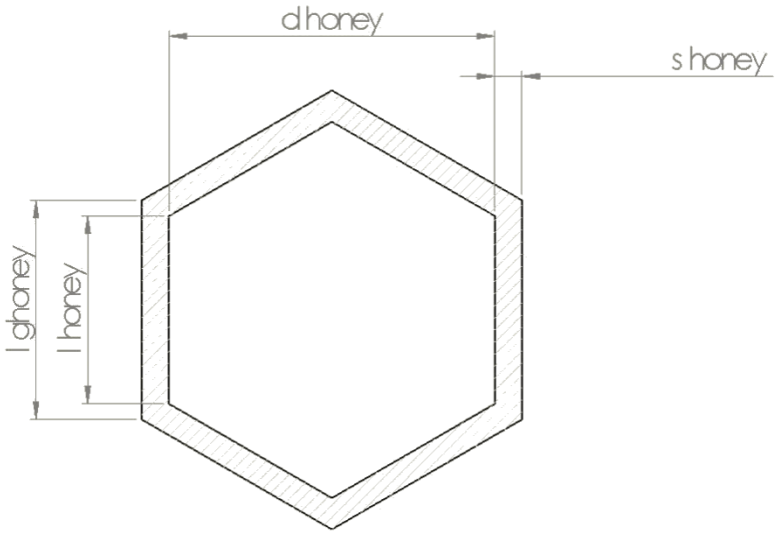

Length of the Honeycomb (L_{honey})	50 mm
Thickness of the cell (s_{honey})	0.1 mm
Size of the cell (d_{honey})	6.35 mm

Appendix B: Datasheet for the fans

Ferrari Ventilatori (KA – 451 – PA):

SERIE **KA**

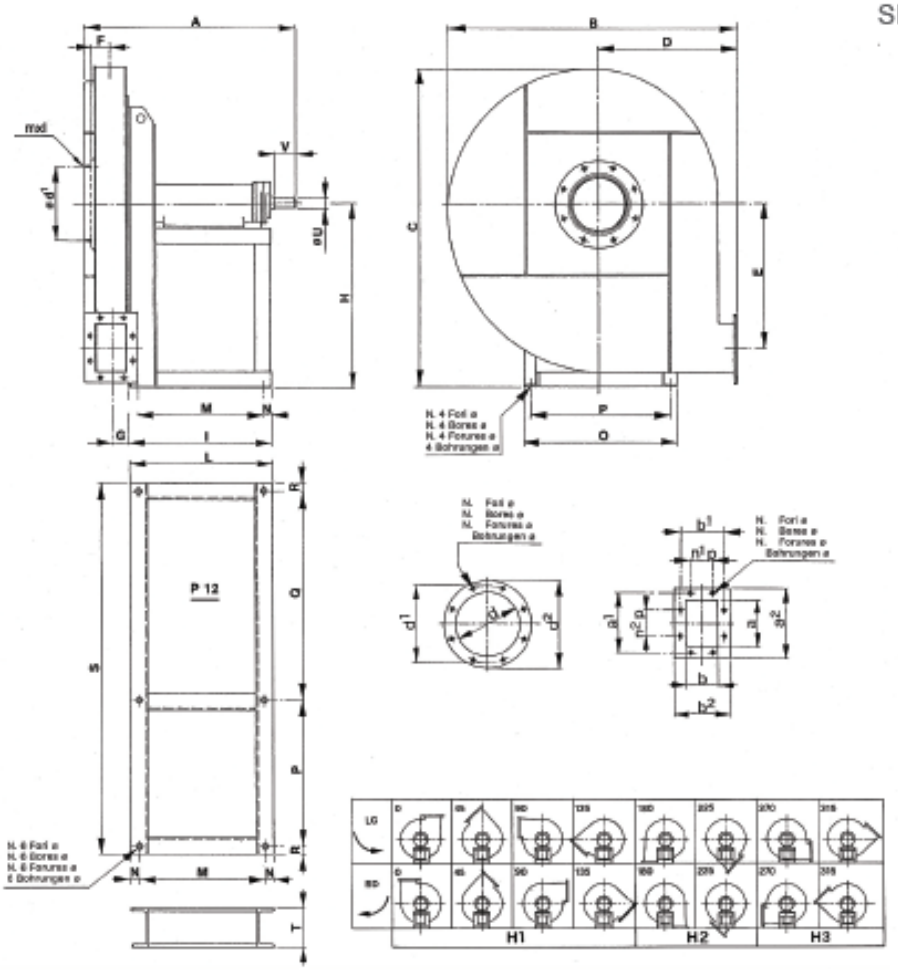

Tipo/Type/Type/Typ	Ventilatore Fan Ventilateur Ventilator										Basamento Base Chassis Socket											Peso Weight Poids Gewicht	Albero Shaft Arbre Welle	
Ventilatore Fan Ventilateur Ventilator	A	B	C	D	E	F	G	H1	H2	H3	I	L	M	N	O	P	Q	R	S	T	Ø	Kg	U	V
KA 401 P1A	490	590	660	280	273	40	37	375	375	375	333	333	299	17	324	288	528	18	850	100	12	13	24	50
KA 451 P1A	500	645	715	300	305	44	42	400	400	400	328	328	294	17	324	288	578	18	900	100	12	13	24	50
KA 501 P1A	555	715	800	335	342	50	47	450	450	450	463	463	417	23	400	355	660	22,5	1060	120	14	21	28	60
KA 561 P1A	685	805	890	375	387	55	52	500	500	500	457	457	411	23	400	355	720	22,5	1120	120	14	21	28	60
KA 631 P1A	710	910	1000	425	438	60	58	560	560	560	475	475	429	23	400	355	780	22,5	1180	120	14	23	38	80
KA 711 P1A	855	1015	1120	475	488	68	64	630	630	630	575	575	519	28	588	534	862	27	1250	160	17	32	42	110
KA 801 P1A	885	1140	1260	530	551	75	71	600	600	710	575	575	519	28	628	574	772	27	1400	160	17	35	42	110
KA 901 P1A	880	1285	1420	600	620	81	83	670	670	800	580	580	524	28	708	654	792	27	1500	160	17	45	48	110
KA 1001 P1A	1000	1420	1590	670	690	93	90	750	750	900	642	642	576	33	828	762	874	32	1700	180	19	60	48	110

Tipo/Type/Type/Typ	Flangia aspirante Inlet flange Bride à l'aspiration Flansch saugseitig						Flangia premente Outlet flange Bride en refoulement Flansch druckseitig										Peso Weight Poids Gewicht	J
Ventilatore Fan Ventilateur Ventilator	d	d1	d2	n°	Ø	m x l	a	b	a1	b1	a2	b2	n1p	n2p	n°	Ø	Kg	Kgfm²
KA 401 P1A	129	165	189	4	8	M8x20	95	68	129	102	145	128	-	-	4	10	35	0,09
KA 451 P1A	144	182	214	8	8		105	78	139	110	165	136	-	-	4	10	39	0,18
KA 501 P1A	184	200	234	8	8		117	85	151	119	177	145		-	4	10	54	0,25
KA 561 P1A	184	219	254	8	8		131	95	165	129	191	155	-	1-100	6	10	79	0,43
KA 631 P1A	204	241	274	8	8		146	105	182	139	216	175	-	1-112	6	12	105	0,85
KA 711 P1A	228	265	298	8	8		164	117	200	151	234	187	-	1-112	6	12	148	1,38
KA 801 P1A	254	292	324	8	10	M8x25	183	131	219	165	253	201		1-112	6	12	193	2,5
KA 901 P1A	285	332	365	8	10		205	146	241	182	275	216	1-112	1-112	8	12	278	4,2
KA 1001 P1A	320	368	400	8	10		229	164	265	200	299	234	1-112	1-112	8	12	398	8,8

Peso ventilatore in kg
Fan weight in kg
Poids du ventilateur en kg
Ventilatorgewicht in kg

Tabella non impegnativa
The above data are unbinding
Tableau sans engagement
Unverbindliche Tabelle

KA 451 P1A

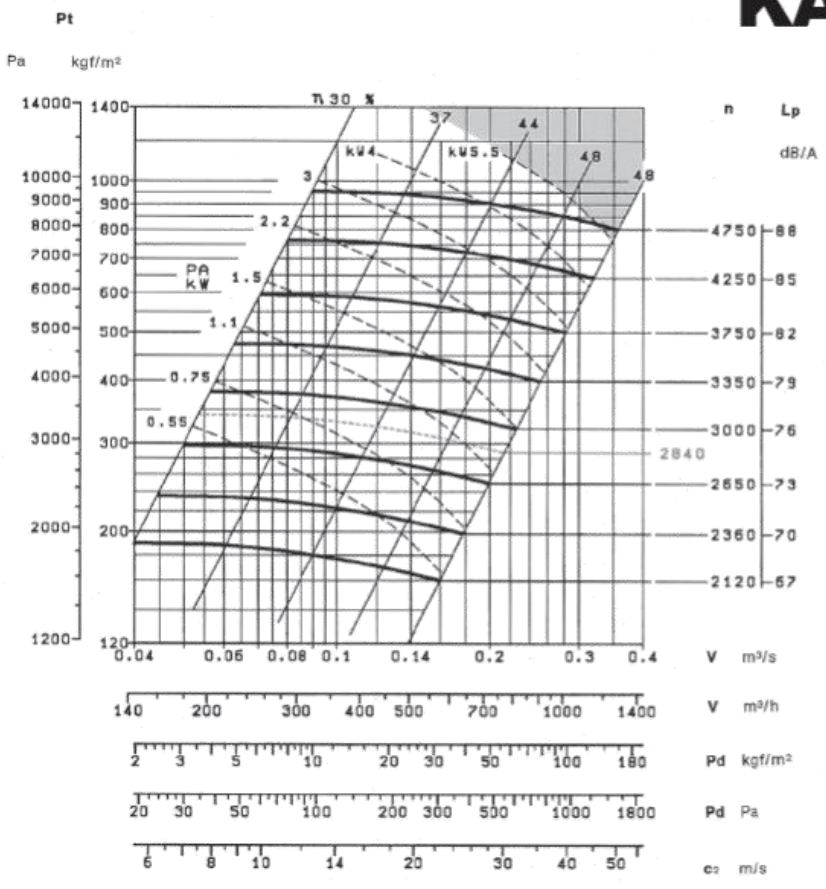

Giri massimi ammissibili
Maximum permissible rpm
vitesse de rotation maximale admissible
maximal zulässige Drehzahl:

≤ 100°C = 4750
101 ÷ 200°C = 4250

J = 0,18 kg • m²

Tolleranza sulla rumorosità + 3 dB/A
Noise level tolerance + 3 dB/A
Tolérance sur niveau sonore + 3 dB/A
Toleranz Schallpegel + 3dB/A

kW assorbiti ventilatore tolleranza ± 3%
kW consumed fan tolerance ± 3%
Tolérance sur Pabs kW ± 3%
Toleranz für Wellenleistung ± 3%

MZ aspiratori (VP/P 400):

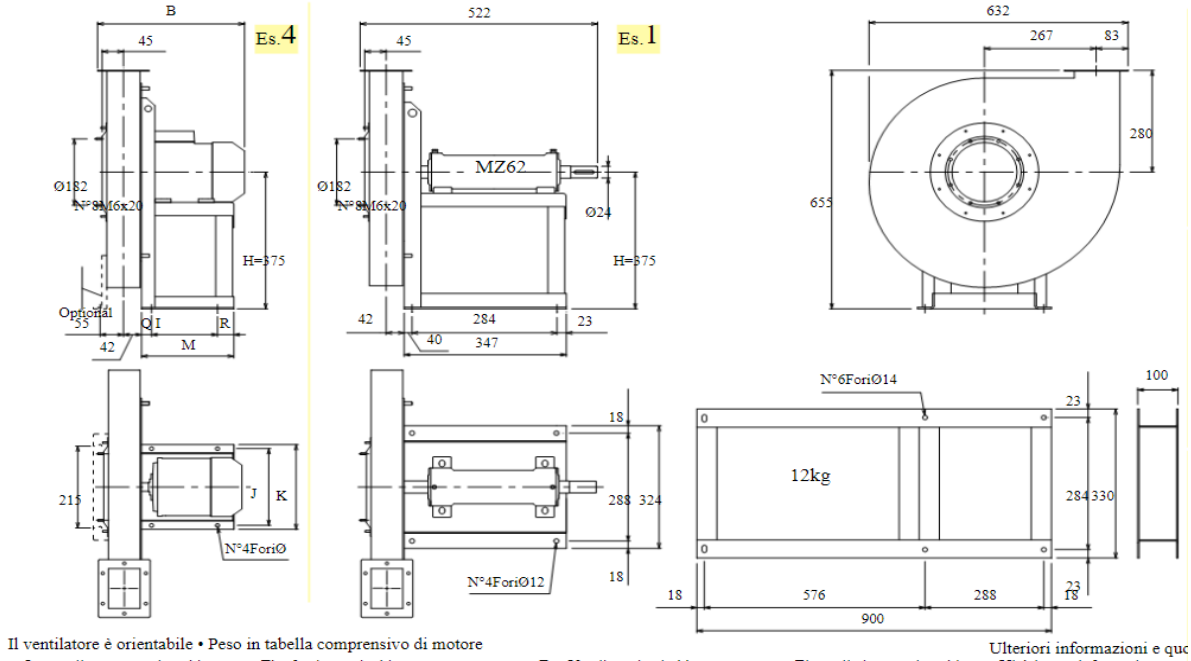

Il ventilatore è orientabile • Peso in tabella comprensivo di motore

■ Le ventilateur est orientable ■ The fan is revolvable ■ Der Ventilator ist drehbar ■ El ventilador es orientable

Lepoidsdans le tableau inclut lemoteur The weight indicated in the table includesmotor Das Gewicht imTafel schließtdenMotor El pesoen la tabla incluyeelmotor

Ulteriori informazioni e quo
Ultérieures informations et c
Further information and size
Weitere Infos und Größen:
Más informaciones y medid

TIPO Type VENTILATORE Fan	MOTORE Motor	PESO Weight Kg	PD Kgf x s²/m	B	I	H	H1	H2	J	K	M	Q	R	Ø
VP400/P2	80 A2	49	0,6	344	121	375	375*	375	203	225	217	48	48	10
VP400/P2	80 B2	49	0,6	344	121	375	375*	375	203	225	217	48	48	10
VP400/P/T		40	0,6			375	280	375						

pg. 4.6/S.

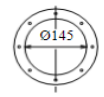

pg. 4.5/S.

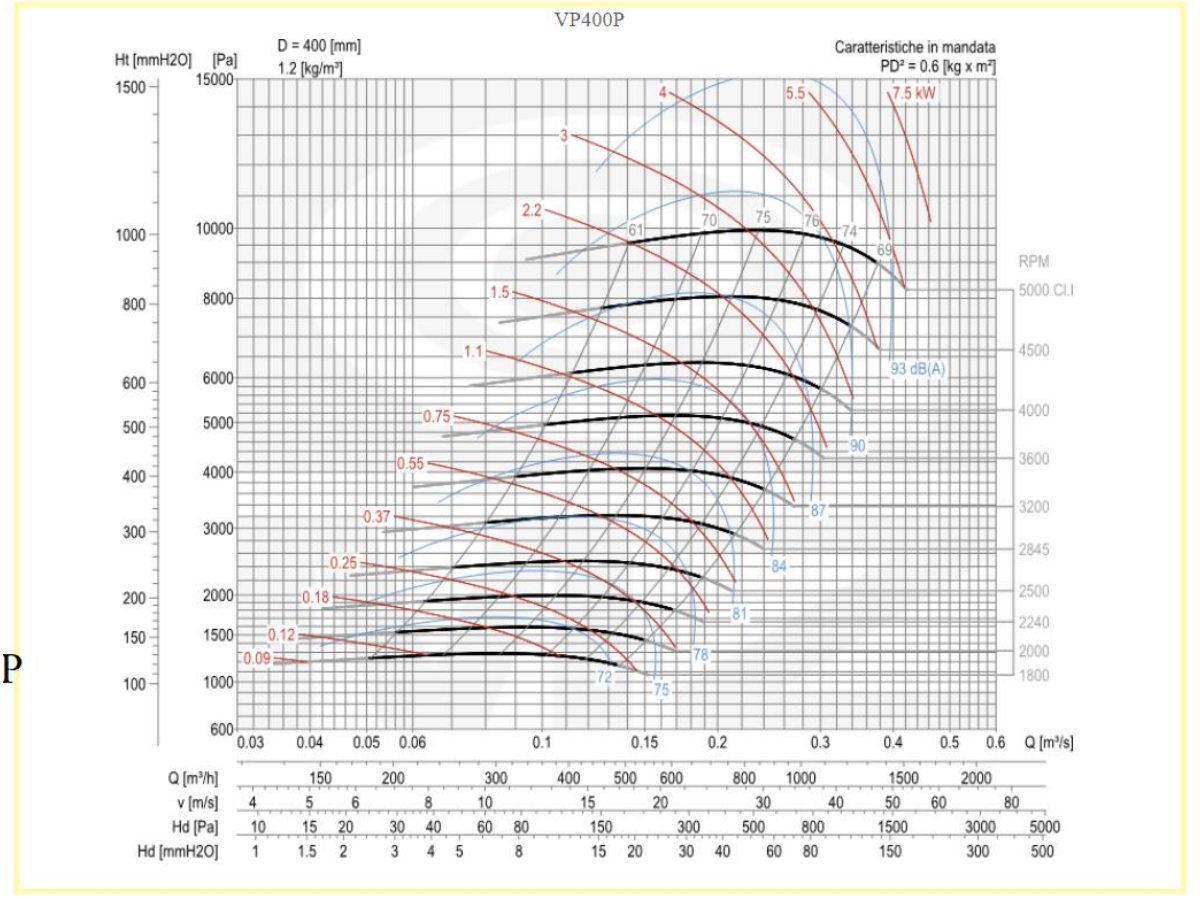

P